BHLHE40 positively regulates the differentiation of human airway basal cells

Inauguraldissertation
zur Erlangung des Grades eines Doktors der Medizin (Humanbiologie) des Fachbereichs Medizin
der Justus-Liebig-Universität Gießen

vorgelegt von

Ghoul, Maroua

aus

Tunis, Tunisia

Gießen, 2025

Aus dem Fachbereich Medizin der Justus-Liebig-Universität Gießen

Cardio-Pulmonary Institute, Klinik für Innere Medizin II

Gutachter: Prof. Dr. Samakovlis, Christos

Gutachter: PD Dr. Deckmann, Klaus

Tag der Disputation:

23.06.25

Ehrenwörtliche Erklärung

„Hiermit erkläre ich, dass ich die vorliegende Arbeit selbständig und ohne unzulässige Hilfe oder Benutzung anderer als der angegebenen Hilfsmittel angefertigt habe. Alle Textstellen, die wörtlich oder sinngemäß aus veröffentlichten oder nichtveröffentlichten Schriften entnommen sind, und alle Angaben, die auf mündlichen Auskünften beruhen, sind als solche kenntlich gemacht. Bei den von mir durchgeführten und in der Dissertation erwähnten Untersuchungen habe ich die Grundsätze guter wissenschaftlicher Praxis, wie sie in der „Satzung der Justus-Liebig-Universität Gießen zur Sicherung guter wissenschaftlicher Praxis“ niedergelegt sind, eingehalten sowie ethische, datenschutzrechtliche und tierschutzrechtliche Grundsätze befolgt. Ich versichere, dass Dritte von mir weder unmittelbar noch mittelbar geldwerte Leistungen für Arbeiten erhalten haben, die im Zusammenhang mit dem Inhalt der vorgelegten Dissertation stehen, und dass die vorgelegte Arbeit weder im Inland noch im Ausland in gleicher oder ähnlicher Form einer anderen Prüfungsbehörde zum Zweck einer Promotion oder eines anderen Prüfungsverfahrens vorgelegt wurde. Alles aus anderen Quellen und von anderen Personen übernommene Material, das in der Arbeit verwendet wurde oder auf das direkt Bezug genommen wird, wurde als solches kenntlich gemacht. Insbesondere wurden alle Personen genannt, die direkt und indirekt an der Entstehung der vorliegenden Arbeit beteiligt waren. Mit der Überprüfung meiner Arbeit durch eine Plagiatserkennungssoftware bzw. ein internetbasiertes Softwareprogramm erkläre ich mich einverstanden.“

_____ _____

Ort/Datum Unterschrift

Table of Contents

Abbreviations

ALI	Air liquid interface
APS	Ammonium persulphate
BASCs	Bronchioalveolar stem cells
BADJ	Bronchioalveolar duct junction
BBS	Borate buffered saline
BSA	Bovine serum albumin
$CaCl_2$	Calcium chloride
cDNA	Complementary deoxyribonucleic acid
Chip	Chromatin immunoprecipitation
CUT&RUN	Cleavage under targets and release using nuclease
DMEM	Dulbecco's Modified Eagle Medium
DNA	Deoxyribonucleic acid
DNase	Deoxyribonuclease
DOX	Doxycycline
DTT	Dithiothreitol
EDTA	Ethylenediaminetetraacetic acid
EdU	5-Ethynyl-2′-deoxyuridine
eGFP	Enhanced GFP
ENCODE	Encyclopedia of DNA elements
FACS	Fluorescence-activated cell sorting
FCS	Fetal Calf Serum
HBSS	Hanks' balanced salt solution
HCL	Hydrochloric acid
HEK293T	Human embryonic kidney 293T cells
Hepes	*N*-2-Hydroxyethylpiperazine-*N*'-2-ethane sulphonic acid
HLH	Helix-loop-helix
IF	Immunofluorescence
IGV	Integrative genomic viewer
IP	Immunoprecipitation
Kb	Kilobase
Kcl	Potassium chloride
KDa	Kilodalton

LB	Lysogeny broth
LNEP	Lineage negative epithelial stem cells
$MnCl_2$	Manganese(II) chloride
MOPS	3-(N-morpholino) propane sulfonic acid
mRNA	Messenger Ribonucleic acid
NaCl	Sodium chloride
Na-DOC	Sodium deoxycholate
$Nahco_3$	Sodium bicarbonate
Na_2HPO_4	Sodium phosphate dibasic anhydrous
NaH_2PO_4	Sodium dihydrogen phosphate
NaN_3	Sodium azide
NaOH	Sodium hydroxide
NEB	Neuroepithelial bodies
NEC	Neuroepithelial cells
nt	Nucleotide
N1ICD	Notch1 intracellular domain
PAGE	Polyacrylamide gel electrophoresis
PBS	Phosphate- buffered saline
PCR	Polymerase chain reaction
pHBECs	Primary human bronchiolar epithelial cells
RbCl	Rubidium chloride
RIN	RNA Integrity Number
RIPA	Radio-immunoprecipitation assay buffer
RNase	Ribonuclease
RPM	Revolutions per minute
RT	Reverse transcriptase
RT qPCR	Real-time quantitative PCR
SD	Standard deviation
SDS	Sodium dodecyl sulfate
SMG	Submucosal glands
TAE	Tris-acetate-EDTA
TEMED	Tetramethyl ethylenediamine
tGFP	Turbo GFP

1 Introduction

1.1 Human airway epithelium: stem cell populations and differentiated cell types

The human airway epithelium serves as the first line of defense against inhaled pathogens, primarily through mucociliary clearance. It also conducts gases to the alveolar compartment, where gas exchange takes place. Regenerative, secretory, protective, and sensory functions are carried out by the various epithelial cell populations that compose the airway lining. Among them are basal, secretory, ciliated, neuroendocrine, ionocyte, and tuft cells (Montoro et al., 2018; Travaglini et al., 2020).

1.1.1 Basal cells

The basal cells are attached to the basement membrane of the pseudostratified epithelium and are morphologically characterized by their small height in comparison to the adjacent luminal differentiated cells. They compose 30% of the human airway epithelium and are present throughout the entire airways, including small bronchioles. However, in rodents, they are restricted to the trachea and main bronchi. Basal cells are multipotent stem cell progenitors able to self-renew and differentiate into the ciliated and secretory lineage but also tuft, neuroendocrine, and ionocytes cells (Montoro et al., 2018; Rock et al., 2009) to maintain the pseudostratified epithelium. Basal cells are characterized by the expression of the transcription factor transformation-related protein 63 (TP63), cytokeratin 5 (KRT5), nerve growth factor receptor (NGFR), Integrin Subunit Alpha 6 (ITGA6), and podoplanin (PDPN) (Hogan et al., 2014; Rock & Hogan, 2011; Rock et al., 2009). In addition to their stem cell function, basal cells have also an immunomodulatory function, since they recruit immune cells by secreting IL33 in the airways (Byers et al., 2013). Several studies have suggested the existence of two transcriptionally distinct basal cell populations in proximal human airway epithelium: proliferating and differentiating basal cells. The proliferative basal cells express cell cycle genes, while the differentiating basal cells were characterized by a decreased expression of KRT5 and increased expression of differentiation markers (e.g., SCGB3A2, HES1) (Travaglini et al., 2020). In mouse airway epithelium, previous studies have also described two molecularly distinct basal cell subpopulations: putative (dividing) stem cells and luminal precursors characterized by the increased expression of luminal markers (e.g., KRT8) (Watson et al., 2015).

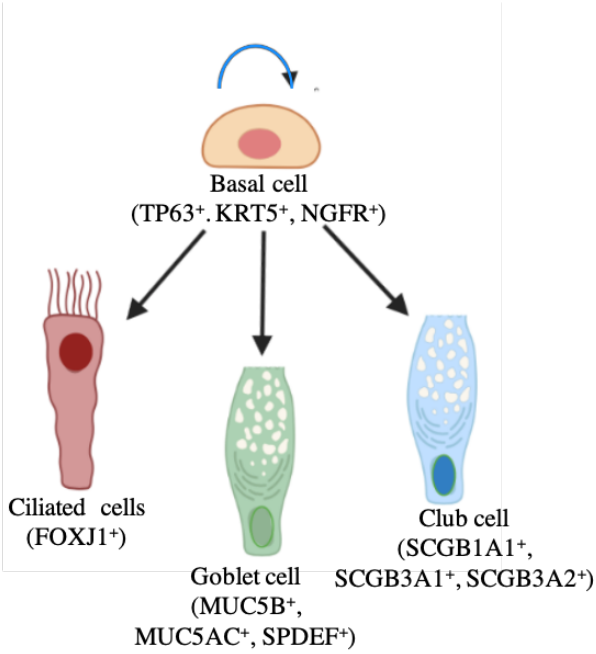

Figure 1. Schematic representation of airway basal cell differentiation. Basal cells are multipotent progenitors of the airway epithelium that can give rise to different cell types including ciliated, goblet, and club cells.

1.1.2 Submucosal glands

A second stem cell population was identified in the submucosal glands (SMGs) ducts, which are located under the surface airway epithelium (SAE) within the mesenchyme and have duct and acinar compartments. In humans, SMGs are located in the cartilaginous airways, from the larynx down to the main bronchi. However, in the mouse, they are restricted to the trachea. Interestingly, SMGs duct progenitors have a basal cell-like morphology and were shown to express KRT5, KRT14, α-SMA, IGFBP4, and NGFR. In mouse trachea, these cells were able to regenerate goblet and ciliated cells of the surface epithelium after Naphthalene injury, (Hegab et al., 2011; Lynch et al., 2018).

1.1.3 Bronchioalveolar stem cells

Another stem cell population identified in the murine lung is the bronchioalveolar stem cells (BASCs). These rare epithelial cells are located in the bronchioalveolar duct junction (BADJ), the transition between the terminal bronchioles to the alveoli. These cells co-express cell-specific markers from both club and alveolar type 2 cells, Secretoglobulin1a1 (SCGB1A1) and surfactant protein c (SP-C), respectively. They have been shown to function as dual progenitors *in vivo*, by maintaining the bronchiolar club cells and alveolar cells of the distal lung in response to injury (Kim et al., 2005; Liu et al., 2019; Salwig et al., 2019).

1.1.4 Lineage-negative epithelial stem cells

A rare group of stem cells has also been identified as lineage-negative epithelial stem cells (LNEP) in the distal part of the lung. During homeostasis, these rare stem cells are quiescent, however, upon injury (bleomycin, Influenza), LNEPs activate TP63/KRT5 programs and migrate to regenerate the damaged alveolar region. The Activation of TP63 and KRT5 gene expression is Notch-dependent (Kathiriya et al., 2020; Vaughan et al., 2015).

1.1.5 Club cells

Club cells are characterized by a domed morphology oriented toward the lumen and by the presence of secretory vesicles in their cytoplasm (Hogan et al., 2014). They are scattered throughout the human and murine airway epithelium and arise from basal cells in a Notch1-dependent manner. Interestingly, club cells act as progenitor cells that can both self-renew and produce differentiated secretory and ciliated cells (Rawlins et al., 2009; Rock & Hogan, 2011). Lineage tracing experiments have shown that secretory cells can also dedifferentiate into functional basal cells, and regenerate the epithelium after murine basal cell ablation with Diphtheria toxin injury, suggesting the existence of a communication signal from basal toward secretory cells. Furthermore, the dedifferentiated basal-like cells were multipotent and able to give rise to the 3 cell populations: basal, secretory, and ciliated cells when cultured in ALI culture (Tata et al., 2013). In addition to their progenitor potential, club cells have secretory and detoxifying functions, as they secrete proteins that contribute to the protective lining fluid of the airways, and metabolize xenobiotic substances inhaled from the air through cytochrome P450 enzymes (Rokicki et al., 2016). Specific markers for club cells include Secretoglobin SCGB1A1 (also known as CCSP or CC10) (Hogan et al., 2014), but also SCGB3A1, SCGB3A2, and SSEA1 (Reynolds et al., 2002; Tata et al., 2013).

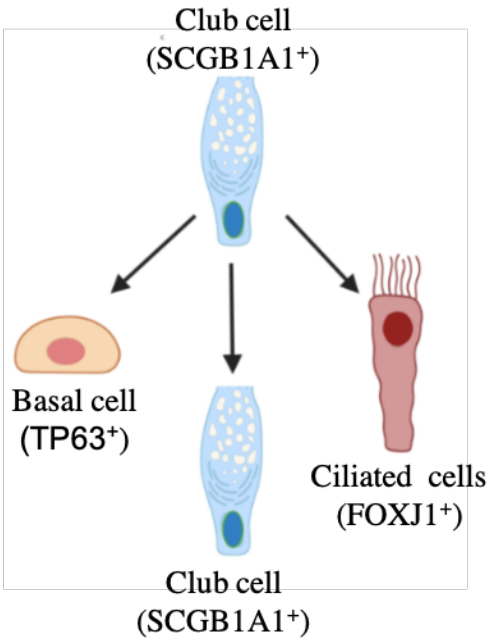

Figure 2. Schematic representation of the progenitor potential of club cells. Club cells act as progenitor cells that can self-renew and give rise to ciliated and basal cells upon injury.

A club cell sub-population is the naphthalene-resistant or variant club cells, which are characterized by the expression of Uroplakin 3A (UPK3A) and SCGB3A2 but low SCGB1A1 expression. Unlike the other club cells, the variant-club cells do not express the cytochrome P450 CYP2F2, which confers them resistance to Naphthalene injury, as CYP2F2 metabolizes naphthalene into a cytotoxic compound lethal for the cells. Previous studies describe their location near the Neuroepithelial bodies (NEBs) and bronchioalveolar duct junctions (BADJs). Interestingly, the variant club cells restored the airway epithelium after naphthalene-induced club cell depletion (Guha et al., 2017; Guha et al., 2012).

1.1.6 Ciliated cells

Ciliated airway epithelial cells are morphologically characterized by the presence of multi-cilia on their apical surface. They are scattered throughout the large and small airways (Tata et al, 2017). However, ciliated cell density and cilia length decrease along the murine tracheobronchial airways (Toscala et al, 2005). Under steady-state, ciliated cells arise mainly from club cells, and fewer from basal cells (Rawlins et al., 2009; Ruiz Garcia et al., 2019). Nonetheless, following injury and after the loss of club cells, ciliated cells are regenerated mainly from basal cells (Pardo-Saganta, Law, et al., 2015). Unlike club cells, ciliated cells are terminally differentiated (Rawlins & Hogan, 2008), they do not self-renew or trans-differentiate to regenerate the epithelium after injury (Rawlins et al., 2007). Thanks to the

beating of their cilia, these cells enable mucociliary clearance, a process where inhaled particles and pathogens are moved out of the airways (Knowles & Boucher, 2002). Also, ciliated cells are molecularly characterized by the expression of the transcription factors TP73, MYB, and FOXJ1, required for their differentiation (Marshall et al., 2016; Rawlins & Hogan, 2008).

1.1.7 Goblet cells

Goblet cells are morphologically characterized by large vesicles required for mucus secretion in response to airway injury or irritation. This mucus contributes to the protective liquid layer of the lung. With their apical surfaces toward the lumen, they compose almost 25% of the bronchial epithelium in humans and larger mammals. Also, goblet cells arise either from basal cells (Danahay et al., 2015; Rogers, 1994, 2003) or from Scgb1a1 expressing club cells, and SPDEF is required for their differentiation in the normal tracheal-laryngeal airways (Chen et al., 2009). In addition, goblet cells are characterized by the expression of the mucins MUC5AC, MUC5B, and the transcription factor FOXA3 (Danahay et al., 2015).

1.2 Notch signaling and airway epithelial cell differentiation

1.2.1 Notch signaling is required for basal cell differentiation

Previous studies have shown that Notch signaling is required for basal cell differentiation into early progenitors. Mouse basal cells cultured in the presence of Notch inhibitor DPZ failed to form a lumen and were composed of a single layer of $TP63^+$ cells. In addition, sustained activation of Notch1 intracellular domain (N1ICD) in basal cells under the *Krt5* promoter drives their differentiation. Notch signaling activation was associated with the downregulation of basal cell genes and upregulation of luminal secretory genes, predominantly *SCGB1A1*. In the human ALI system, constitutive expression of Notch downstream targets *HES1* or *HEY1* in primary epithelial cells showed fewer $TP63^+$ cells in comparison with control cells. Also, FACS-sorted HES1-GFP^+ cells showed reduced *JAG2* expression (which is the most differentially expressed ligand among basal-luminal cells of the steady-state mouse tracheobronchial epithelium) and increased *NOTCH2* expression (Rock et al., 2011).

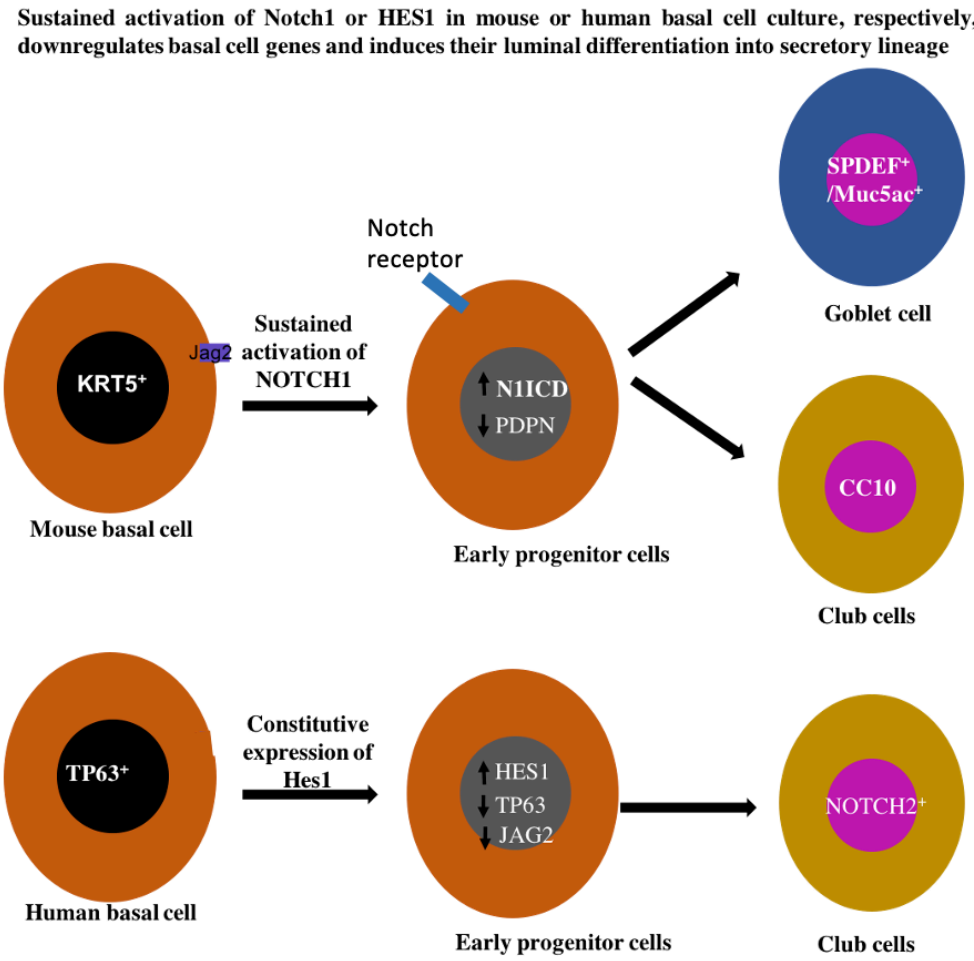

Figure 3. Notch activation promotes basal cell differentiation. Sustained activation of Notch signaling downregulates basal cell genes and promotes their differentiation into the secretory lineage.

1.2.2 Jag2 and Jag1 maintain secretory cell identity via Notch2 activation

Previous studies have shown that Jag1 inhibition in mice, using selective anti-Jag1 antibody led to increased ciliated cells at the expense of secretory cells, via direct trans-differentiation of club cells into ciliated cells (proliferation and cell apoptosis remained unchanged after JAG1 blockade). Near the NEBs and the BADJs, a few remaining club cells were not affected by Jag1 inhibition. Consistently, NOTCH2 inhibition using anti-NOTCH2 antagonist antibody or genetic deletion in secretory cells increased ciliated cells at the expense of secretory cells (Lafkas et al., 2015; Pardo-Saganta, Law, et al., 2015). In addition, genetic deletion of *Jag1* in shh-Cre mice, induced a significant increase in FOXJ1^{+} cells with decreased SCGB3A2^{+} and SCGB1A1^{+} cells (Stupnikov et al., 2019b). Also, genetic deletion of *Jag2* by *Krt5*-Cre in mice induced an increase in FOXJ1^{+} cells, and a decrease in CC10^{+}, SCGB3A2 $^{+}$, and SSEA1^{+} secretory cells. This deletion also reduced N2ICD^{+} Suprabasal cells. Similarly, in the human ALI culture, *JAG2* knockdown in primary human bronchiolar

cells induced the same phenotype: reduced secretory (*SCGB1A1*, *SCGB3A2*) and increased ciliated cell gene expression (*FOXJ1*, *MYB*) (Pardo-Saganta, Tata, et al., 2015).

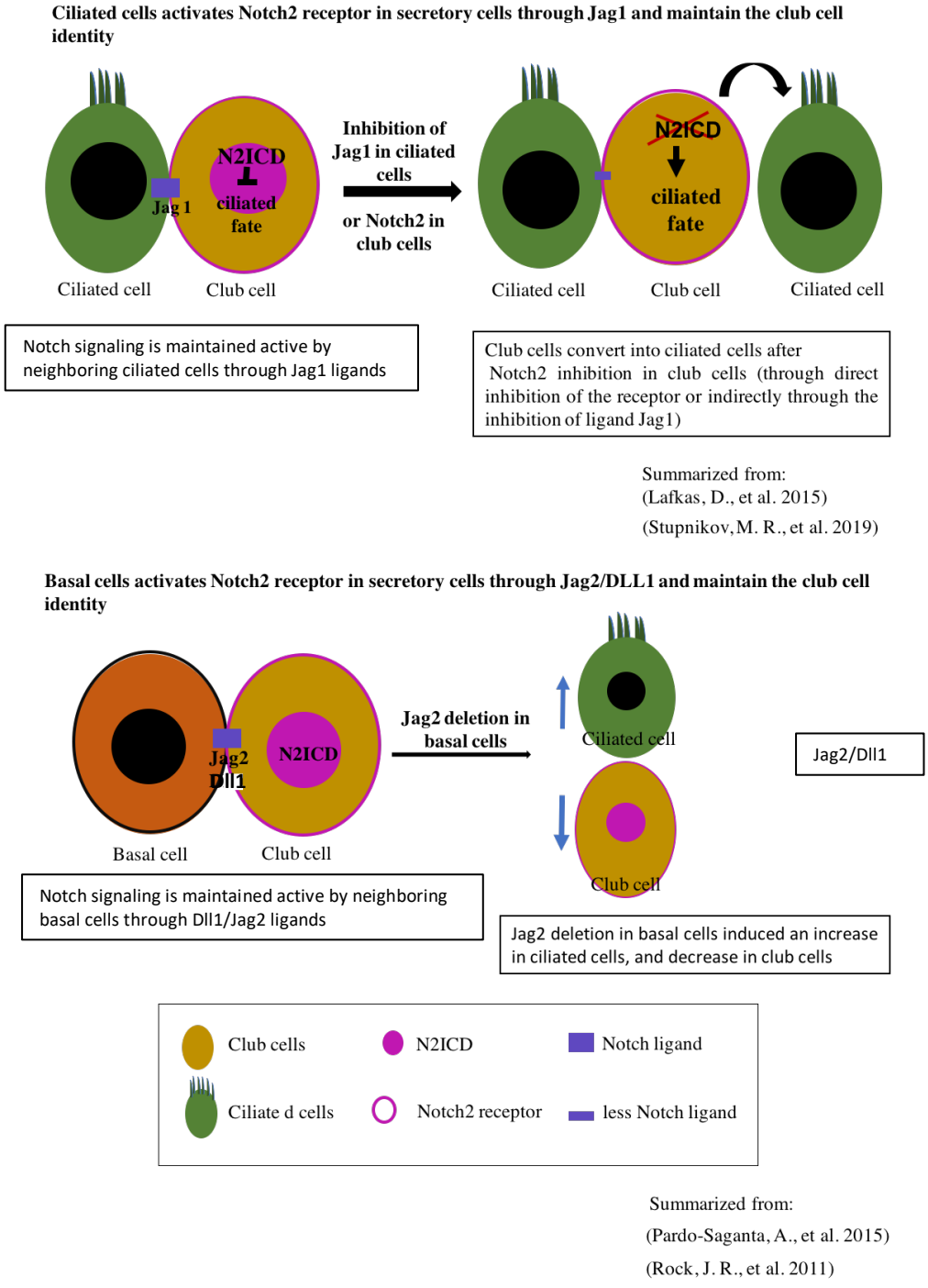

Figure 4. Active Notch2 signaling is required to maintain the club cell fate. Notch2 signaling in club cells is activated by DLL1/JAG2 ligands expressed by the neighboring basal cell. The deletion of *Jag2* decreases club cells and increases ciliated cells.

1.3 The transcription factor BHLHE40

1.3.1 BHLHE40: a transcription factor with diverse mechanisms, binding sites, and cellular functions

BHLHE40 protein is composed of a basic region and a Helix Loop Helix (HLH) region: the basic region of BHLHE40 is associated with DNA binding, while the HLH region is associated with protein dimerization (Ivanova et al., 2005). Moreover, BHLHE40 has two nuclear localization signals and one nuclear export signal motif (Boudjelal et al., 1997). Previous studies have shown that BHLHE40 is involved in circadian rhythm regulation and is a transcriptional repressor of clock-controlled genes. It was shown to repress Clock/Bmal1-induced transactivation of clock genes, through direct protein interaction with BMAL1 or through competing with Clock/Bmal1 E-boxes binding region (Honma et al., 2002; Nakashima et al., 2008). In addition, BHLHE40 negatively auto-regulated its expression via repression of its own promoter. This repression required the C-terminal domain that covers the α-helices through an HDAC-dependent mechanism. Also, BHLHE40 strongly reduced *c-Myc* promoter activity, a proliferation-associated gene. However, HDAC recruitment was not required for this repression (Sun & Taneja, 2000). In another context, BHLHE40 repressed LKB1 promoter activity, an activator of AMP-activated protein kinase which is important for many metabolic processes. The repression required the binding to the E-box region through the N-terminal basic region (Sato et al., 2015).

Similarly, BHLHE40 transcriptionally repressed the expression of drug-metabolizing enzymes in the liver. In addition, BHLHE40 repressed the transcription of *CYP4A1 in vitro*, using primary human hepatocyte, not through E box binding, but through a similar sequence to the *SP1* binding site (CCCTGC). This repression required the DNA binding domain in the N-terminal region of BHLHE40 (Zhao et al., 2012). BHLHE40 has also been reported to interact with RXR receptors through N-terminal LXXLL nuclear receptor motif and repressed RXR ligand-dependent activation of the RXR reporter (Cho et al., 2009). Another report showed that BHLHE40 negatively regulated the expression of genes involved in peroxisomal fatty acid oxidation and the biogenesis of peroxisomes (Chang et al., 2019). Interestingly, in muscle cells, BHLHE40 repressed Notch transcriptional activity by interacting with NICD and preventing its binding with RBPJk, which in turn, repressed the transcription of Notch downstream effectors *Hes1* and *Hey1*. Consistently, increased levels of NICD were detected in regenerating *BHLHE40* $^{-/-}$ mouse myoblast after injury (Sun et al., 2007). However, BHLHE40 has also been described as a transcriptional activator in several

studies (Qian et al., 2014; Jarjour et al., 2019; Nguyen et al., 2024). It has been shown that BHLHE40 in cooperation with HDAC8, transcriptionally increased the expression of *TP73*, a master regulator of ciliogenesis (Qian et al., 2014; Wallmeier et al., 2021).

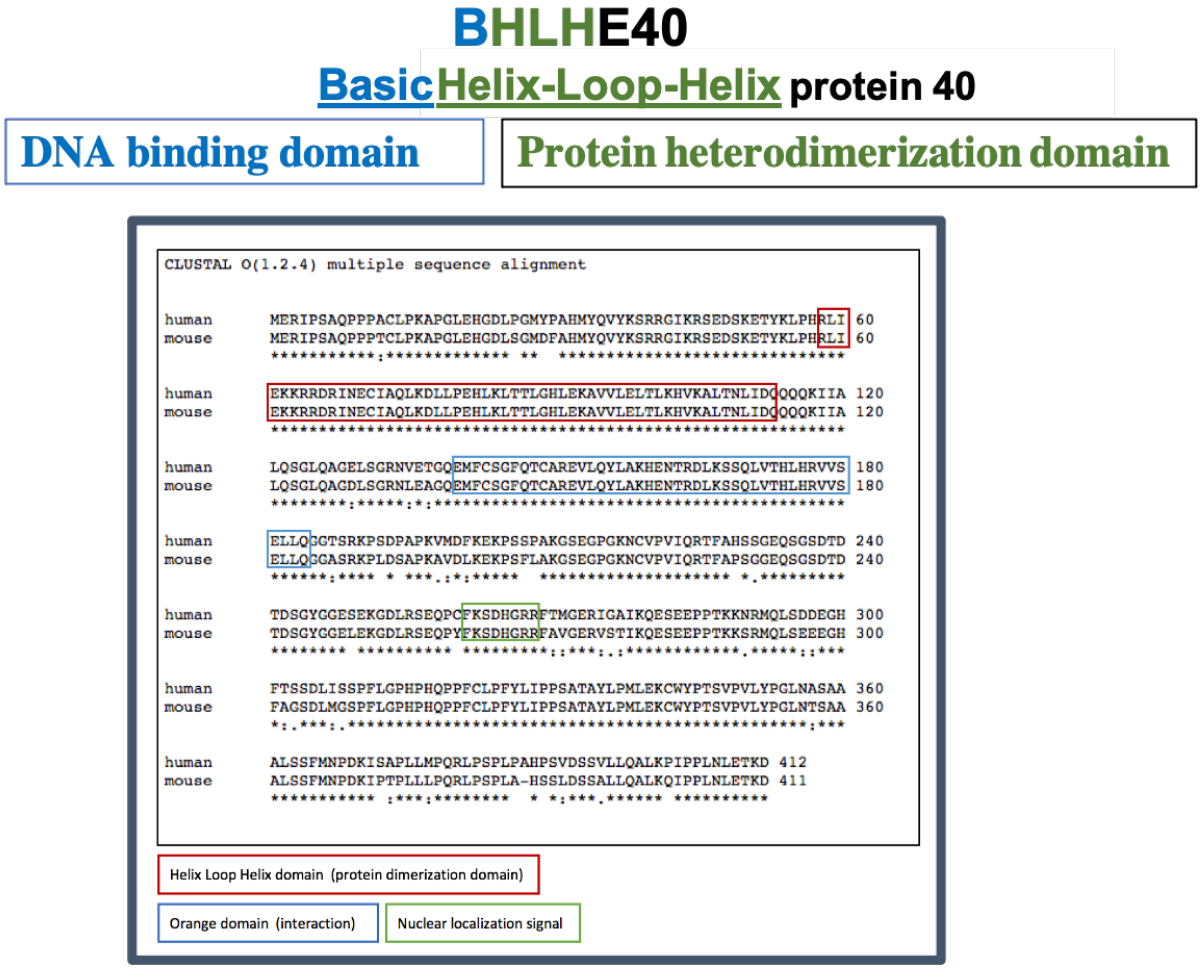

Figure 5. BHLHE40 functional domains. BHLHE40 is composed of a DNA binding domain (B: Basic domain) and a protein heterodimerization domain (HLH: Helix Loop Helix) for protein interaction.

1.3.2 The role of BHLHE40 in cellular differentiation and proliferation

Previous studies have shown that the overexpression of BHLHE40 in chondrogenic cell lines promoted chondrocyte differentiation. In addition, in the chondrocyte *in vitro* differentiation model, *BHLHE40* expression was low during the proliferation phase and upregulated during the differentiation phase (Shen et al., 2002). Similarly, forced expression of BHLHE40 in human mesenchymal stem cells, cultured in the presence of an osteogenic medium, increased the expression of bone-related genes and accelerated osteogenic differentiation and calcification (Sato et al., 2015). Also, ectopic expression of BHLHE40 in cultured mouse trophoblast stem cells, inhibited cell proliferation and promoted the differentiation into

trophoblast giant cells (Hughes et al., 2004). However, in another cellular context, BHLHE40 overexpression inhibited muscle cell differentiation through transcriptional repression of *Myog* promoter, an important transcription factor for myogenic differentiation (Wang et al., 2015). Another report showed that BHLHE40 promoted myogenic differentiation by reducing Notch transcriptional activity (Sun et al., 2007). Furthermore, BHLHE40 overexpression inhibited cell cycle progression and accumulation in the S-phase in MCF-7 cells via reducing Cyclin E interaction with the ubiquitin ligase, increasing its stability. Cyclin E needs to be degraded by ubiquitination in the G1/S phase to allow the transition S/G2 phase (Bi et al., 2015). However, BHLHE40 positively regulated large peritoneal macrophage proliferation through transcriptional activation of cell-cycle-related genes (Jarjour et al., 2019). Also, BHLHE40 promoted alveolar macrophage proliferation in addition to maintaining their identity (Rauschmeier et al., 2019). Taken together, BHLHE40 can either promote or inhibit differentiation and proliferation depending on the cellular context.

1.4 The Air-Liquid Interface (ALI) culture system as a model for studying cell proliferation and differentiation

Air Liquid Interface (ALI) is an *in vitro* differentiation model that mimics the human proximal airway epithelium and reproduces its cellular composition (Silva et al., 2023). The ALI culture can be established from primary human bronchiolar epithelial cells (pHBECs), which are cultured on a trans-well and differentiated over 21 days to give rise to a polarized pseudostratified airway epithelium. The cells in ALI culture are found in two phases: a proliferation phase from day 0 to 7, during which the cells form a confluent monolayer, followed by a differentiation phase from day 7 to 21, where differentiation increases progressively (Fig. 6A). Similar to the human proximal airway epithelium, our pHBECs-derived ALI culture is composed of basal progenitor cells $TP63^{+}$ that form the basal layer, along with differentiated epithelial cells that compose the luminal surface: mature ciliated cells $FOXJ1^{+}$ Acetylated $Tubulin^{+}$, club cells $CC10^{+,}$ and goblet cells $MUC5B^{+}$. The airway epithelial barrier was assessed by the expression of the tight junction protein Zonula occludens-1 (ZO-1) (Fig. 6B, C).

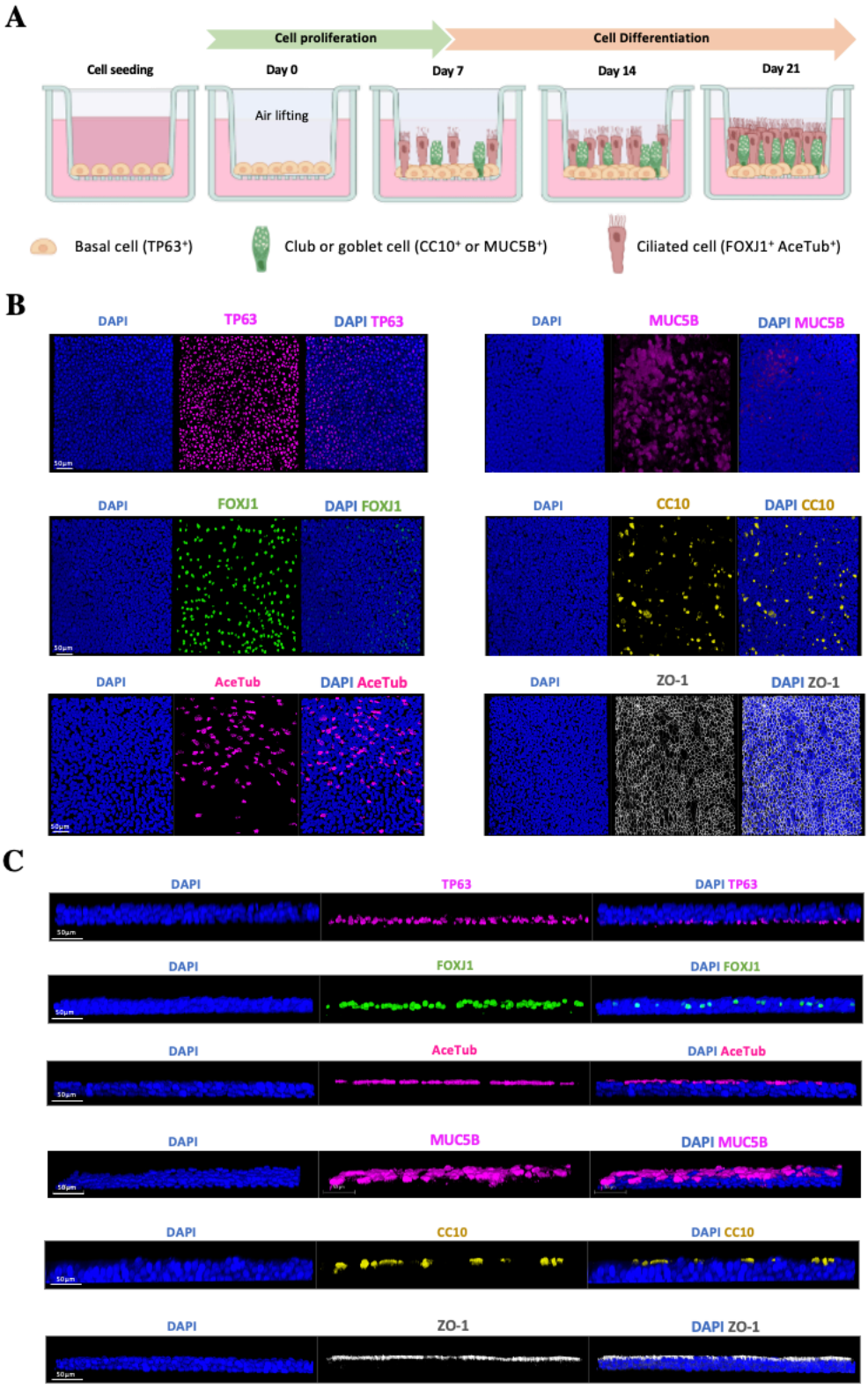

Figure 6. Mucociliary differentiation of human adult basal stem cells in Air Liquid Interface culture. **(A)** Schematic representation of the ALI culture proliferation and differentiation phase. Airway epithelial cells in ALI culture from day 21 were stained with the following specific antibodies for differentiation and polarization markers: **(B)** Anti-TP63 antibodies for basal cells, anti-FOXJ1 or Acetylated Tubulin antibodies for ciliated cells, anti-MUC5B or anti-CC10 antibodies for goblet and club cells, respectively, anti-Zonula occludens-1 (ZO-1) antibodies to assess the airway epithelial barrier. The images are 3D

reconstructions of the entire z-stack and **(C)** their corresponding optical sections. All nuclei were stained with DAPI.

1.5 Single-cell RNA sequencing analysis of pHBECs-derived ALI culture

1.5.1 BHLHE40 is selectively upregulated in differentiating epithelial cells

Airway basal cells are multipotent stem cell progenitors, which are crucial to maintaining the pseudostratified epithelium. They are able to self-renew and differentiate into the ciliated and secretory lineage, during homeostatic and repair conditions (Rock et al., 2011; Rock et al., 2009). Understanding the molecular mechanisms that regulate human basal cell differentiation is essential to unravel how normal and pathological regeneration occurs (Ruiz Garcia et al., 2019). Accordingly, to better understand the differentiation mechanisms of human airway basal progenitor cells, we performed single-cell RNA sequencing of pHBECs differentiated in the ALI culture (unpublished data). To include the proliferation and differentiation phases in our analysis, we performed single-cell RNA sequencing at different time points: days 0, 5, 9, and 14. We analyzed 5000 cells per time point and identified 14 epithelial cell clusters based on the expression of 5 known cell type-specific markers. Among the clusters identified are ionocyte-tuft, ciliated, basal (default, proliferative, transitioning, or SMG-like), and immature/mature secretory cells (Fig. 7A, B), recapitulating the composition of the human proximal airway epithelium.

We ordered the differentially expressed genes along a differentiation trajectory starting from the SMG-like basal cell-to-immature secretory-to-secretory cells and defined gene modules with a similar expression pattern (Fig. 7C, D). This pseudotime analysis of differentiating ALI cultures from different time points revealed a selective upregulation of the transcription factor *BHLHE40* in differentiating epithelial cells. These differentiating epithelial cells were characterized by the distinctive expression of immature secretory cell genes, highlighted in the box (Fig. 7D), which preceded the expression of mature secretory cell markers. This suggests a potential role of BHLHE40 in the differentiation toward secretory cells.

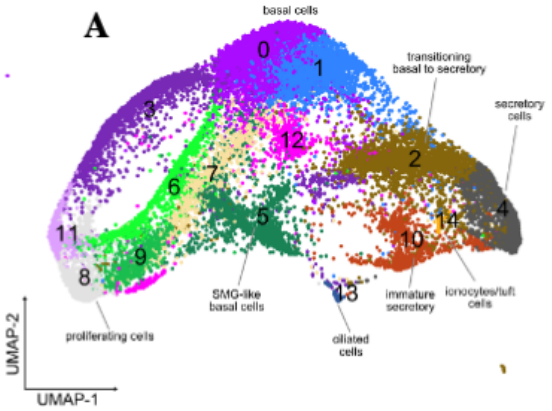
A
basal cells
transitioning basal to secretory
secretory cells
SMG-like basal cells
immature secretory
ionocytes/tuft cells
proliferating cells
ciliated cells
UMAP-2
UMAP-1

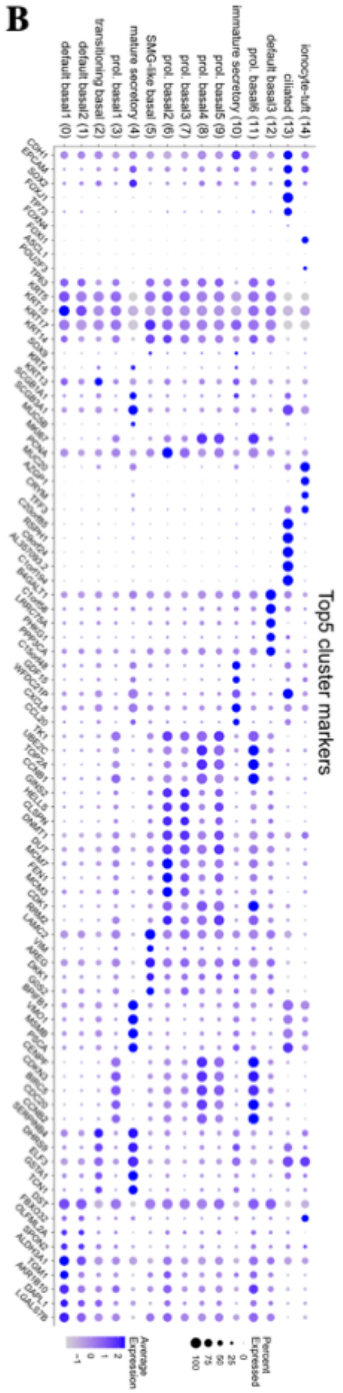
B
Top5 cluster markers
Average Expression
Percent Expressed

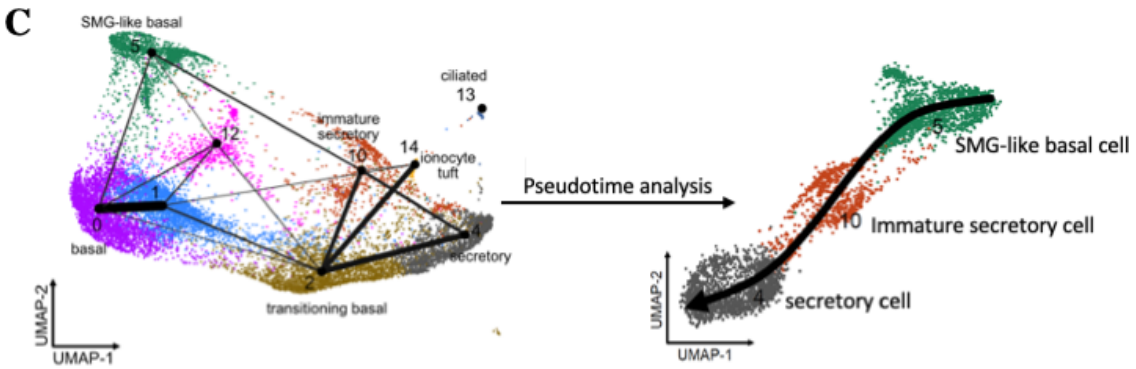
C
SMG-like basal
ciliated
immature secretory
ionocyte tuft
basal
secretory
transitioning basal
UMAP-2
UMAP-1
Pseudotime analysis
SMG-like basal cell
Immature secretory cell
secretory cell

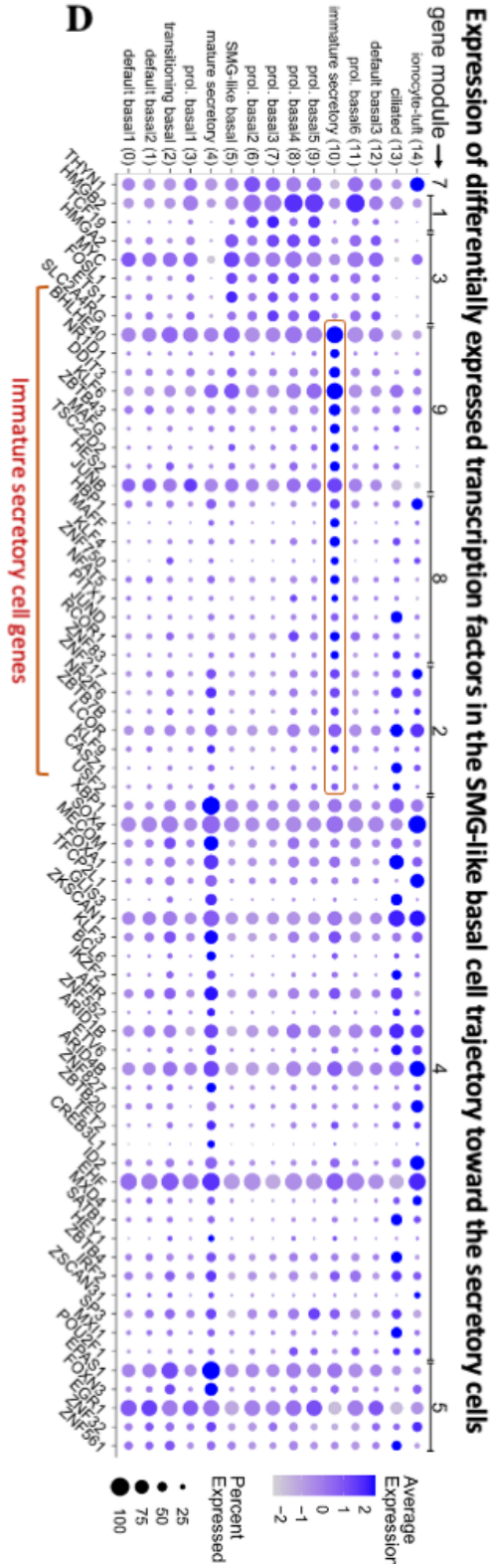
D
Expression of differentially expressed transcription factors in the SMG-like basal cell trajectory toward the secretory cells
gene module
Immature secretory cell genes
Percent Expressed
Average Expression

Figure 7. Single-cell RNA sequencing from human pHBECs-derived ALI cultures revealed a selective upregulation of the transcription factor *BHLHE40* in differentiating epithelial cells. (A) UMAP plot showing the epithelial cell-specific clusters identified by single-cell RNA sequencing of human primary bronchial epithelial cells differentiated in an air-liquid-interface (ALI) culture at different time points: day 0, 5, 9, and 14 (all clusters combined). **(B)** Dot plot showing the top 5 specific markers per cluster. **(C)** PAGA plot of non-proliferating cells showing two distinct differentiation trajectories (conventional differentiation and SMG-like basal cell trajectory) towards secretory cells. **(D)** Transcription factor trajectory interference analysis from clusters 5, 10, and 4 (shown in (C)): the differentially expressed transcription factors were plotted along the SMG-like basal cell trajectory toward the secretory cells. The dot plot shows a selective upregulation of the transcription factor *BHLHE40* in the differentiating immature secretory cells cluster (single-cell RNA sequencing data and figures were kindly provided by Janine Koepke and Alexandros Sountoulidis).

1.5.2 High expression of *BHLHE40* correlated with upregulation of Notch genes

Since Notch is a key signaling in airway epithelial cell differentiation (Rock et al., 2011), we further investigated the potential role of BHLHE40 in the differentiation process by correlating its expression with epithelial cell-specific markers and Notch signaling genes, using differential gene expression analysis in each cluster against all others per individual timepoints of the ALI culture. Since *BHLHE40* was ubiquitously expressed in all clusters (Fig. 8A, B, C, D), we focused our attention on the cluster showing the highest *BHLHE40* expression, namely ''the *BHLHE40*-high cluster'', to establish a distinct correlation that could be extrapolated to a potential unique function.

Interestingly, in the pre-secretory cell cluster from day 0 (Fig. 8A), the *BHLHE40*-high cluster showed a distinct correlation with high expression of Notch signaling genes: *NOTCH2*, *NOTCH3*, *HES1*, *HES2*, and *NRARP,* but not the ligands *DLL1*, *JAG1*, or *JAG2*. To a lesser extent, the *BHLHE40*-high cluster distinctly correlated with *NOTCH1* gene expression. According to gene expression, this cluster is composed of undifferentiated cells that distinctly express very low levels of *TP63* transcripts compared to the other clusters, with no differentiation markers present yet. Later on day 5, in the pre-secretory cell cluster (Fig. 8B), the same correlation was observed but with an additional selective high expression of the secretory cell markers *SCGB1A1* and *SCGB3A1* and Notch downstream effector *HEY1*.

On day 9 (Fig. 8C), in the secretory cell cluster, *BHLHE40*-high expression remains strongly correlated with high expression of *SCGB1A1*, *HES1*, *HES2*, and *NRARP* genes. However, no distinct correlations were observed with *SCGB1A1*, Notch receptors, or ligands when compared to the other clusters. On day 14, in the secretory cell cluster (Fig. 8D), the

BHLHE40-high cluster was only correlated with high expression of *SCGB1A1*, *HES1*, and *NRARP* genes.

Taken together, these data reveal a correlation between the *BHLHE40*-high cluster and high expression of Notch signaling genes (*NOTCH2*, *NOTCH3*, *HES1*, and *HES2*) on days 0 and 5 of the ALI culture. However, at later time points, the correlation with high expression of Notch receptors was no longer observed, while a correlation with high expression of *HES1* and *SCGB1A1* emerged.

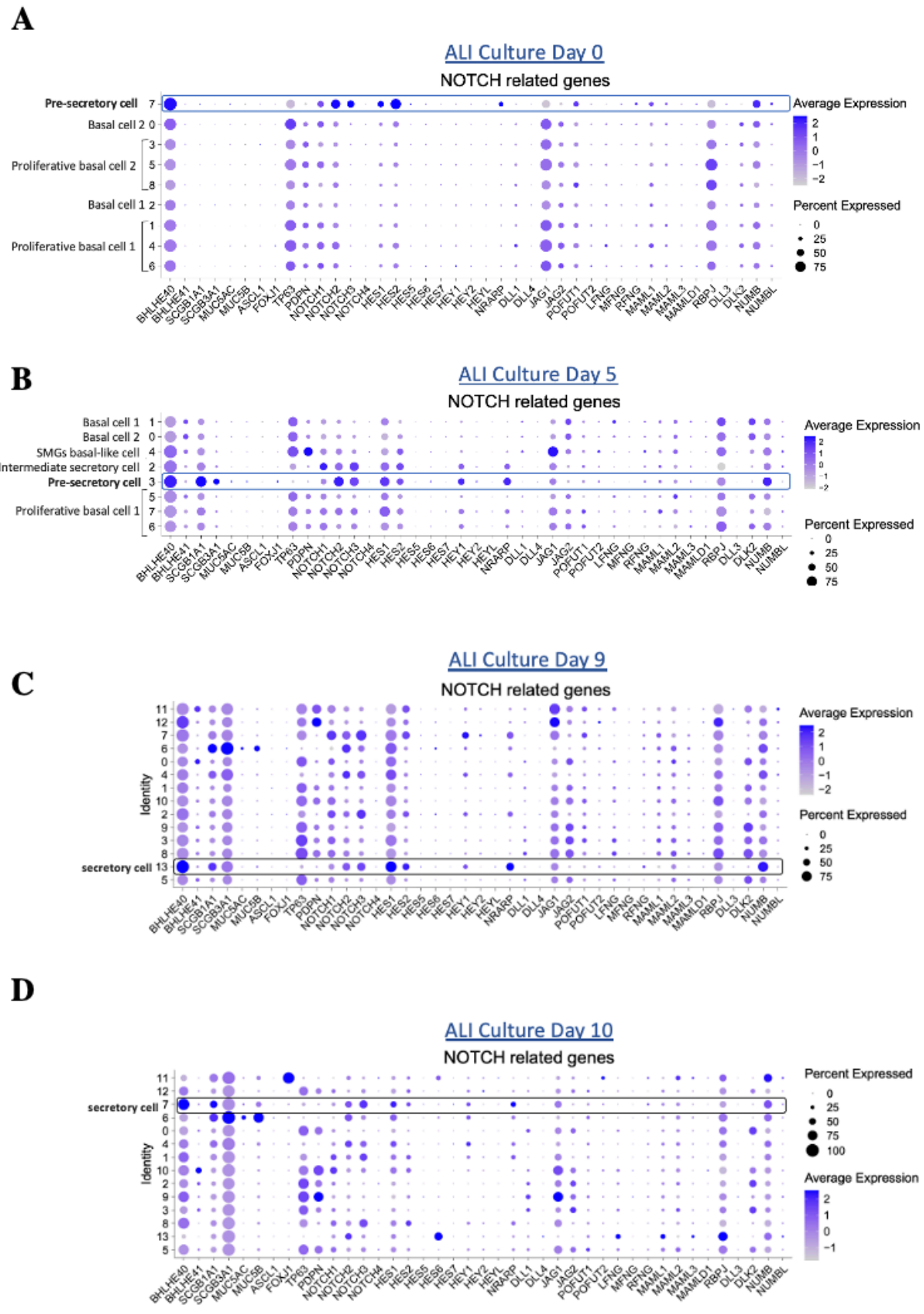

(Janine Koepke and Alexandros Sountoulidis)

.

Figure 8. BHLHE40 selective upregulation correlated with increased Notch signaling gene expression. Dot plots showing the correlation between *BHLHE40* expression, Notch-related genes, and epithelial cell-specific markers in the different clusters identified by single-cell RNA sequencing at individual timepoints of culture: **(A)** day 0, **(B)** day 5, **(C)** day 9, and **(D)** day 14 (Single-cell RNA sequencing data and figures were kindly provided by Janine Koepke and Alexandros Sountoulidis).

1.6 Hypothesis and aim

Previous studies have shown that the transcription factor BHLHE40 can either promote or inhibit cell differentiation depending on the cellular context (Boudjelal et al., 1997; Iwata et al., 2006; Shen et al., 2002; Wang et al., 2015). Based on our single-cell RNA sequencing and pseudotime analysis of differentiating pHBECs in ALI cultures, we found that *BHLHE40* expression was selectively upregulated in differentiating cells and interestingly correlated with the upregulation of Notch signaling genes. Given that Notch is a key signaling pathway in airway epithelial cell differentiation and its activation in basal cells promotes their luminal differentiation (Rock et al., 2011), we hypothesize that BHLHE40 may play a role in human airway basal cell differentiation through a Notch-dependent manner. Therefore, the aim of this study is to:

1. Characterize the molecular role of BHLHE40 in the differentiation of human airway basal cells, using pHBECs-derived ALI culture in combination with lentiviral-based gene transfer to overexpress and knockdown BHLHE40.

2. Investigate whether the function of BHLHE40 is linked to the Notch signaling pathway.

3. Identify potential transcriptional targets of BHLHE40 involved in the differentiation mechanism of human airway basal cells.

2 Materials

2.1 Chemicals and reagents

Table 1. Transfection reagents

Product	Company/Catalogue number
Calcium chloride	Merck, 1002440500
Lipofectamine 2000	Invitrogen, 11668019
DNase free water	Invitrogen, 10977-035

Table 2. Cell culture products

Product	Company/Catalogue number
Collagen Type I	SIGMA, C9791
PBS 1X	Capricorn, PBS-1A
Trans-well plate (0.4μm pore)	Corning, 3460

Table 3. Western blot product

Product	Company/ Catalogue number
Acrylamide/Bis Solution	Carl Roth, 3029.2
TEMED	Carl Roth, 2367.3
Pierce ECL western blotting substrate	ThermoFischer, 32106
SuperSignal West pico PLUS Chemiluminescent substrate	ThermoFischer, 34580
PageRuler pre-stained protein ladder	ThermoFischer, 26616
Nitrocellulose blotting membrane	GE Healthcare, 10600002
Extra Thick blot paper	BioRad, 1703966
Glass plates-Spacer plates (1mm spacers)	BioRad, 1653311
Glass plates-short plates	BioRad, 1653308
Milk pouder	Carl Roth, T145.2
Tween 20	Sigma, P7949

Table 4. Others

Product	Company/ Catalogue number
Triton X-100	Merck, 1086031000
Hoechst 33342	Sigma, B2261
Fluoromount	Serva, 21634.01
Doxycycline hyclate	Sigma, D9891
TRIzol reagent	ThermoFischer, 15596018
GlycoBlue Coprecipitant	ThermoFischer, AM9515
Agarose	Carl Roth, 2267.4
SYBR Safe DNA Gel Stain	Invitrogen, S33102
1kb DNA ladder	Promega, G5711
Blue/Orange Loading Dye (6X)	Promega, G1881
Filtropur (0.22µm)	Sarstedt, 831.823.001

Table 5. FACS product

Product	Company/ Catalogue number
BSA	Sigma, A3059
HBSS	Sigma, H6648
Sterile wide orifice pipet tips (1000µl)	VWR, 89049-168
5ml polystyrene tube with cell-strainer cap	Corning, 352235

2.2 Buffers

- Buffers for DNA preparations

P1 buffer:

Tris -50mM

EDTA -10mM

RNase -0.4mg/ml

pH 8, stored at 4°C

P2 buffer:

NaOH -0.2M

SDS -1%

Stored at room temperature

P3 buffer:

Potassium Acetate -3M

pH 5.5, stored at room temperature

All buffers were dissolved in distilled water

- Buffers for Agarose gel electrophoresis

10XTAE Buffer

Tris-acetate -400mM

EDTA -10mM

Dissolved in distilled water

- Buffers for SDS-Polyacrylamide gel (SDS-PAGE)

Stock buffer for separating gel

Tris-HCl -1M, pH 8.8

Stock buffer for stacking gel

Tris-HCl -0.5M, pH 6.8

- Buffers for western blot

Radioimmunoprecipitation assay buffer (RIPA) buffer (100ml)

NaCl (5M) -12ml

Tris pH 7.4 (2M) -10ml

EDTA pH 8 (0.5 M) -4ml

SDS (20%) -2ml

Na-DOC (10%) -20ml

Triton X-100 -4ml

Dissolved in distilled water and protease inhibitor cocktail was added to 50 ml of RIPA buffer

4X Laemmli Buffer (10ml)

Tris -2ml of 1M, pH 6.8

SDS -0.8g

EDTA -1ml of 0.5M

H_2O -6ml

100% Glycerol -4ml

ß-Mercaptoethanol -0.4ml of 14.7M

Bromophenolblue -8mg

Running buffer

10XTris-glycine (1000ml)

Tris -30.27g

Glycine -144.0g

For the 1X running buffer, 5ml of 20% SDS was added (for 1000ml)

All buffers were dissolved in distilled water

10X transfer buffer(1000ml)

Tris-base -30.27g

Glycine. -144g

No methanol

pH 8.5

All buffers were dissolved in distilled water

1X transfer buffer (1000ml)

10X Transfer buffer -100ml

Methanol -200ml

ddH2o -700ml

Ponceau

Ponceau S - 0.1% (X/V)

Acetic acid - 1.0%

Dissolved in distilled water

1XPBS Tween

PBS -1X

Tween -0.1%

Blocking buffer

Milk powder -6%

Dissolved in 0.1%PBS tween and stored at 4°C

- Buffer for FACS

Washing and resuspension buffer

HBSS -1X

BSA -1%

- Buffers for HEK293T cells transfection

2X BBS buffer

BES -50.0mM

NaCl -280.0mM

Na_2HPO_4 -1.5mM

Dissolved in 500 ml of distilled water and pH 7.0 was adjusted followed by sterilization using a 0.22μM filter

2M CaCl2

2M $CaCl_2$ was dissolved in 500ml distilled water and sterilized using 0.22μM filter

- Buffers for immunofluorescence

10X PBS: Glycine (500ml):

NaCl -38.00g

Na_2HPO_4 -9.38g

NaH_2PO_4 -2.07g

Glycine -37.50g

Diluted in distilled water

pH 7.4 and filter sterilized

10X IF-wash (500ml):

NaCl -38.00g

Na2HPO4 -9.38g

NaH2PO4 -2.07g

NaN3 -2.5g

BSA (Fraction V) -5.0g

Triton X-100 -10.00 ml

Tween-20 -2.5ml

Diluted in distilled water

pH 7.4 and filter sterilize

Permeabilization buffer:

Triton X-100 -0.5%

Diluted in PBS

Blocking buffer

IF wash buffer -1X

FCS -10%

Diluted in distilled water

- Collagen solution

Collagen Type I (SIGMA, C9791)

Stock solution: 10mg of collagen was re-suspended in 10ml Acetic acid (0,1M)

- Buffers for competent cells

RF1 solution (stored at 4°C, pH 5,8)

	100 ml	1000 ml
100mM RbCl	1,2g	12,0g
50 mM $MnCl_2$x $4H_2O$	0,99g	9,9g
30mM Calcium acetate	3ml	30ml
10mM $CaCl_2$ x$2H_2O$	0,15g	1,5g
15% Glycerol	15,0g	150,0g

pH was adjusted to 5.8 then filter-sterilized

RF2 solution (stored at 4°C, pH 5.8)

	100 ml	1000 ml
10mM MOPS	2ml	20ml
10mM RbCl	0,12g	1,2g

75mM $CaCl_2$ x2H_2O	1,1g	11g
15% Glycerol	15,0g	150,0g

pH was adjusted to 5.8 then filter sterilized

2.3 Media

- HEK293T cell culture media

DMEM(1X) (500.0ml)
(Gibco, 10938-025)

- Sodium Pyruvate 100mM (100X) -5.0ml
  (Gibco, 11360-039)
- L-Glutamine 200mM (100X) -5.0ml
  (Gibco, 25030-024)
- Heat inactivated FBS (10%) -50.0ml
  (Gibco, 10270-106)
- Penicillin-streptomycin (100X) -5.0ml
  (Capricorn, PS-B)

- Primary bronchiolar epithelial cell culture media

Airway Epithelial Cell Growth Medium (500.0ml)
(PromoCell, C-21060)

- Penicillin-streptomycin (100X) -5.0ml
  (Capricorn, PS-B)

DMEM High glucose (500ml)
(Sigma, D5796)

- Penicillin-streptomycin (100X) -5.0ml
  (Capricorn, PS-B)

Differentiation Medium

- 50% Airway Epithelial Cell Growth Medium
- 50% DMEM High glucose

- 0.05% Retinoic acid (5mg/ml stock solution): 0,5μl in 50ml medium with 50ng/ml final concentration

2.4 Enzymes

- Restriction enzymes and Antarctic phosphatase (New England BioLabs)
- Accutase (Capricorn, ACC-1B)
- Trypsin-EDTA-0.05% (Capricorn, TRY-1B)
- Trypsin-EDTA-0.25% (Gibco, 25200-056)
- AccuPrime Pfx polymerase was obtained from (Invitrogen: 12344-024)
- T4 DNA Ligase (New England BioLabs, M0202S)
- DNase I- 1000 U (Thermofisher, EN0525)
- Protease from Streptomyces griseus (Sigma, P5147)
- RNase A (740505, Takarabio)

2.5 Kits

- RNeasy Mini Kit (Qiagen, 74106)
- QIAshredder (Qiagen, 79656)
- iScript cDNA Synthesis Kit (BIO-RAD, 1708890)
- iTaq Universal SYBR Green Supermix (BIO-RAD, 1725121)
- QIAamp Viral RNA Mini Kit (Qiagen, 52904)
- Lenti-X qRT-PCR Titration Kit (Takara, 631235)
- QIAGEN Plasmid Maxi Kit (Qiagen, 12163)
- QIAGEN Plasmid Midi Kit (25) (Qiagen, 12143)
- QIAquick PCR purification kit (Qiagen, 28104)
- QIAquick Gel Extraction Kit (Qiagen, 28704)
- Click-iT Plus EdU Cell Proliferation, Alexa Fluor 647 (Thermofisher, C10640)
- Click-iT Plus TUNEL Assay, Alexa Fluor 647 (Thermofisher, C10619)
- CUT&RUN Assay Kit (Cell signaling, 86652)
- Minute™ Detergent-Free Single Nuclei Isolation Kit (Invent Biotech, NI-024)
- NEBNext® Ultra™ II DNA Library Prep kit (NEB, E7645S)

- NEBNext Multiplex Oligos (NEB, E7710S)
- Agilent High Sensitivity DNA Chip (Agilent, 5067-4626)
- Agilent RNA 6000 Pico Kit (Agilent, 5067-1513)
- Agilent RNA 6000 Nano Kit (Agilent, 5067-1511)

2.6 Antibodies

Table 6. List of antibodies

Primary antibody	Source	Company & catalogue number	Dilution	Application
GFP	Chicken polyclonal	Abcam, ab13970	1:1000	IF, WB
BHLHE40	Rabbit polyclonal	Sigma, HPA028922	1:200	IF
Turbo GFP	Mouse monoclonal	Origene, TA150041	1:500	IF
Turbo GFP	Rabbit polyclonal	ThermoFisher, PA5-22688	1:500	IF
FLAG	Rabbit monoclonal	Cell signalling, 14793S	1:500	IF, WB
CC10	Mouse monoclonal	Santa Cruz, sc-365992	1:500	IF, WB
SCGB3A1	Goat polyclonal	R&D Systems, AF2954	1:100	IF
MUC5B	Rabbit polyclonal	Novus Biologicals, NBP1-92151	1:500	IF
RFX3	Rabbit polyclonal	Sigma, HPA035689	1:500	IF
FOXJ1	Mouse monoclonal	eBioscience, 14-9965-82	1:400	IF
Acetylated Tubulin	Mouse monoclonal	Sigma, T7451	1:1000	IF
TP63	Mouse monoclonal	Abcam, ab735	1:500	IF
NGFR	Goat polyclonal	Santa Cruz, sc-6188	1:500	IF
NME5	Rabbit polyclonal	Sigma, HPA044555	1:500	IF
RSPH1	Rabbit polyclonal	Sigma, HPA017382	1:500	IF
ZO-1	Rabbit		1:500	IF
BNC1	Rabbit polyclonal	Novus Biologicals, NBP2-55855	1:500	IF
IgG Isotype control	Rabbit	ThermoFischer, 02-6102	1:500	CUT&RUN

2.7 Antibiotics

Different antibiotics were dissolved as mentioned below (1000x stocks)

Ampicillin 50mg/ml in distilled water

Chloramphenicol 30mg/ml in ethanol

Doxycycline 50mg/ml in distilled water

Puromycin 50mg/ml in distilled water

Antibiotics were sterilized using 0.22μm filters and stored at -20 °C

2.8 Plasmid

Table 7. List of lentiviral plasmids

Name	**Backbone vector**	**Company**
BHLHE40-GFP (lentiviral plasmid)	pWPXL	cloned
BHLHE40-FLAG (lentiviral plasmid)	pTRIPZ	cloned
BHLHE40 shRNA (lentiviral plasmid)	pGFP-C-shLenti	Origene
Lentiviral supporting plasmid 1	pSPAX	Obtained from Prof. Stefan Offermanns (Max Plank Institute for heart and kung research)
Lentiviral supporting plasmid 2	pMD2.G	Obtained from Prof. Stefan Offermanns (Max Plank Institute for Heart and Lung research)

2.9 Primers

Table 8. List of cloning primers

Name	**Forward**	**Reverse**
BHLHE40-GFP	GGTGGTGTTTAAACATGGAGC GGATCCCCAGC	GGTGGTACGCGTAAGTCTT TGGTTTCTAAGTTTAA
BHLHE40-FLAG	GGTGGTACCGGTATGGAG CGGATCCCCAGC	GGTGGTACGCGTAAGTCTT TGGTTTCTAAGTTTAA

Table 9. List of Real-time qPCR Primers

Gene name	**Forward primer**	**Reverse primer**
BHLHE40	CACCTTCAGCGACTGCCTAC	CTGGCACTGAGGTGGGATAC
eGFP	GAAGCGCGATCACATGGT	CCATGCCGAGAGTGATCC

NOTCH1	CGGGGCTAACAAAGATATGC	CACCTTGGCGGTCTCGTA
NOTCH2	TGGTGGCAGAACTGATCAAC	CTGCCCAGTGAAGAGCAGAT
NOTCH3	TGCAGCGTGACCGAGATA	CACCCATTATAAATAAAGGAAGACTGA
JAG1	GAATGGCAACAAAACTTGCAT	AGCCTTGTCGGCAAATAGC
JAG2	GAGCTCTGCGACACCAATC	TCATTGACCAGGTCGTAGCA
DLL1	CTGCAGGAGTTCGTCAACAA	CACACGCGGAAGAAGGTC
HES1	TTACGGCGGACTCCATGT	AGAGGTGGGTTGGGGAGT
HEY1	GATGATCAGCTTTATCCAAGAAAGA	CAGTTTGTACATTCACCTTTCTGC
HES6	TGGGCTAAACAAAAGCTTGAA	AAGATGTACAGAGCATCACAGCTC
RPLP0	CCAGCAGGTGTTCGACAAT	CAGGAAGCGAGAATGCAGA
FOXJ1	CAGCTGCCATCAGATTCAAG	GAGGAGGCAGCGATTCTG
MYB	CCGGGAAGAGGATGAAAAAC	TTTCCAGTCATCTGTTCCATTC
TP73	CCACTGGTGGACTCCTATCG	CTGTAGGTGACTCGGCCTCT
RFX3	TCCATCACCCACCAACAAC	AAATGCCAGAATGACCAAGTG
TP63	GAAGATCAAAGAGTCCCTGGAA	GCTGTTGCCTGTACGTTTCA
SCGB1A1	CTCACCCTGGTCACACTGG	CTGAAAGCTCGGGCAGAT
SCGB3A1	CGGGTATAAGAAGCCTCGTG	GCCCACTAAGAAAGCAGCAG
FOS	GGTGCATTACAGAGAGGAGAAA	GTGTGTTTCACGCACAGATAAG
MYC	AAGCTGAGGCACACAAAGA	GCTTGGACAGGTTAGGAGTAAA
HMGA2	GTGGGAGGAGCGAAATCTAAA	AAAGAGAGAGGGAGAGGAAGAG
BNC1	CATGGTGTTCAGCTCCCTAAG	GAGGTCTTTGTCCCGGTTATTT
ZFP36L1	ACT GCA CCT TCC CTC ATT TC	TGGTCTGGCAACAACTCTTC
FOSL1	GACAGTATCCCACATCCAACTC	GGCCAGCTCAAGAGAAACA
SOX9	AACGCCTTCATGGTGTGG	GTTGTGCAAGTGCGGGTA

2.10 Cells

Table 10. List of human cells

Cell Name	Company/institute
Primary human bronchiolar epithelial cells: pHBECs	Isolated in our lab from human bronchus as described in part 3.4
Human embryonic kidney 293T cells: HEK293T	ATCC stock
Human adenocarcinomic alveolar epithelial cells: A549	ATCC stock

2.11 Bacterial strain and growth medium

Bacterial strain

E. *coli* top 10 competent cells were prepared as described in method part 3.16.

Liquid and solid growth medium

-25g of LB (Luria-Bertani) powder was dissolved in 1L of distilled water and autoclaved.

-12g of agar powder was dissolved in 1L of LB medium and autoclaved. After cooling down to 50°C, the respective antibiotic was added, and the mixture was plated in sterile Petri dishes. Once the agar was solidified, the dishes were sealed and stored at 4°C for later use.

3 Methods

3.1 Cloning

3.1.1 Isolation of the DNA of interest

A. Amplification with Polymerase chain reaction (PCR)

The target double-stranded DNA sequence(s) were amplified by PCR using specific primers with appropriate restriction sites. The reaction mixture was prepared as follows:

Template DNA	-100ng
Forward primer	-2µl (10µM)
Reverse primer	-2µl (10µM)
AccuPrime reaction buffer	-5µl
AccuPrime Pfx polymerase	-1µl
Sterile distilled water	-up to 50µl

PCR Program:

- Initial Denaturation
  - 95°C - 2 minutes

25 cycles of:

- Denaturation
  - 95°C - 15 seconds
- Annealing
  - 58°C - 30 seconds
- Extension
  - 68°C -1 minute per kb
  - 4°C - forever

B. Agarose gel electrophoresis

To visualize the amplified PCR product and assess its specificity, 5µl of the amplified DNA was loaded in an agarose gel. Depending on the size of the amplicon, gels of 0.8-2% were prepared by melting agarose powder in 1xTAE buffer. After adding SYBR Safe DNA Gel Stain (Invitrogen), the gel solution was poured into the chamber and allowed to polymerize. After that, the PCR-amplified DNA product was mixed with the DNA loading dye and loaded into the gel followed by electrophoresis for 40 min at 80-100 volts. DNA was then visualized and imaged under UV light using Gel Doc XR+ (BIO-RAD).

C. Restriction digestion of the amplified DNA

The amplified DNA of interest as well as the plasmid was digested using the appropriate restriction enzymes, with the appropriate buffer. To ensure efficient digestion, buffer compatibility with each endonuclease was checked using the online tool: New England BioLabs double digest finder https://nebcloner.neb.com/#!/redigest.

The reaction mix is prepared as follows:

DNA (amplified insert or Plasmid):	- 10µg
Respective buffer (1X)	- 10µl
Respective enzyme 1	- 5µl
Respective enzyme 2	- 5µl
Sterile distilled water	- up to 100µl

For the amplified insert, the remaining 45µl was used for this digestion step.

The mixture was then incubated at 37°C for 3 hours or at the optimum temperature/time suggested by the company instructions (NEB). In the case of enzymes that generate compatible ends, digested plasmids were treated with Antarctic phosphatase enzyme, to reduce the chance of vector re-ligation. The following mixture was added to the plasmid digestion mix and incubated for 30min at 37°C.

Antarctic phosphatase Buffer (1X)	-12µl
Antarctic phosphatase enzyme	-5µl
Sterile distilled water	-3µl

The digested PCR product was cleaned up using QIAquick (Qiagen).
The digested plasmid was loaded on an agarose gel (V_f=120µl) and the band corresponding to the digested plasmid was cut out and gel purified using QIAquick Gel Extraction Kit (Qiagen).

3.1.2 Ligation

After digestion and purification of the PCR product and the vector, the ligation reaction was done as follows:

Vector: PCR product	-1:5 molar ratio
Ligase buffer (1x)	-1µl
T4 DNA Ligase	-1µl
Sterile distilled water	-up to 10µl

The ligation mixture was incubated overnight at 16°C. Negative control for plasmid re-ligation was used for this step, which included the digested plasmid alone without the insert.
The amount of insert used for 100ng vector was calculated using the online tool ''*in silico* uni-duesseldorf'', which calculates the amount of insert to add based on the vector and insert size.

3.1.3 Transformation of the ligated plasmid into competent TOP 10 E. *coli* cells

5-10µl of ligation mixture was added to100μl of competent cells and incubated on ice for 10 minutes. The mixture was then heat pulsed as described previously in method part 3.2. 500μl of LB medium without antibiotic was added to the mixture, which was then incubated at 37°C for 1-2h at 800rpm. A negative control to check for uncut plasmid contamination in the

digested plasmid involved transforming the digested, non-ligated plasmid into the competent cells. After that, the transformed bacteria were spread on LB-agar plates containing the selective antibiotic, and were grown overnight at 37°C. The next day, single-positive clones were picked up, inoculated into 5ml of LB medium with selective antibiotic, and grown overnight at 37°C with shaking at 250 rpm.

3.1.4 Isolation of the plasmid

5 ml of the bacterial culture grown overnight were centrifuged at 4000 rpm for 10 minutes at room temperature. The supernatant was discarded and the pellet was re-suspended in 250µl of P1 buffer to degrade the bacterial RNA. The mixture was then transferred to 1.5ml Eppendorf followed by the addition of 250µl of P2 solution to lysate the bacterial membrane. The tubes were inverted upside down 5 times and incubated for 5 minutes. 500µl of P3 in order buffer was added to the suspension and the tubes were inverted upside down 5 times followed by centrifugation at 14000 rpm for 10 minutes at 4°C. The supernatant was collected in a fresh 1.5ml Eppendorf followed by mixing with 500µl of Isopropanol and centrifugation at 14000rpm for 30 minutes at 4°C. The supernatant was discarded and the pellet was washed once with 70 % ethanol and dried for 5-10 minutes at 55°C. 50µl of sterile distilled water was added to dissolve the plasmid DNA (P1, P2, and P3 buffer compositions are described in Material 2.2).

3.1.5 Restriction digestion analysis and validation of the positive clones

Restriction digestion was performed using the appropriate restriction enzyme(s) to confirm that the ligation of the insert into the plasmid was successful. Two bands should be seen: one corresponding to the digested plasmid and the other one to the insert DNA (Fig. 9).

Purified Plasmid	-10µl
Respective buffer (1X)	-2µl
Enzyme 1	-1µl
Enzyme 2	-1µl
Sterile distilled water	-16µl

The digested plasmids were run on an agarose gel as previously described in methods part 3.1.1.B. True positive clones were then sent for sequencing (Microsynth Seqlab) to confirm

the presence of the target DNA sequence, and the correct reading frame (in case of fusion to a tag).

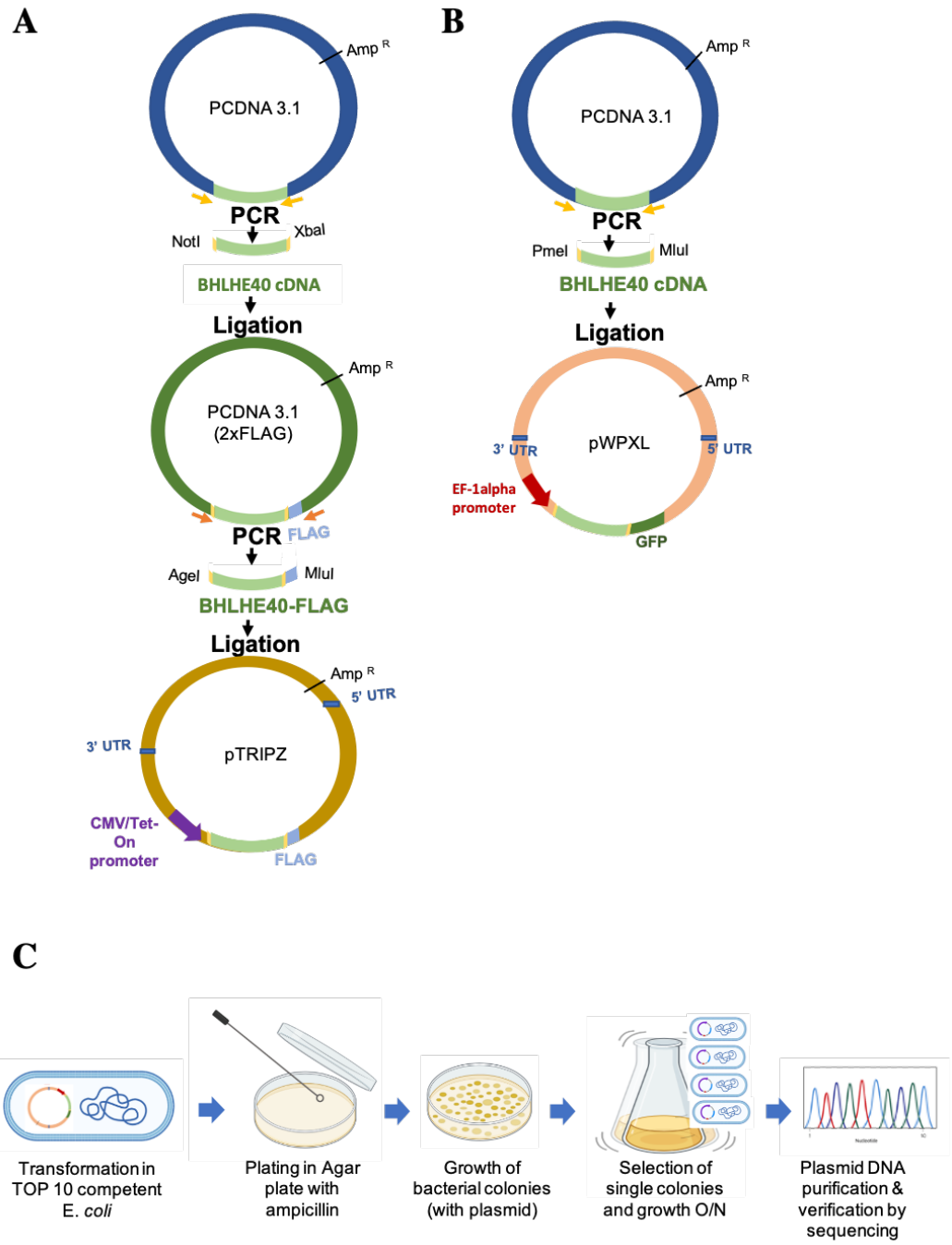

Figure 9. Representation of BHLHE40 cloning strategy into pTRIPZ and pWPXL lentiviral plasmids. (A) BHLHE40 cDNA was amplified with PCR using primers containing the indicated restriction sites, then ligated into PCDNA 3.1 upstream of the C-terminal double FLAG tag. BHLHE40-Flag was then amplified with PCR and cloned into the lentiviral plasmid pTRIPZ. **(B)** BHLHE40 cDNA was amplified with PCR using primers with the indicated restriction sites then ligated into the lentiviral vector pWPXL upstream of the C-terminal GFP tag **(C)** The cloned lentiviral plasmids were then transformed into TOP10 E. *coli* grown in Agar plate and LB medium with Ampicillin, then purified and sequenced.

3.2 Transformation of plasmid DNA into competent Top 10 E. *coli* cells (retransformation) and storage in glycerol stock

An aliquot of competent E. *coli* TOP10 was thawed on ice. 100ng of plasmid was mixed with 100μl of competent cells and incubated on ice for 10 minutes. Then, the mixture was heat-pulsed at 42°C for 1 minute 30 seconds and immediately returned to the ice for 2 minutes. 500μl of LB medium without antibiotic was added and the mixture was incubated at 37°C for 1-2h at 800rpm. The mixture was then transferred to a sterile 500ml flask containing 25ml LB medium with the selective antibiotic. Transformed competent cells were grown overnight at 37°C with shaking at 250 rpm. The next day, 500µl of the overnight culture was mixed with 500µl of sterile 50% glycerol in a cryotube, mixed gently, and frozen at -80°C for later use. For the remaining culture, DNA preps were performed using Plasmid Midi Kit (Qiagen) according to the Manufacturer's instructions.

3.3 Cell culture

Mammalian cell culture

HEK293T cells were cultured in the DMEM(1X) medium described in Materials part 2.3., and incubated at 37°C with 5% CO_2. Confluent cells were washed once with 1X PBS and treated with 2ml of 0.25% Trypsin-EDTA solution for 2-5 minutes at room temperature until complete dissociation of the cells. Then, 8ml of the DMEM(1X) medium was added and cells were split according to the needs of the experiment (e.g., one confluent 10cm dish can be split into three 10cm dishes and used for transfection the following day).

Primary human bronchiolar epithelial cell culture

Primary cells were cultured in the airway growth medium described in Materials part 2.3., and incubated at 37°C with 5% CO_2. Confluent cells were washed once with 1X PBS and treated with 5ml of 0.05% Trypsin-EDTA solution for 5-7 minutes at 37°C until complete dissociation of the cells. Then, 10ml FCS was added to inactivate the enzyme and the mix was transferred to a 50ml falcon tube to be centrifuged at 1500 rpm for 10 minutes. Finally, the supernatant was removed, the cell pellet was re-suspended in 1ml of the airway growth medium, and seeded in T-75 flasks or trans-wells for ALI culture.

Collagen treatment of the ALI trans-wells (12-well plate)

The collagen stock solution (described in Material part 2.2) was diluted 1:10 with distilled water and 500µl of the diluted collagen was added per trans-well, followed by overnight

incubation at 37°C (alternatively, incubating for 1 hour at 37°C was also successful). The following day, the collagen was removed and the plates were UV-treated for 1h before cell seeding.

3.4 Isolation of primary human bronchiolar epithelial cells from a human bronchus

- Preparation of the bronchus

The fresh bronchus was opened and then cut into small pieces (≤ 2 cm) with a sterile scalpel, after which the remaining lung tissue was carefully removed. The bronchus pieces were then placed into a Petri dish with the epithelial side facing down and rinsed thoroughly with 1XPBS.

- Treatment with Dithiothreitol (DTT)

DMEM was prepared with 1% P/S, Amphotericin B (2.5µg/ml), and DTT (0.5mg/ml).
The bronchus pieces were covered with this media in the petri dish and incubated overnight at 4° C. The bronchus pieces were then washed twice with 1XPBS.

- Treatment with protease

DMEM was prepared with 1% P/S, Amphotericin B (2.5µg/ml), and Protease 14 from *Streptomyces griseus* (1mg/ml). The bronchus pieces were then covered with this media and incubated overnight at 4°C.

- Cell isolation from the bronchus pieces, culture, cryopreservation, and seeding in trans-wells

<u>Cell isolation, culture, and cryopreservation</u>

The bronchus pieces were washed twice with 1XPBS and fixed by a pair of tweezers. The epithelial cells were then carefully scraped using a scalpel, collected in 50mlPBS, and centrifuged at 1600rpm for 10 minutes at room temperature. After that, the supernatant was discarded and the cell pellet was re-suspended in 15ml of the airway epithelial medium with Antimycotics (Amphotericin B 2.5µg/ml), then seeded in a T75 flask until confluence was reached. Finally, the cells were frozen in 20% FCS, 10% DMSO, and 70% airway medium (cryotubes) in liquid nitrogen for later use. The steps for primary cell dissociation and cleanup from the trypsin and FCS were previously described in part 3.3.

Cell seeding in Air-liquid trans-wells and differentiation

Once the cells reached 80% confluency, the media was removed and replaced by 5ml of 0.05% trypsin-EDTA, followed by incubation for 5 minutes at 37°C. When the cells were de-attached, 10ml of FCS was added to inactivate the enzyme, then the mix was transferred to a 50ml falcon tube and centrifuged at 1500rpm for 10 minutes. Finally, the supernatant was removed, cell pellet was re-suspended in 1ml of the airway growth medium. To seed the cells, trans-wells were equilibrated with airway medium (1ml on the bottom, 250µl on the top) and incubated at 37°C for 30 minutes. Then, 200.000 cells were seeded in 250µl of medium per well. The following day, once the cells had formed a confluent monolayer, the media on the apical surface was removed (airlifting), and the basal media was replaced with differentiation medium (described in Materials part 2.3). The differentiation medium would then diffuse to the apical surface cells through the membrane pores of the trans-well. This day is considered to be day 0. The differentiation medium was changed every 48h.

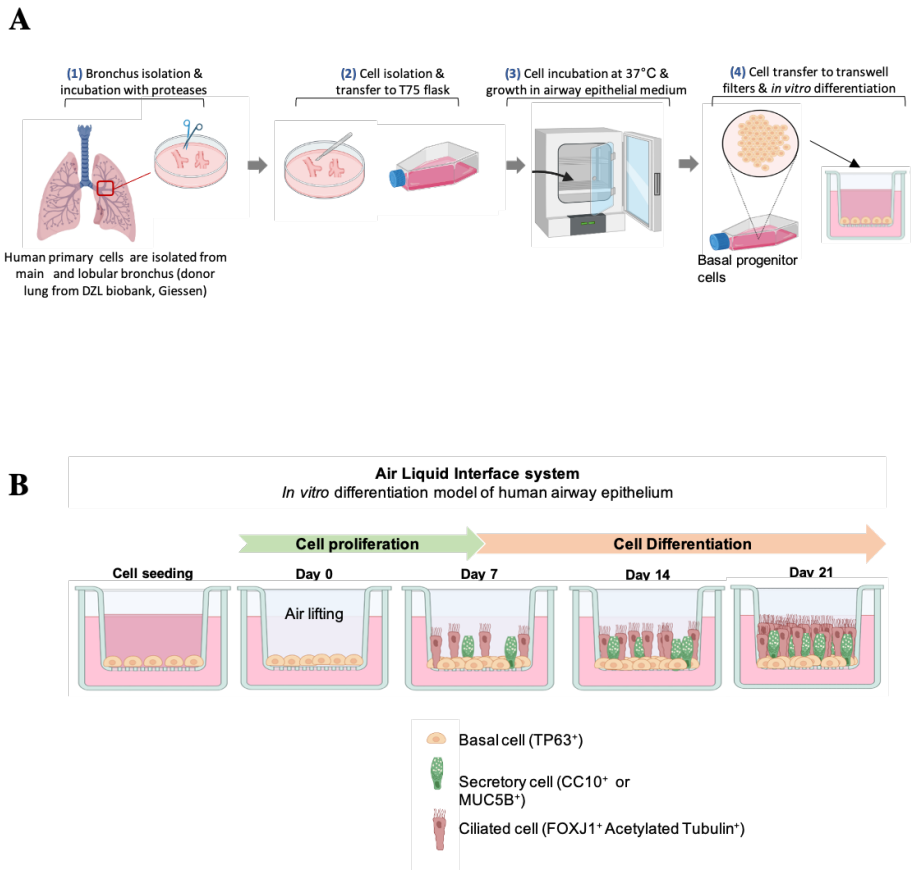

Figure 10. Isolation of primary human airway epithelial cells and *in vitro* differentiation. (A) Primary cells were isolated from human bronchus obtained from the DZL biobank, then incubated at 37°C in a T75-flask in the presence of airway epithelial medium. **(B)** Primary cells were seeded in ALI filters. Then, they were airlifted once confluent, and a differentiation medium was added to the bottom. The cells were allowed to differentiate over 21 days to give rise to a pseudostratified epithelium.

3.5 Transfection

HEK293T cells were transfected with plasmid DNA (pTRIPZ, pWPXL or pGFP-C-shLenti) using the calcium chloride method. Before adding the transfection mix, the antibiotic-containing media was removed from HEK293T cells and replaced by 9ml (for 10 cm plate) or 1.5ml (for 6-well plates) of fresh media antibiotic-free. HEK293T cells were split 1 day before transfection and were 70%-80% confluent at the time of transfection.

<u>For cells in 10 cm plate</u>

Plasmid (pTRIPZ, pWPXL or pGFP-C-shLenti)	-	10µg
Sterile water	-	450µl
BBS 2X	-	500µl
$CaCl_2$ (2M)	-	50µl

<u>For cells in 6 well plate</u>

Plasmid (pTRIPZ, pWPXL or pGFP-C-shLenti)	-	3.0µg
Sterile water	-	112.5µl
BBS 2X	-	125.0µl
$CaCl_2$ (2M)	-	12.5µl

The mixture was vortexed and incubated at room temperature for 20 minutes, then added dropwise to HEK293T cells. After 4 hours of incubation at 37°C with 5% CO_2, the media was changed to an antibiotic-containing medium and the cells were re-incubated (usually, 24 to 48 hours are needed to see the expression of the tag/protein of interest).

3.6 Lentivirus transduction

<u>Transfection of lentiviral constructs in HEK293T cells</u>

HEK293T cells were transfected with Lentiviral constructs (pTRIPZ, pWPXL, or pGFP-C-shLenti) together with the packaging and envelop plasmids (pMD2.G and pSPAX) using the calcium chloride method. Media change and cell splitting are as previously described.

<u>For cells in a 10 cm dish</u>

Lentiviral plasmid (pTRIPZ, pWPXL or pGFP-C-shLenti)	-	10µg
Supporting plasmid (pMD2.G)	-	1µg
Supporting plasmid (pSPAX)	-	1µg

Sterile water	-	450µl
BBS 2X	-	500µl
$CaCl_2$ (2M)	-	50µl

The mixture was vortexed and incubated at room temperature for 20 minutes, then added dropwise to HEK293T cells. Media was changed to an antibiotic-containing medium after 4 hours and cells were incubated for 3 days at 37°C and 5% CO_2 to isolate the virus. For pTRIPZ plasmid, which has a doxycycline-inducible promoter, 5ug/ml of doxycycline was added to the antibiotic-containing medium after 4 hours of transfection (during the media change).

Lentivirus concentration

Viral supernatant was collected from HEK293T cells and centrifuged at 1500 rpm for 10 minutes to remove cellular debris. The supernatant was carefully transferred to the ultracentrifuge tubes without disturbing the pellet. The supernatant was centrifuged at 25.000 rpm for 2 hours at 4°C, then discarded carefully without disturbing the pellet. The viral pellet was resuspended in 100µl PBS for each virus isolated from a single 10cm HEK293T cell plate, followed by incubation at 4°C overnight (alternatively, 2 hours incubation at 4°C was also successful). The following day, the viral suspension was diluted in the airway media to have 150µl virus per well (or frozen at -80°C for later use). Virus isolated from a single 10cm HEK293T cells plate was sufficient to successfully infect an entire 12-trans-well plate of pHBECs culture, meaning that the dilution will be as follows: 100µl of resuspended virus diluted in 1700µl media to infect one entire 12-trans-well plate of pHBECs. However, transduction efficiencies may vary depending on the insert size and the lentiviral plasmids, therefore MOI calculation would be needed for new experiments.

Infection of primary bronchial epithelial cells

The pHBECs cells were seeded in 12 trans-well plates and infected the following day with 150µl of the corresponding diluted viral suspension (one day before airlifting). The cells were then incubated with the viral particles overnight at 37°C, and washed twice with PBS prior to airlifting.

3.7 Real-Time qPCR

RNA isolation

Total RNA from pHBECs was isolated using the RNeasy Mini Kit (Qiagen) according to the Manufacturer's instructions, and the RNA concentration was determined using Nanophotometer N60. For the RNA samples used for bulk RNA sequencing, the quality control of the RNA was carried out using the Agilent 2100 Bioanalyzer with Agilent RNA 6000 Nano Kit (Agilent, 5067-1511) according to the manufacturer's instructions.

DNase I treatment

The RNA was treated with DNase I to remove any DNA contamination (DNase I, ThermoFisher). The mixture was then incubated at 37°C for 30 minutes.

Table 11. Reaction mixture for DNase treatment

Component	Volume per reaction (µl)
RNA	1µg (variable)
DNase I (1U/µl)	1.0
10X Reaction Buffer with $MgCl_2$	1.0
Nuclease-free water	Variable
Total	**10.0**

The mixture was then incubated at 65°C for 10 minutes to heat-inactivate the enzyme in the presence of EDTA: 1µl of EDTA (50mM) was added to prevent RNA hydrolysis with divalent cations during heating.

Reverse transcription

Reverse transcription was performed using the iScript cDNA Synthesis Kit (BIO-RAD) according to the manufacturer's instructions. The previously DNase-treated RNA was fully used for this step.

Table 12. Reaction mixture for reverse transcription

Component	Volume per reaction (µl)
5X iScript Reaction Mix	4.0
iScript Reverse Transcriptase	1.0
Nuclease-free water	4.0

RNA template	11.0 (1μg)
Total volume	**20.0**

RT qPCR amplification of the cDNA

Real-Time qPCR reactions were performed using iTaq Universal SYBR Green Supermix and Light Cycler 480 system (Roche) according to a standardized protocol. Primers were designed using the online tool Universal Probe Library (Roche). The reaction mixture for each gene was prepared on ice as follows:

Table 13. Reaction mixture for cDNA amplification (Real-Time qPCR)

Component	Volume per well (μl)
iTaq Universal SYBR Green Supermix	10.0
Forward primer (10μM)	1.0
Reverse primer (10μM)	1.0
Nuclease-free water	3.0
Total volume	**15.0**

15μl of the above master mix was loaded for each gene with 5μl (5ng) of cDNA in the appropriate well. The 96-well plate was then sealed and centrifuged for 30 sec to ensure the mixing of the reaction components and to remove any air bubbles.

3.8 Lentivirus Real-Time qPCR Titration

Viral supernatant collection and viral RNA purification

150μl of PBS was added to the trans-well, mixed, and collected to test the presence of the virus. Genomic viral RNA was purified using QIAamp Viral RNA Mini Kit (Qiagen) according to the Manufacturer's instructions.

Treatment with DNase I and Real-Time qPCR Amplification of Lentiviral Genomic RNA

The RNA was then treated with DNase I to remove any residual plasmid DNA from the transient transfection of the packaging HEK239T cells and the Master Reaction Mix for the Real-Time qPCR was performed using the Lenti-X qRT-PCR Titration kit (Takara), according to the Manufacturer's instructions.

Real-Time qPCR reaction cycles program

- Reverse Transcription reaction
  - 42°C 5 minutes
  - 95°C 10sec

- qPCR x 40 cycles
  - 95°C 5sec
  - 60°C 30 sec

- Dissociation Curve
  - 95°C 15 sec
  - 60°C 30 sec
  - All (60°C – 95°C)

Lentivirus titration

The genomic viral RNA copy number for each sample was determined by finding the copy number that corresponds to its Ct value on the generated standard curve described in the kit protocol.

3.9 Fluorescence Activated Cell sorting (FACS)

The cells were moved to the S1 area after confirming they were virus-free through RT-qPCR testing. 6 wells per condition were used for sorting GFP-positive cells (ALI day 14), where 1.5ml of accutase was added to the top and the bottom of each well. Then, the cells were incubated at room temperature for 60-90 minutes and pipetted up and down using a wide orifice pipette. Cells were constantly checked under the microscope until they were completely dissociated from each other and formed a single-cell suspension. Cells from the 6 wells were pulled together in a 50ml falcon, then centrifuged at 1500rpm for 8 minutes at 4°C. The supernatant was discarded and the cell pellet was re-suspended in 2ml ice-cold 1%BSA/HBSS. The cells were centrifuged twice, re-suspended in the same solution, and transferred to the glass tubes after filtration to start the FACS sort.

3.10 Immunofluorescence

Fixation

Media was removed from trans-wells that were then washed twice with 1XPBS. Cells were fixed with 4% formaldehyde for 15 minutes at room temperature, followed by 3 washes with PBS-Glycine buffer (10 minutes per wash).

Permeabilization

Cells were permeabilized with 0.5% Triton X-100 for 15 minutes at room temperature, then washed 3 times with 1XIF-wash buffer (10 minutes each wash) prepared as described in Materials part 2.2.

Blocking and primary antibody staining

Cells were incubated with the blocking solution (described in Materials 2.2*)* for 1 hour and 50 minutes at room temperature. The primary antibodies were diluted in the blocking solution and incubated with the cells overnight at 4ºC. 150µl of diluted antibodies were added to the bottom and top of each trans-well.

Secondary antibody staining

The next day, the cells were rinsed 3 times with 1XIF-wash buffer at room temperature (10 minutes each wash). They were then incubated with the secondary antibody diluted in the same blocking solution, for 2 hours at room temperature protected from light. 150µl of the diluted secondary antibodies were added to the bottom and top of each trans-well. Cells were then rinsed 3 times, 10 minutes each with 1X IF-wash at room temperature. All secondary antibodies used were Alexa-conjugated from Invitrogen and were used at 1:1000 dilution.

DAPI staining and mounting

Cells were incubated with 1XPBS containing 0.5ng/ml DAPI for 15 minutes and then washed one time with 1XPBS. ALI filters containing the cells were cut using a scalpel, and mounted with Fluoromount solution on the slides (cells facing up). The slides were allowed to dry overnight at room temperature and were then stored at 4ºC.

3.11 Western blot

Cells were lysed in ice-cold RIPA buffer and the protein samples were mixed with 4X Laemmli buffer, and boiled for 5 minutes at 95°C. Denatured proteins were separated by 6 %

or 12 % SDS-PAGE at 100V for 60-90 minutes. Separated proteins were transferred onto nitrocellulose membrane, using semi-dry or wet transfer, at 15V for 30-40minutes or 50V for 120 minutes, respectively. The membrane was placed in a blocking solution (6% milk in 1XPBS Tween) for 1 hour at room temperature (with shaking), washed with 1XPBST (0.1% tween) three times, then incubated with the respective primary antibody(ies) diluted in the blocking solution, overnight at 4°C (with shaking). The next day, the membrane was washed with 1XPBST three times at room temperature (10 minutes each), and incubated with the respective secondary antibody(ies) coupled to horseradish peroxidase (HRP) for 1 hour at room temperature (with shaking), followed by 3 times washes. Target protein(s) were visualized using the enhanced chemiluminescence system (ECL) (Thermofisher), with Amersham Imager 600.

3.12 CUT & RUN: Cleavage Under Target and Release Using Nuclease

CUT&RUN experiment design

The pHBECs from the ALI culture day 14 transduced with BHLHE40-GFP were washed twice with 1XPBS, incubated with accutase for 20-30 minutes at 37°C prior to dissociating them into single cells (1ml accutase in the apical side and 1mvl in the bottom). The cells were examined under a microscope every 15 minutes to confirm complete dissociation, ensuring proper binding to the beads later. Nuclei were then isolated using Minute™ Detergent-Free Single Nuclei Isolation Kit (Invent Biotech) according to the Manufacturer's instructions. Successful nuclei isolation was checked under the microscope. After that, the CUT&RUN experiment was performed using the CUT&RUN Assay Kit (Cell Signaling) according to the Manufacturer's instructions. The number of cells used for each condition was 500,000 cells, and the antibodies used are described in Fig. 11 (500,000 cells represent the double amount recommended by the kit, therefore, all the reagent volumes were adjusted accordingly).

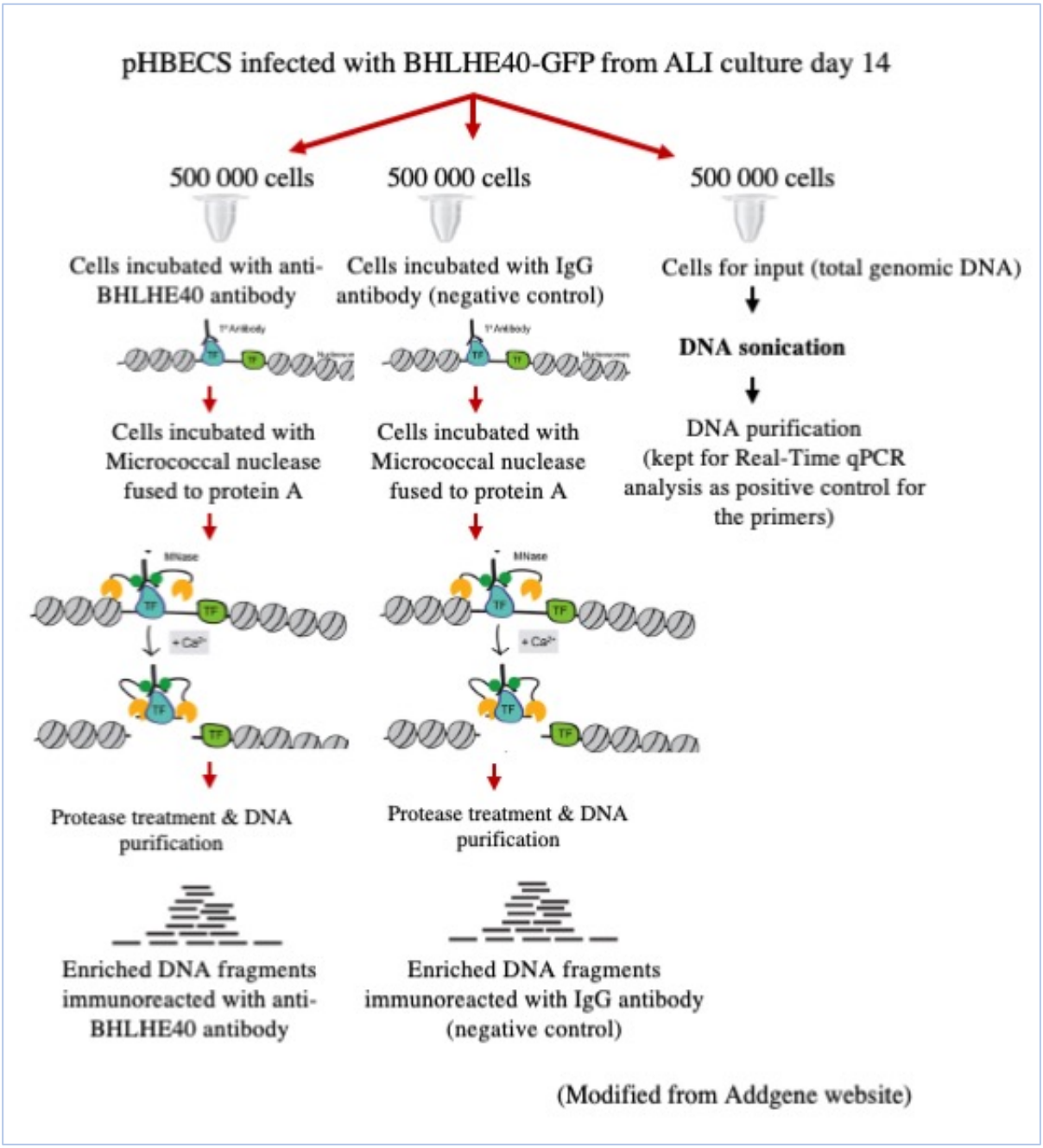

Figure 11. Cleavage Under Targets & Release Using Nuclease. Schematic representation of the CUT&RUN experiment summarizing the main steps.

3.13 BHLHE40 ChIP-sequencing data from ENCODE website

The data of the publicly available ChIP-sequencing of BHLHE40 in A549 cells was downloaded from the Encyclopedia of DNA Elements (ENCODE) consortium website (https://www.encodeproject.org) as follows in the figure.

Figure 12. The steps to download BHLHE40 ChIP-seq peaks in A549 cells using the ENCODE consortium website. Screenshots with boxes summarizing the steps to download the corresponding files.

3.14 Preparation of SDS-Polyacrylamide gel

The SDS gel was prepared as follows:

Table 14. Reagents for the separating gel preparation (12.5%)

Components	Volume to add for 2 gels
1M Tris pH 8.8	6.75ml
30% Acrylamide/Bis	7.5ml
10% SDS	180µl
50% glycerol	450µl
Distilled H2O	3.0ml
APS	90.0µl
TEMED	18.0µl

After pouring the separating gel mix in between the plates, 1ml of isopropanol was added. The gel was allowed to polymerize for 20 minutes. Then, isopropanol was removed, the stacking gel mix was added and allowed to polymerize for 20 minutes.

Table 15. Reagents for the stacking gel preparation

Components	Volume to add for 2 gels
0.5M Tris pH 6.8	1.2ml
30% Acrylamide/Bis	800.0µl
10% SDS	48.0µl
Distilled H2O	2.8ml
APS	25.0µl
TEMED	4.8µl

3.15 Coating of Poly-L-lysine

5 coverslips were added in every well of the 6-well plate. After that, 3ml of poly-L-lysine solution was added to each well and the coverslips were pulled down to be fully covered with the solution. The plate was then incubated for 1 hour at 37°C, the poly-L-lysine solution was removed, and the coverslips were washed once with 1XPBS. Finally, the coverslips were dried for 1 hour or overnight under the cell culture hood, then UV-treated for 1 hour before seeding the cells.

3.16 Preparation of competent Top 10 E. *coli* cells

All solutions and devices were pre-cooled at 4°C. 20 ml of fresh culture was inoculated into 1000 ml of dYT medium, then $MgCl_2$ and $MgSO_4$ were added to a final concentration of 10mM. This culture was then incubated at 37°C, 200 rpm for 2-2.5h until OD O.6 was reached. After that, cells were transferred into 50ml falcon tubes and placed on ice for 30min, then centrifuged at 3000 rpm, 8 minutes at 4°C. The cell pellet was re-suspended in 330 ml (1/3 of the initial volume) of the pre-cooled RF1 solution using pre-cooled glass pipettes and then placed in the refrigerator for 30 minutes. Cells were again centrifuged for 8 minutes, 3000 rpm at 4°C, then re-suspended in 80ml (1/12.5 of the initial volume) of the pre-cooled RF2 solution and transferred to 50 ml falcon tubes. The mixture was incubated on ice, for at least 30 minutes. After that, 100µl aliquots were transferred into the pre-cooled Eppendorf, and snap-frozen in liquid nitrogen for future use.

3.17 Statistical analysis

All data shown are mean with ± SD (standard deviation). Comparisons between the two groups were performed with an unpaired student's t-test, *P < 0.05, **$P < 0.01$, ***$P < 0.001$. All statistical analyses were performed using GraphPad Prism 6.

3.18 Quantification

- Real-Time qPCR

Relative gene expression was quantified using the ΔΔCt (Delta-Delta Ct) method, which compares the Ct values of target genes between the control and treated conditions. For each condition, the Ct values were first normalized to the housekeeping gene *RPLP0* to account for variations in RNA input and reverse transcription efficiency. The normalized expression levels were then compared between the control and treated conditions to determine relative fold changes in gene expression.

- Immunostaining

For the immunostaining data, a minimum of 3 random regions were taken using confocal microscopy (40X objective) before quantification. Nuclear staining counting was performed automatically using IMARIS software and cytoplasmic staining counting was performed manually using LASX 3D image analysis software.

4 Results

4.1 Endogenous *BHLHE40* expression increased during pHBECs differentiation in ALI culture

To analyze the expression of *BHLHE40* during pHBECs-derived ALI culture differentiation, RNA was collected at different time points of proliferation and differentiation (Fig. 13A). *BHLHE40* gene expression was low on day 0, however, it significantly increased on day 7 and was stable between days 7, 14, and 21 (Fig. 13B). Taken together, the increase in *BHLHE40* expression coincides with the beginning of differentiation, suggesting that BHLHE40 may play a role in the differentiation of human airway basal epithelial cells.

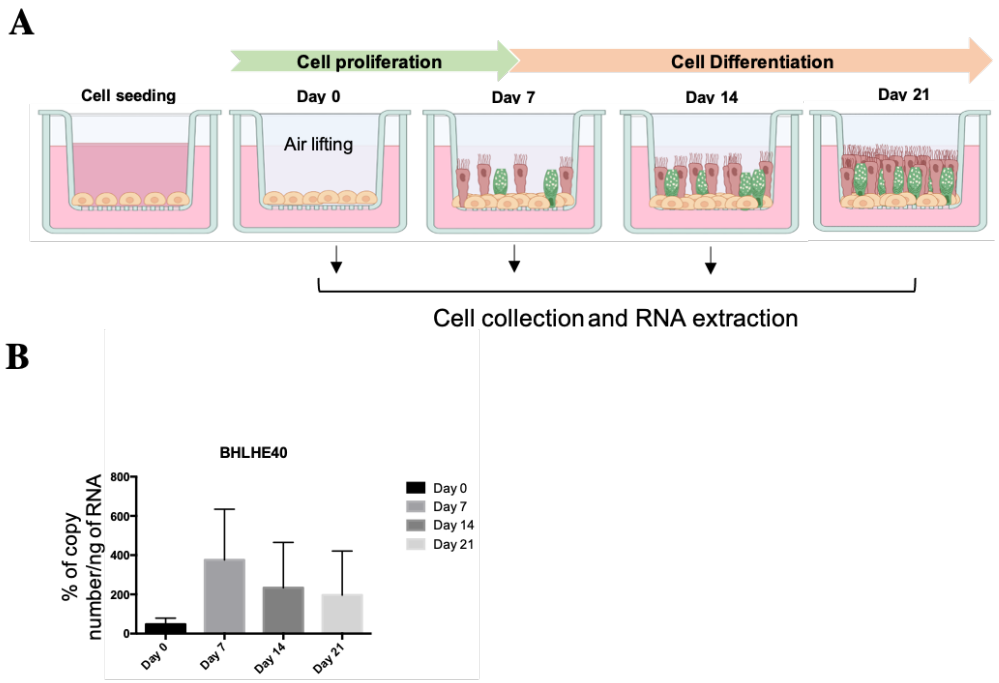

Figure 13. Analysis of BHLHE40 endogenous expression during the ALI culture. **(A)** Schematic representation of the ALI culture. Human primary bronchiolar epithelial cells were seeded in ALI filters and grown over 21 days. Then, cells were collected on days 0, 7, 14, and 21 and total RNA was extracted and reverse transcribed. **(B)** *BHLHE40* gene expression was determined by Real-Time qPCR using the absolute gene quantification method at each indicated time point (before and during differentiation) (n=4).

4.2 Validation of BHLHE40-GFP and BHLHE40-Flag expression in HEK293T cells using lentiviral constructs

BHLHE40-GFP and BHLHE40-FLAG fusions were cloned into pWPXL and pTRIPZ lentiviral vectors, respectively (the cloning strategy for each plasmid is described in Fig. 9). The constructs were then transfected in HEK293T cells to confirm their expression. After that, the cells were fixed 48h post-transfection for immunostaining with anti-GFP or anti-FLAG antibodies (Fig 14A, B). For the GFP constructs, the promoter is constitutive and was therefore expressed directly after transfection. Transfected cells with control GFP showed cytoplasmic staining while the transfected cells with BHLHE40-GFP localized at the nucleus. The transfected cells with BHLHE40-FLAG were treated with doxycycline (5ug/ml) to induce the overexpression. Doxycycline-treated cells showed nuclear FLAG staining, in contrast to the non-treated cells, which suggests that there was no leakiness of the promoter. In addition, the cells were collected 48h post-transfection for immunoblotting using anti-GFP or anti-FLAG antibodies (Fig. 14C, D). BHLHE40-GFP and BHLHE40-FLAG fusions were detected at the correct size of 82 and 55 kDa, respectively.

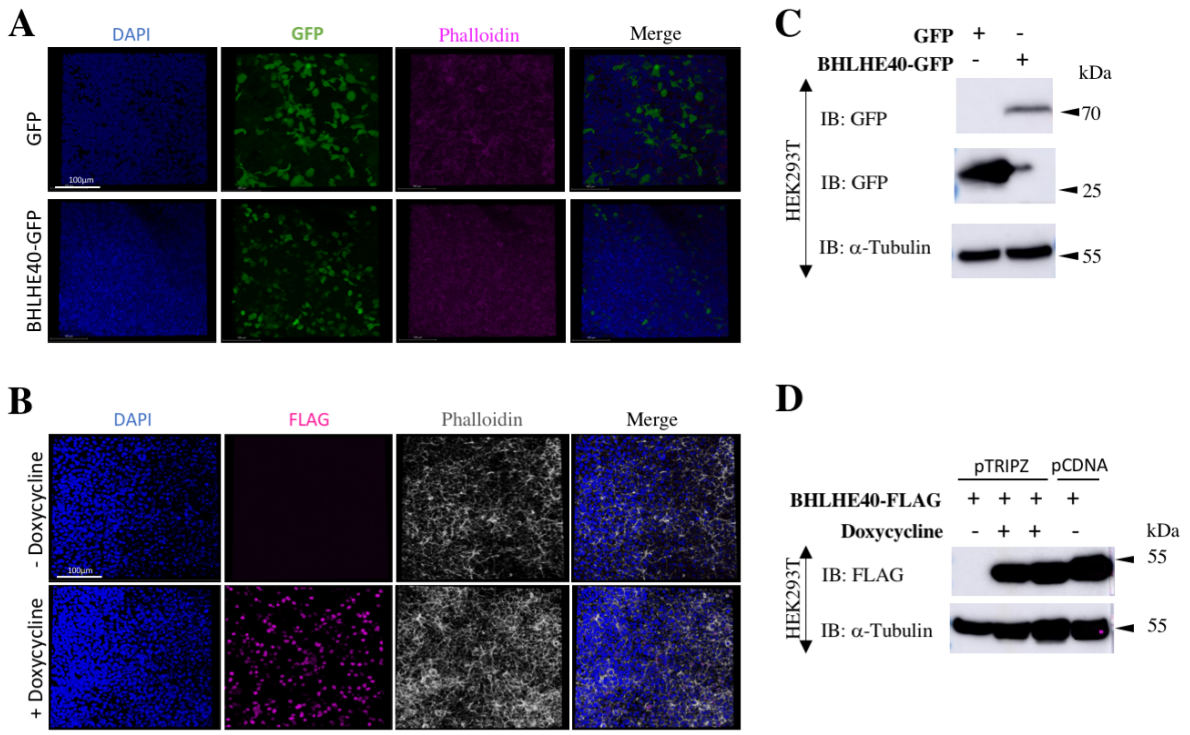

Figure 14. Efficiency of BHLHE40 overexpression in HEK293T cell lines. HEK293T cells transfected with **(A)** BHLHE40-GFP or **(B)** BHLHE40-FLAG constructs were fixed with 4% PFA 48h post-transfection, then stained using **(A)** anti-GFP antibody or (B) anti-FLAG antibodies with Phalloidin. All nuclei were stained with DAPI. For BHLHE40-FLAG, the transfected cells were treated with doxycycline (5ug/ml) 4h post-transfection in order to induce overexpression. Each transfected cell was collected 48h post-transfection and subjected to immunoblotting. Lysates from transfected HEK293T cells with each construct were immunoblotted and the protein expression of **(C)** GFP (BHLHE40-GFP) or **(D)** FLAG (BHLHE40-FLAG) was determined. α-tubulin was used as the loading control.

4.3 Analysis of BHLHE40 overexpression and knockdown efficiency in pHBECs-derived ALI culture using lentiviral transduction

Lentiviral particles encoding the human BHLHE40 fused to GFP (pWPXL) or *BHLHE40* shRNA (pGFP-C-shLenti) and their respective controls were successfully produced in HEK293T (described in method part 3.6), then used to infect the pHBEC-derived ALI culture on day -1. To analyze the overexpression efficiency, transduced cells with GFP or BHLHE40-GFP constructs were FACS sorted after 5 days of ALI culture (Fig. 15A and 16A). For the overexpression experiment, the transduction efficiency of BHLHE40-GFP construct was lower than the GFP construct, also the nuclear GFP signal intensity was lower than the cytoplasmic GFP signal. Therefore, to sort enough BHLHE40-GFP$^+$ cells, a higher cell number was needed compared to the control GFP$^+$ cells, which explains the higher cell number represented in the pseudocolour dot plot of the transduced pHBECs with BHLHE40-

GFP. Similarly, to check the knockdown efficiency, transduced pHBECs cells with scramble or *BHLHE40* shRNA were FACS sorted after 5 days of ALI culture to analyze *BHLHE40* gene expression (Fig. 15B and 16B).

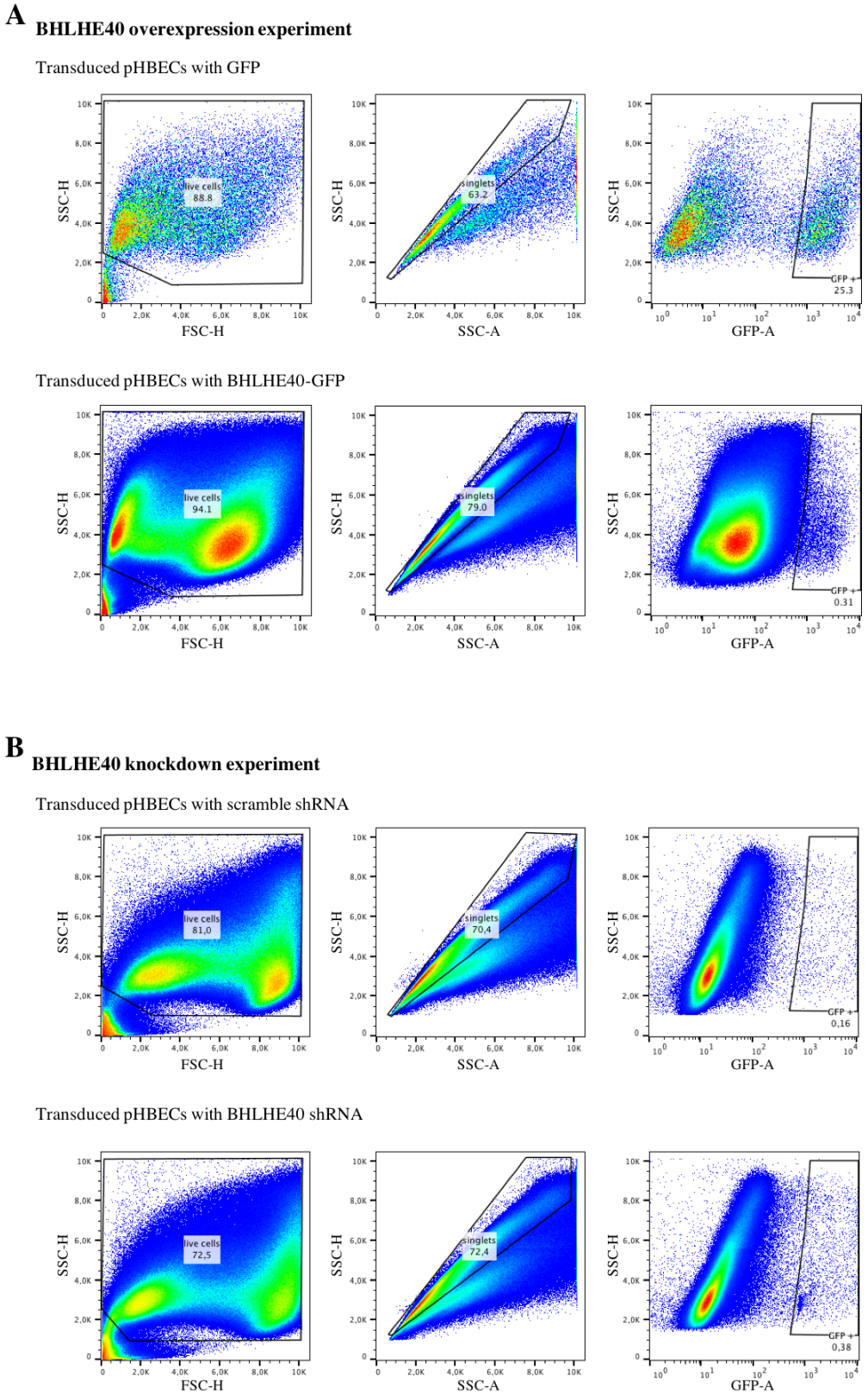

Figure 15. Flow cytometric pseudocolour dot plots showing the gating strategy to FACS sort the transduced pHBECs from BHLHE40 overexpression and knockdown experiment in the ALI culture. Cells were first gated based on their size and granularity (FSC-H vs SSC-H) to remove cell debris, then singlets were sub-gated (SSC-A vs SSC-H) followed by the selection of the GFP^+ transduced cells (GFP-A vs SSC-H) for BHLHE40 **(A)** overexpression and **(B)** knock-down experiments. Values inside the plots represent the percentages from the parent gate. SSC-A: side scatter area, FSC-A: forward scatter area, SSC-H: side scatter height, FSC-H: forward scatter height, GFP-A: GFP area.

Real-time qPCR analysis of the FACS sorted cells from the overexpression experiment, showed that *BHLHE40* transcripts were six-fold increased in BHLHE40-GFP overexpressing cells compared to the control (Fig. 16C). In the knockdown experiment, *BHLHE40* transcripts were reduced by nearly 50% in *BHLHE40* shRNA overexpressing cells compared to the control (Fig16.D). In addition, the overexpression of BHLHE40-GFP was further confirmed in pHBECs by immunostaining of transduced ALI culture from day 14: cytoplasmic GFP staining was observed for the transduced cells with GFP, while nuclear staining was observed for the transduced cells with BHLHE40-GFP (Fig. 16E). Similarly, for the transduced cells with BHLHE40-FLAG, a nuclear FLAG staining was observed (Fig. 16F).

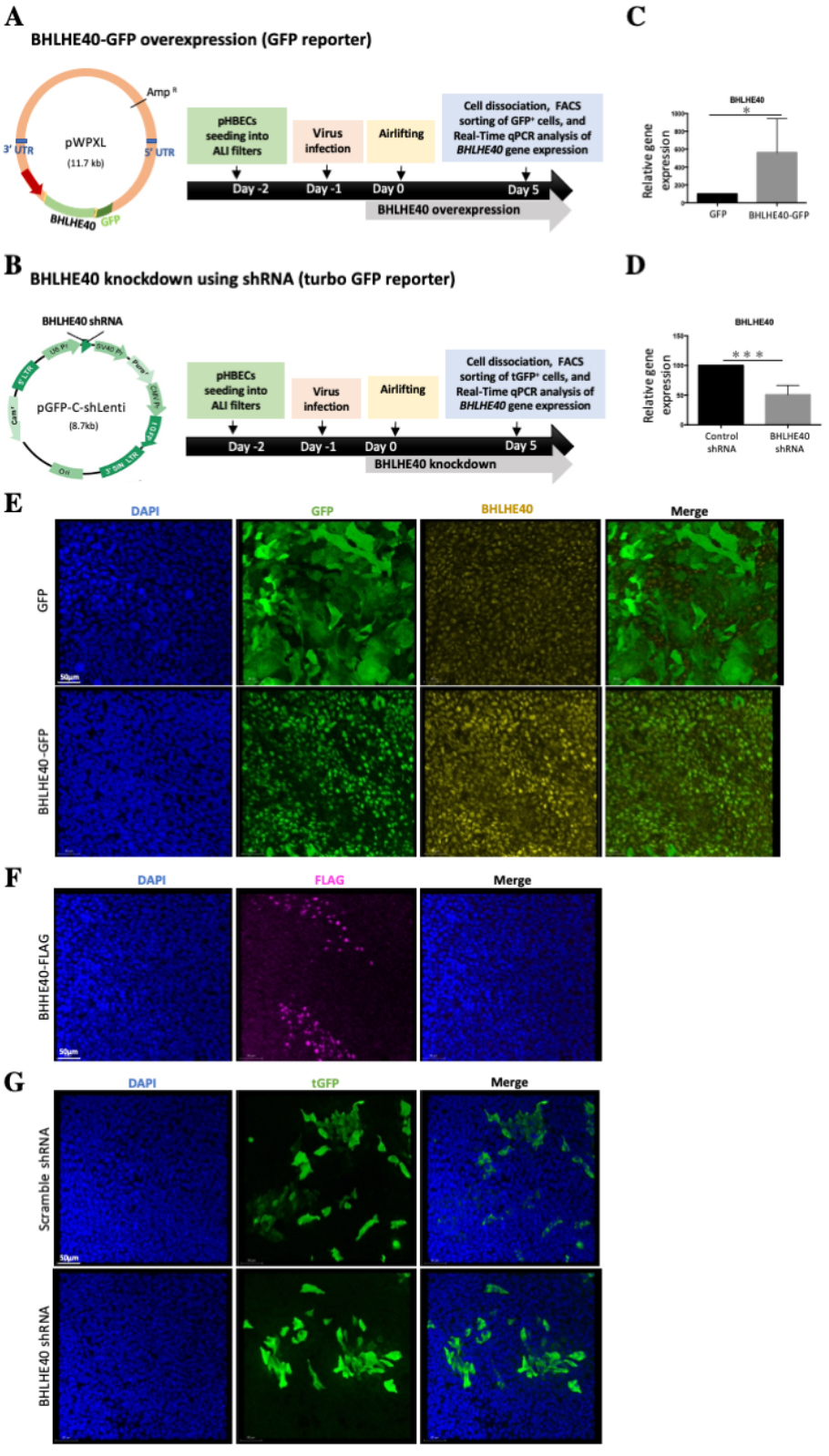

Figure 16. Lentiviral transduction efficiency for BHLHE40 overexpression and knockdown in pHBECs derived-ALI culture. Schematic representation of BHLHE40 overexpression or knockdown strategies using the ALI system. Primary cells were seeded in ALI filters and infected the next day with the lentiviral particles: **(A)** BHLHE40-GFP overexpression or **(B)** shRNA knockdown constructs. The next day, the cells were airlifted and allowed to grow for 5 days. Then, they were dissociated into single-cell suspension to FACS sort the GFP positively transduced cells prior to Real-Time qPCR analysis. Gene expression of *BHLHE40* was analyzed by Real-Time qPCR in the FACS-sorted cells from the **(C)**

overexpression and **(D)** knockdown experiments. *BHLHE40* gene expression was normalized to housekeeping gene RPLP0. **(E)** and **(F)** Confocal microscopy pictures of transduced cells with GFP/BHLHE40-GFP or BHLHE40-FLAG from the ALI culture on days 14 and 21, respectively. To analyze the transduction efficiency, the cells were stained with anti-GFP and anti-BHLHE40 antibodies or with anti-FLAG antibodies. Cell nuclei were stained with DAPI.

4.4 BHLHE40 overexpression and knockdown in the ALI culture interfered with Notch signaling in basal cells but did not affect their fate early in the culture

Single-cell RNA sequencing of human primary bronchial epithelial cells differentiated on the ALI culture revealed that *BHLHE40* gene expression was selectively upregulated in differentiating cells and interestingly correlated with the upregulation of Notch signaling genes (Fig. 7 and 8).

To test if BHLHE40 positively regulates Notch signaling in the pHBECs-derived ALI culture, we analyzed genes involved in Notch signaling by Real-Time qPCR on FACS-sorted BHLHE40-GFP^{+} cells from day 5 (Fig. 17A). At this timepoint, cell differentiation starts and the culture is composed mainly of basal cells. BHLHE40-GFP overexpressing cells showed a significantly higher expression of *NOTCH1*, *NOTCH2*, *NOTCH3* receptors (Fig. 17C), and of the downstream effector *HEY2*, while *HES1* was unchanged (Fig. 17E). BHLHE40-GFP overexpression slightly increased *JAG1/2* gene expression but this was not significant. The lack of statistical significance is likely due to the high variability among biological replicates, as reflected in the standard deviation (Fig. 17C).

Similarly, for the knockdown experiment, Notch signaling gene expression was analyzed in FACS-sorted *BHLHE40* shRNA tGFP $^{+}$ cells from day 5 (Fig. 17B). *BHLHE40* shRNA-expressing cells had a significantly lower expression of *NOTCH1/2* receptors and *JAG1/2* ligands (Fig. 17D) with unchanged level of *HES1* (Fig. 17F), which is consistent with the overexpression data. However, no significant changes were observed for *NOTCH3* or *HEY2* (Fig. 17D, F). Our data suggest that BHLHE40 positively regulates components of Notch signaling.

Notch signaling activation in basal cells is associated with the downregulation of basal cell genes prior to luminal differentiation (Rock et al., 2011). Since BHLHE40 overexpression increased Notch signaling in basal cells from the ALI culture day 5, we hypothesized that this could correlate with the downregulation of basal cell gene markers prior to differentiation. To

this end, basal cell gene expression was analyzed by Real-Time qPCR in GFP and BHLHE40-GFP sorted cells from ALI culture day 5. Surprisingly, BHLHE40-GFP overexpression had no significant effect on *TP63*, *ITGA6*, *KRT5*, or *NGFR* basal cell gene expression (Fig. 17G). Similarly, to investigate if *BHLHE40* knockdown maintains basal cell gene expression, their gene expression was analyzed in *BHLHE40* shRNA FACS sorted cells from ALI day 5 by Real-Time qPCR. Consistent with the overexpression data, the knockdown of *BHLHE40* had no significant effect on any of the basal cell genes (Fig. 17H).

Since Notch signaling is required for basal cell differentiation into early progenitors (Rock et al., 2011), we hypothesized that the transduced basal cells did not lose their fate but started to co-express an intermediate differentiation cell marker *KRT13*, as suggested by our single-cell RNA sequencing analysis (data not shown). However, BHLHE40 overexpression or knockdown did not interfere with the expression of *KRT13* as early as day 5 (Fig. 17I, J). Taken together, our data suggest that BHLHE40 overexpression or knockdown did not affect the basal cell fate on day 5, even though it interfered with the expression of Notch signaling components.

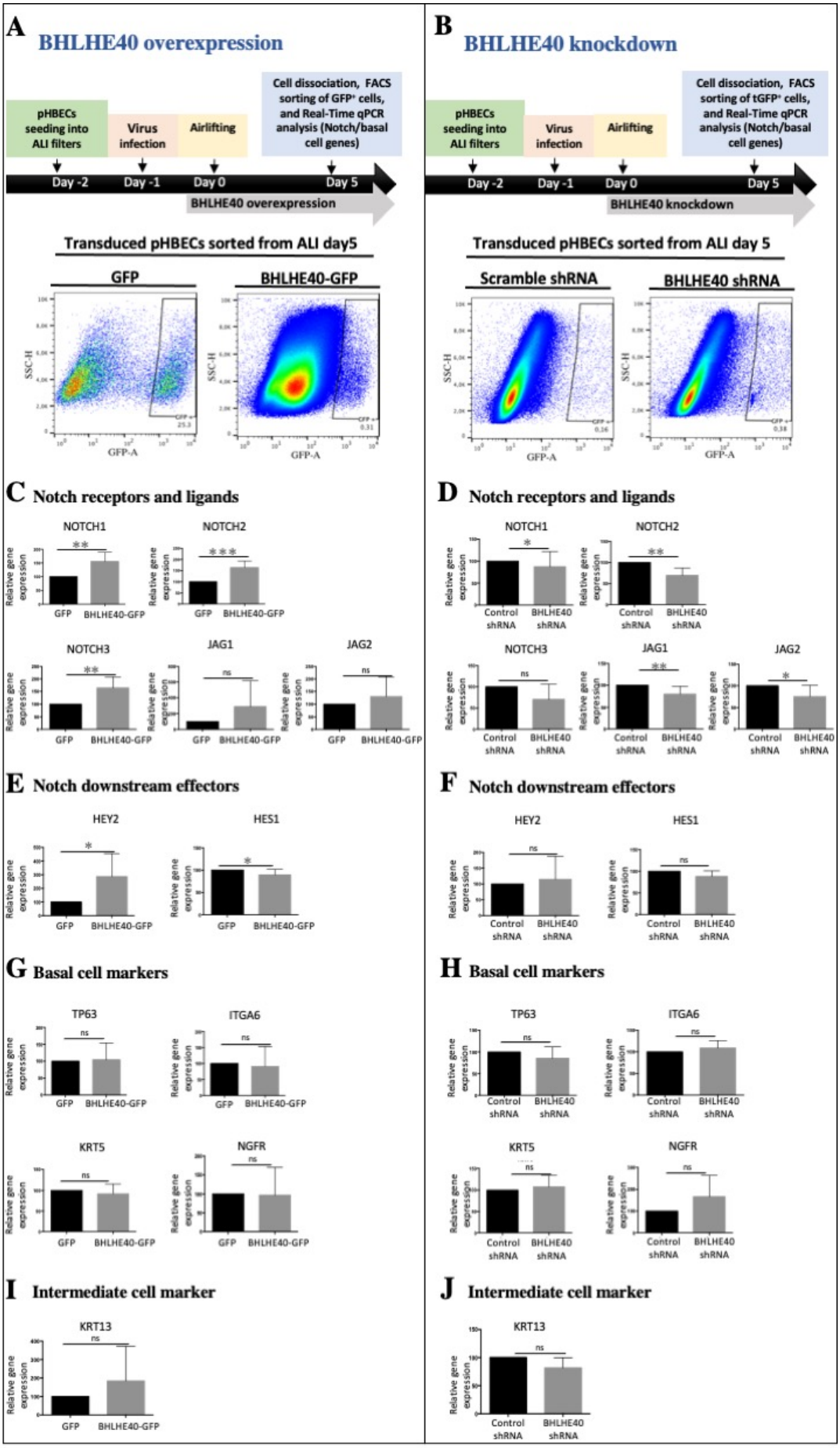
A
BHLHE40 overexpression
pHBECs seeding into ALI filters
Virus infection
Airlifting
Cell dissociation, FACS sorting of GFP+ cells, and Real-Time qPCR analysis (Notch/basal cell genes)
Day -2
Day -1
Day 0
Day 5
BHLHE40 overexpression
Transduced pHBECs sorted from ALI day5
GFP
BHLHE40-GFP
SSC-H
GFP-A
B
BHLHE40 knockdown
pHBECs seeding into ALI filters
Virus infection
Airlifting
Cell dissociation, FACS sorting of tGFP+ cells, and Real-Time qPCR analysis (Notch/basal cell genes)
Day -2
Day -1
Day 0
Day 5
BHLHE40 knockdown
Transduced pHBECs sorted from ALI day 5
Scramble shRNA
BHLHE40 shRNA
SSC-H
GFP-A
C Notch receptors and ligands
NOTCH1
NOTCH2
NOTCH3
JAG1
JAG2
Relative gene expression
GFP
BHLHE40-GFP
D Notch receptors and ligands
NOTCH1
NOTCH2
NOTCH3
JAG1
JAG2
Relative gene expression
Control shRNA
BHLHE40 shRNA
E Notch downstream effectors
HEY2
HES1
Relative gene expression
GFP
BHLHE40-GFP
F Notch downstream effectors
HEY2
HES1
Relative gene expression
Control shRNA
BHLHE40 shRNA
G Basal cell markers
TP63
ITGA6
KRT5
NGFR
Relative gene expression
GFP
BHLHE40-GFP
H Basal cell markers
TP63
ITGA6
KRT5
NGFR
Relative gene expression
Control shRNA
BHLHE40 shRNA
I Intermediate cell marker
KRT13
Relative gene expression
GFP
BHLHE40-GFP
J Intermediate cell marker
KRT13
Relative gene expression
Control shRNA
BHLHE40 shRNA

Figure 17. BHLHE40 overexpression and knockdown in the ALI culture interfered with Notch signaling in basal cells but did not affect their fate at the early time point of culture. Transduced airway epithelial cells from the BHLHE40 overexpression **(A)** or knockdown experiment **(B)** were FACS sorted from the ALI culture on day 5. The pseudocolor density plots show the fraction of sorted GFP$^+$ cells (GFP or BHLHE40-GFP) or tGFP$^+$ cells (scramble or *BHLHE40* shRNA). Gene expression of **(C-D)** Notch receptors and ligands, **(E-F)** downstream effectors, **(G-H)** basal cell markers, and **(I-J)** intermediate cell markers were analyzed by Real-Time qPCR in the overexpression (left panel) and knockdown experiment (right panel). A minimum of 5000 cells were sorted per patient per condition (n=5), $^{**}P < 0.01$, $^{***}P < 0.001$.

4.5 BHLHE40-GFP overexpression in the ALI culture increased airway basal cell differentiation into club, goblet, and ciliated cells on days 14 and 21

To analyze the effect of BHLHE40 overexpression at a later time point of differentiation/maturation, and investigate potentially interesting targets, we overexpressed BHLHE40-GFP as previously described. Transduced GFP$^+$ or BHLHE40-GFP$^+$ were sorted on day 14 prior to bulk RNA sequencing after confirming the RNA quality (Fig. 18A, B). BHLHE40-GFP overexpressing cells showed lower *TP63*, *ITGA6*, *KRT5*, and *NGFR* basal cell gene expression, and also a lower level of the intermediate marker *KRT13*. These results suggest that BHLHE40 overexpression in differentiating basal cells after 5 days of ALI culture leads to a decrease in basal cell gene expression. Supporting that, BHLHE40-GFP overexpressing cells had increased gene expression of ciliated (*FOXJ1*, *MYB*, *TP73*, *RFX3*, *RSPH1*, *FAM161A*), club and goblet cell markers (*SCGB1A1* and *MUC5B*) (Fig. 18C) indicating that the decrease in basal fate markers in BHLHE40-GFP overexpressing cells is due to their differentiation.

We further analyzed a set of epithelial cell-specific genes with Real-Time qPCR: BHLHE40-GFP overexpressing cells had a significantly lower expression of *TP63* and higher expression of the club cell marker *SCGB1A1* and the ciliated cell markers *FOXJ1*, *TP73*, and *MYB* (Fig. 18D), which are known to be master regulators of ciliogenesis (Jackson & Attardi, 2016). Taking together, our results indicate that overexpressing BHLHE40-GFP in pHBEC-derived ALI culture on day 14 decreased basal cell gene expression prior to their differentiation into ciliated, club, and goblet cells.

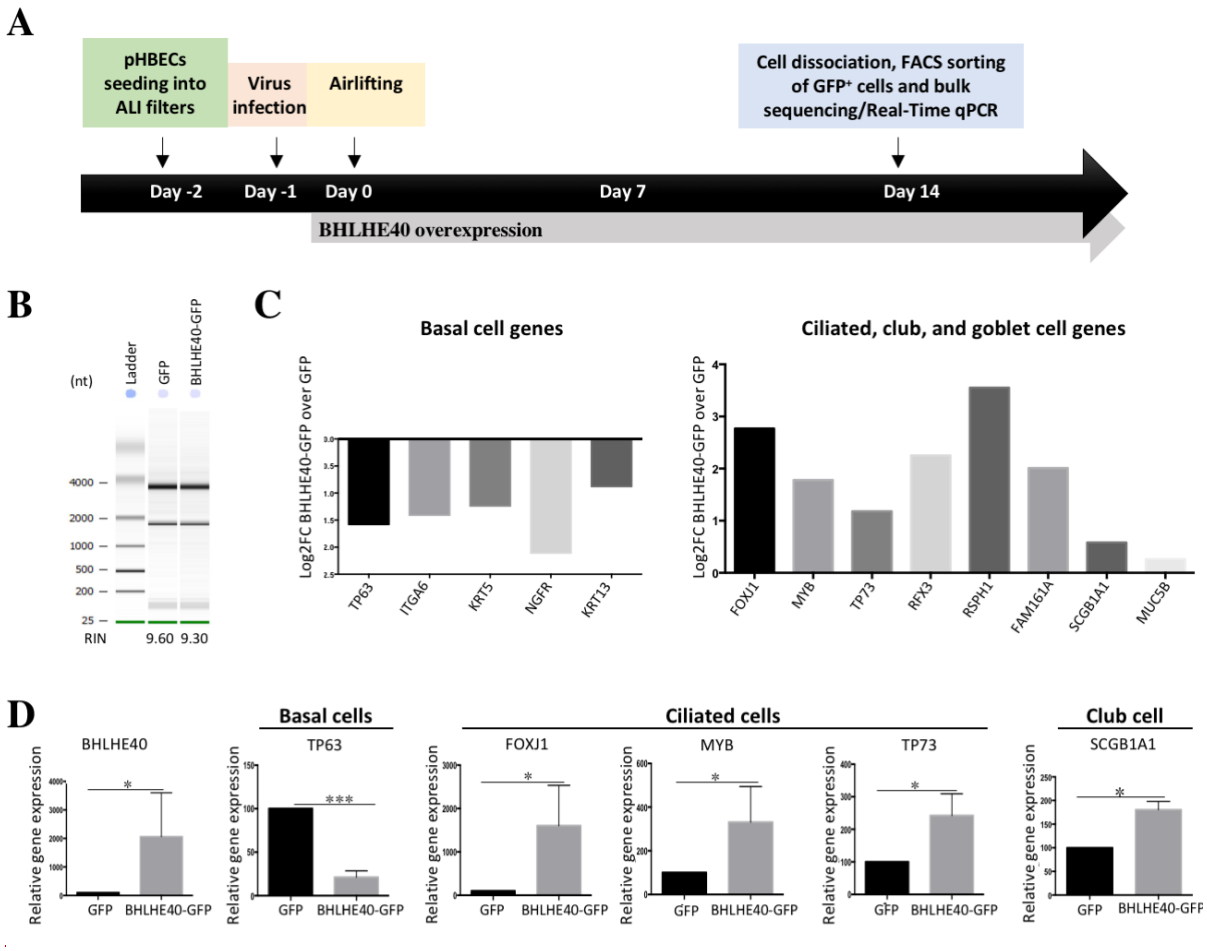

Figure 18. BHLHE40-GFP overexpression decreased basal cell gene expression and increased club, goblet, and ciliated cell gene expression on day 14. (A) Schematic representation of BHLHE40-GFP overexpression experimental setup using the ALI system: cells were infected with GFP or BHLHE40-GFP lentiviral particles one day before airlifting. The next day, the cells were airlifted and allowed to differentiate. On day 14, the cells were dissociated with accutase for 1h at room temperature and the transduced GFP⁺ cells were FACS sorted prior to bulk sequencing and real-time qPCR analysis. **(B)** RNA electrophoresis gel image of the isolated total RNA from the GFP and BHLHE40-GFP sorted cells run with Agilent RNA 6000 Nano Kit. **(C)** Bulk RNA sequencing analysis of basal and differentiated epithelial cell genes of the FACS sorted cells GFP⁺ or BHLHE40-GFP⁺ (n=1). **(D)** Real-time qPCR analysis of basal, ciliated, and club cell genes (n=3) of the FACS sorted cells GFP⁺ or BHLHE40-GFP⁺ cells (n=3), to validate the results in (C). BHLHE40 was used as a positive control for the overexpression. RIN: RNA Integrity Number.

To confirm this finding at the protein level, ALI culture transduced cells with GFP or BHLHE40-GFP from day 14 were stained for epithelial cell-specific markers (Fig.19A). Consistent with the bulk RNA sequencing and RT-qPCR data, BHLHE40-GFP overexpression significantly reduced the percentage of TP63⁺ basal cells compared to the control (Fig. 19B, E) and increased the percentage of ciliated cells RFX3⁺ and goblet cells MUC5B⁺ (Fig. 19C, D, F, H). For the club cells CC10⁺, a non-significant increase was observed at this time point (Fig. D, G).

To further characterize the role of BHLHE40 throughout the differentiation process, we also stained ALI cultures on day 21 with the same markers. The previously observed BHLHE40-induced decrease in basal cells and increase in the differentiated epithelial cells became more prominent (Fig. 19I): BHLHE40-GFP overexpressing cells did not express TP63^{+} basal cells compared to GFP^{+} cells and included an increased percentage of ciliated cells RFX3^{+} and club cells CC10^{+}. The increase in goblet cells MUC5B^{+} was not significant, which may be explained by the high variability between patient-derived basal cells.

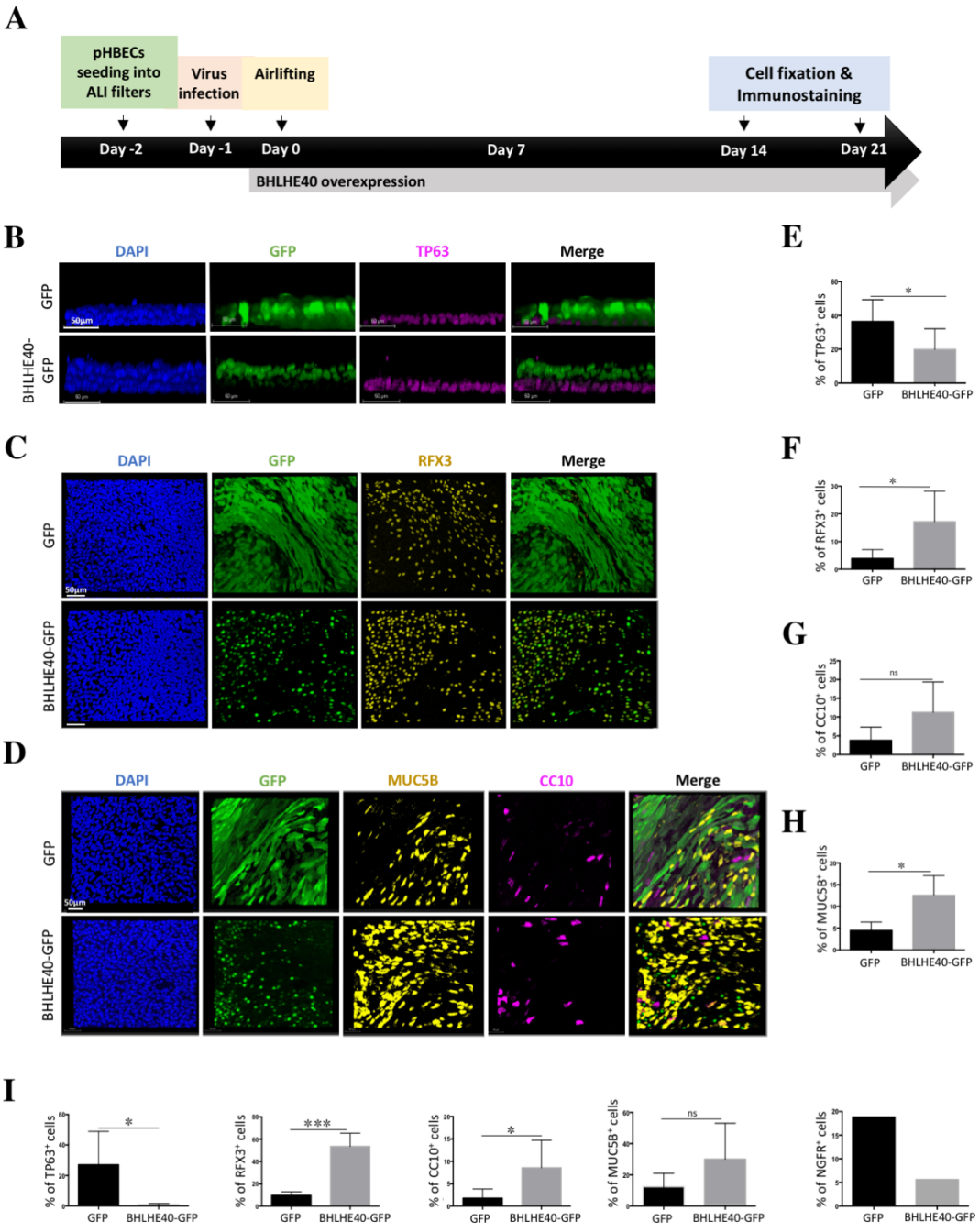

Figure 19. BHLHE40-GFP overexpression at day 0 induced an increase in airway epithelial cell differentiation in the ALI culture. (A) Schematic representation of BHLHE40-GFP overexpression strategy using the ALI culture: cells were infected with GFP or BHLHE40-GFP lentiviral particles one day before airlifting (day 0). The next day, the cells were airlifted and allowed to differentiate over 21 days. Transduced cells were fixed with 4% PFA on days 14 and 21 prior to immunostaining with epithelial cell-specific markers and confocal microscopy imaging. Airway epithelial cells in ALI culture from day 14 transduced with GFP or BHLHE40-GFP were co-stained with anti-GFP antibody and **(B)** anti-TP63 antibody for basal cells (optical section image), **(C)** anti-RFX3 antibody for ciliated cells or **(D)** anti-MUC5B and anti-CC10 antibodies for secretory cells. Bar graph showing the percentage of **(E)** $TP63^+$ basal cells, **(F)** $RFX3^+$ ciliated cells, **(G)** $CC10^+$ club cells, or **(H)** $MUC5B^+$ goblet cells, in the transduced cells with GFP or BHLHE40-GFP on day 14. A minimum of 2000 transduced cells were counted for day 14 (n=4), $^{**}P < 0.01$, $^{***}P < 0.001$. **(I)** Bar graph showing epithelial cell quantification of the ALI culture from day 21 transduced with GFP or BHLHE40-GFP (same markers as day 14). NGFR was used as an additional basal cell marker to confirm the decrease in basal cell number (n=1). A minimum of 2000 transduced cells were counted for day 21 (n=4), $^{**}P < 0.01$, $^{***}P < 0.001$.

Also, BHLHE40-induced increase in ciliated cells was further confirmed with additional ciliated cell-specific markers on day 21. Consistent with the bulk RNA sequencing data, BHLHE40-GFP overexpressing cells had increased $FOXJ1^+$ ciliated cells, which colocalized with RSPH1 (Fig. 20A, C). In addition, a prominent co-localization of BHLHE40-GFP^+ cells with FAM161A and Acetylated Tubulin was observed (Fig. 20B). Taken together, BHLHE40 overexpression in the ALI culture on day 0 progressively increased basal cell differentiation mainly into ciliated and club cells.

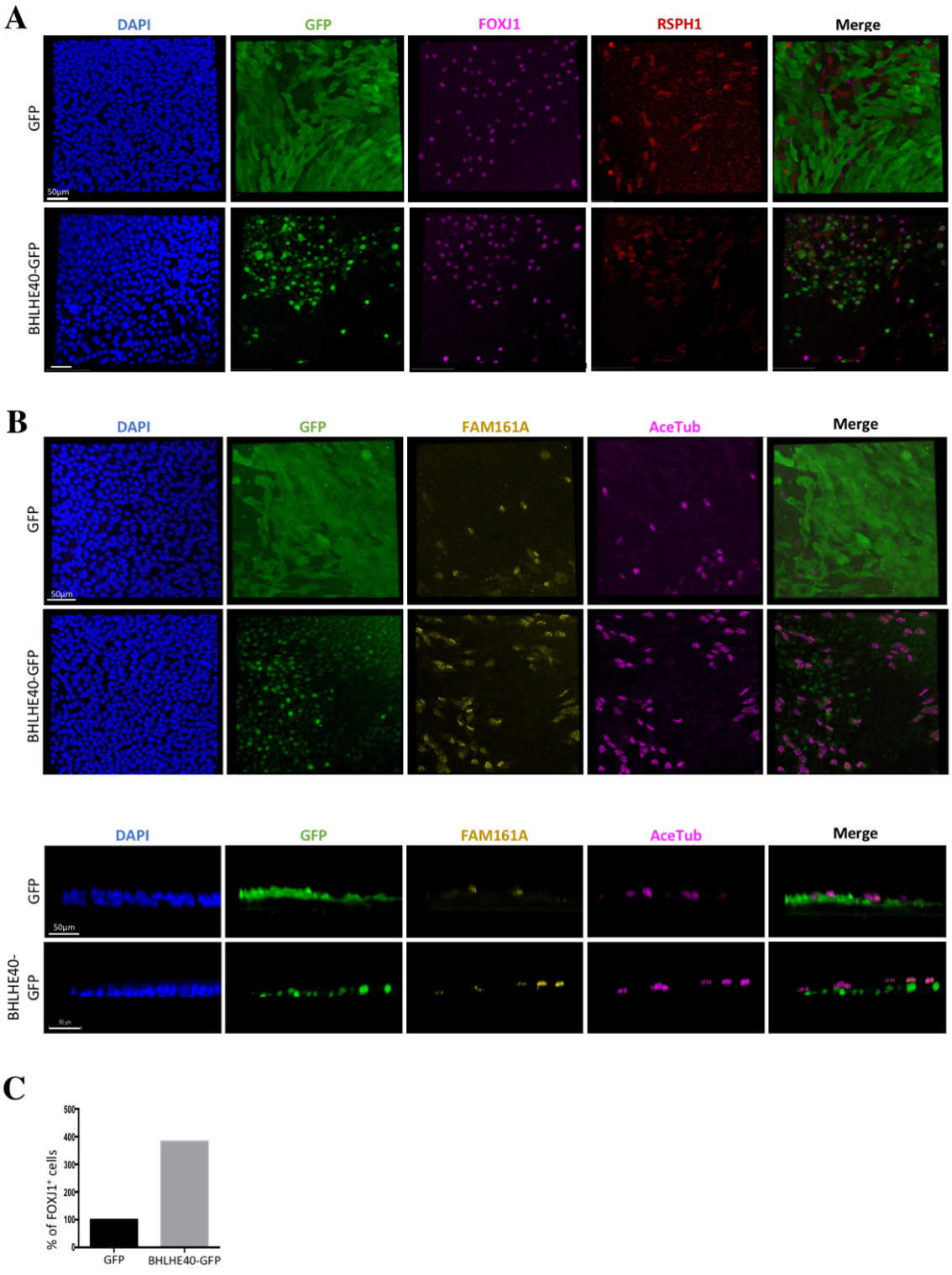

Figure 20. BHLHE40-GFP overexpression at day 0 induced an increase in ciliated cells in ALI culture. ALI culture from day 21 transduced with GFP or BHLHE40-GFP were stained with the following specific antibodies for ciliated cells: **(A)** anti-FOXJ1 and anti-RSPH1 antibodies, **(B)** anti-FAM161A and anti-Acetylated tubulin antibodies (3D reconstructions of the entire z-stack and its corresponding optical section image). All nuclei were stained with DAPI. **(C)** Quantification of FOXJ1^{+} ciliated cells in the transduced cells with GFP or BHLHE40-GFP on day 21 (n=1).

4.6 BHLHE40-GFP overexpression did not induce a precocious differentiation

To rule out the possibility that BHLHE40-induced increase in differentiated cells is due to precocious differentiation of basal cells, the transcript levels of the club cell marker *SCGB1A1* and the early ciliogenesis marker *TP73* and activator of *FOXJ1* and *RFX3* (Nemajerova et al., 2016), were analyzed in the ALI culture on day 5, a timepoint that precedes basal cell differentiation. BHLHE40-GFP overexpression was not sufficient to induce any precocious increase in *SCGB1A1* or *TP73* gene expression (Fig. 21), suggesting that BHLHE40-induced increase in differentiated cells is not due to precocious differentiation of basal cells.

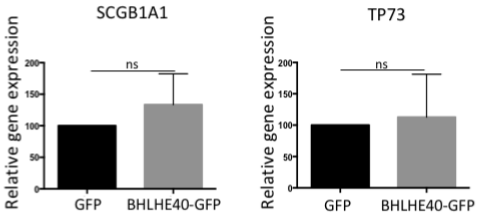

Figure 21. BHLHE40-GFP overexpression at day 0 did not induce an earlier differentiation into ciliated or club cells at ALI day 5. *SCGB1A1* and *TP73* gene expression were analyzed by Real-time qPCR in the FACS-sorted GFP$^+$ or BHLHE40-GFP$^+$ cells from ALI day 5, (n=3).

4.7 *BHLHE40* knockdown in the ALI culture reduced airway basal cell differentiation

BHLHE40 was shown to positively regulate epithelial cell differentiation into ciliated, club, and goblet cells. To test if it is necessary to drive differentiation, we knocked down *BHLHE40* starting from day 0 and fixed the ALI culture on day 14 to analyze epithelial cell differentiation (Fig. 22A). In agreement with the overexpression data, *BHLHE40* knockdown significantly increased basal cells TP63$^+$ (Fig. 22B, F) and decreased ciliated cells RFX3$^+$ (Fig. 22C, G), however, it significantly increased CC10$^+$ club cells (Fig. D, H) without affecting the number of goblet cells MUC5B$^+$ (Fig. 22E, I). The lower number of ciliated cells RFX3$^+$ was further confirmed by FOXJ1 staining (Fig. 22K, L).

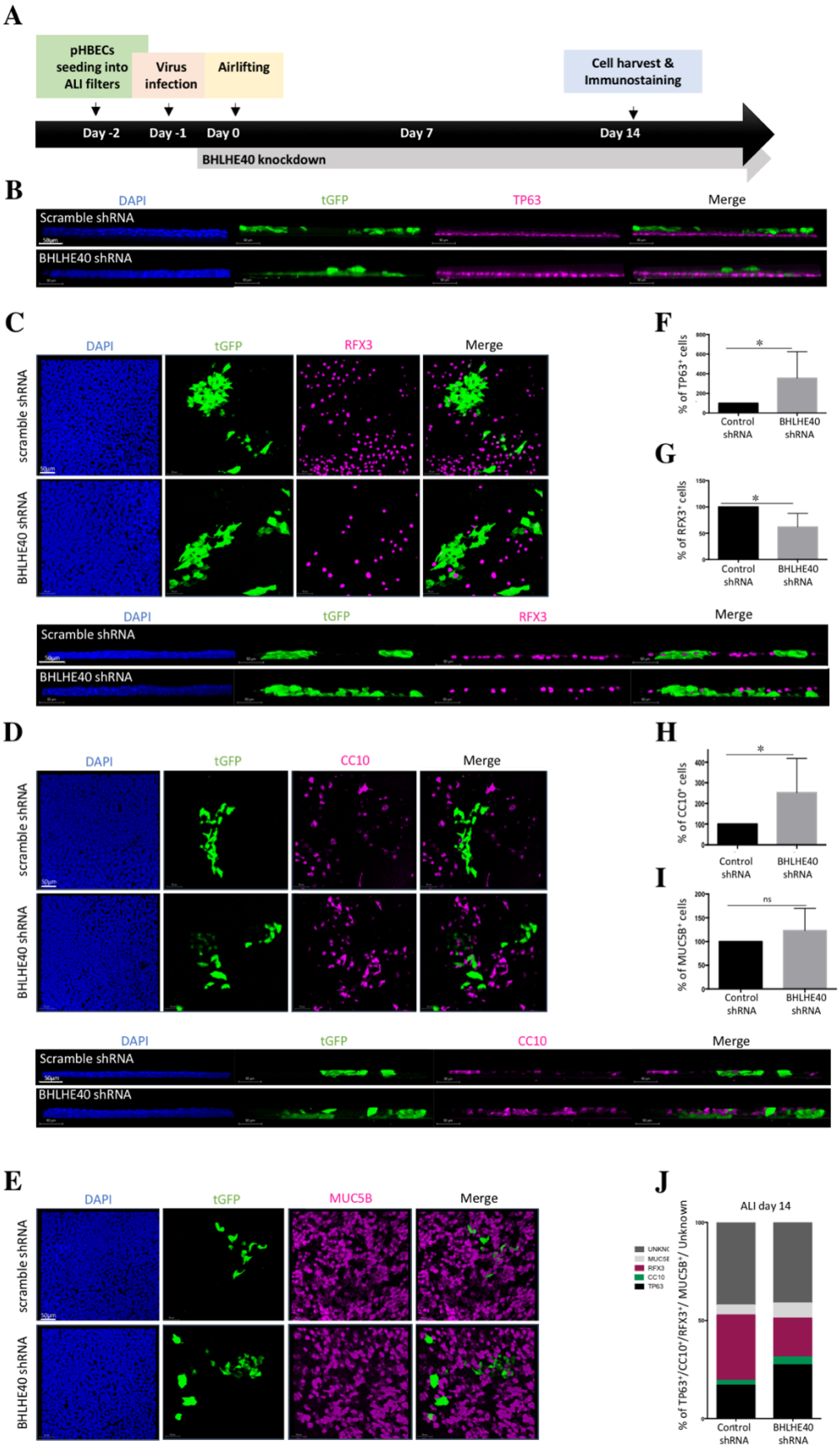
A
pHBECs seeding into ALI filters
Virus infection
Airlifting
Cell harvest & Immunostaining
Day -2
Day -1
Day 0
Day 7
Day 14
BHLHE40 knockdown
B
DAPI
tGFP
TP63
Merge
Scramble shRNA
BHLHE40 shRNA
C
DAPI
tGFP
RFX3
Merge
scramble shRNA
BHLHE40 shRNA
F
% of TP63+ cells
Control shRNA
BHLHE40 shRNA
G
% of RFX3+ cells
D
DAPI
tGFP
CC10
Merge
H
% of CC10+ cells
I
% of MUC5B+ cells
ns
E
DAPI
tGFP
MUC5B
Merge
J
ALI day 14
% of TP63+/CC10+/RFX3+/ MUC5B+/ Unknown
UNKNOWN
MUC5B
RFX3
CC10
TP63

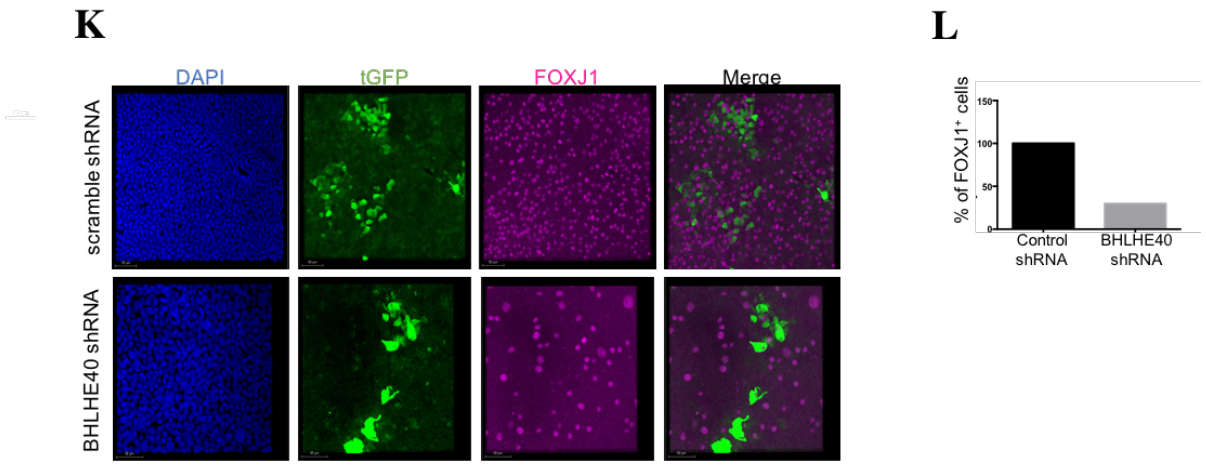

Figure 22. *BHLHE40* knockdown on day 0 reduced epithelial cell differentiation into ciliated cells on day 14. (A) Schematic representation of *BHLHE40* knockdown strategy using ALI system: cells were infected with scramble or *BHLHE40* shRNA lentiviral particles one day before airlifting. The next day, the cells were airlifted and allowed to differentiate for 14 days. Cells were fixed with 4% PFA on day 14 prior to immunostaining with epithelial cell-specific markers: **(B)** anti-TP63 (optical section image), **(C)** anti-RFX3, **(D)** anti-CC10, and **(E)** anti-MUC5B antibodies. All nuclei were stained with DAPI and transduced cells were stained with anti-turbo GFP antibody. In (C) and (D) are represented additional optical section images of the corresponding 3D reconstruction). Bar graph showing the percentage of **(F)** $TP63^+$ **(G)** $RFX3^+$, **(H)** $CC10^+$, or **(I)** $MUC5B^+$ cells, in the transduced cells with scramble or *BHLHE40* shRNA at day 14, (n=3), $^{**}P < 0.01$. **(J)** Bar graph showing the percentage of all epithelial markers grouped (TP63, CC10, RFX3, MUC5B, Unknown) in the transduced cells with scramble or *BHLHE40* shRNA on day 14 (n=3). 200 transduced cells were counted for each condition. **(K)** Transduced cells from ALI day 14 were stained with the ciliated cell marker FOXJ1. **(L)** Bar graph showing the percentage of $FOXJ1^+$ ciliated cells in the transduced cells with scramble or *BHLHE40* shRNA, (n=1).

Since the transduction efficiency with the shRNA constructs for this experiment was low, we repeated the experiment and sorted the cells expressing scramble shRNA or *BHLHE40* shRNA on day 14. We analyzed FACS sorted cells by Real-Time qPCR to evaluate gene expression of airway epithelial cells' specific markers (Fig. 23A). *BHLHE40* knockdown diminished *RFX3*, *SCGB1A1*, and *MUC5B* gene expression compared to the control but did not increase *TP63* gene expression (Fig. 23B). These findings suggest that BHLHE40 acts in an intermediate cell state $TP63^-$ to increase the differentiation rather than directly on the $TP63^+$ progenitors. Collectively, *BHLHE40* knockdown reduced epithelial cell differentiation into club, goblet, and ciliated cells.

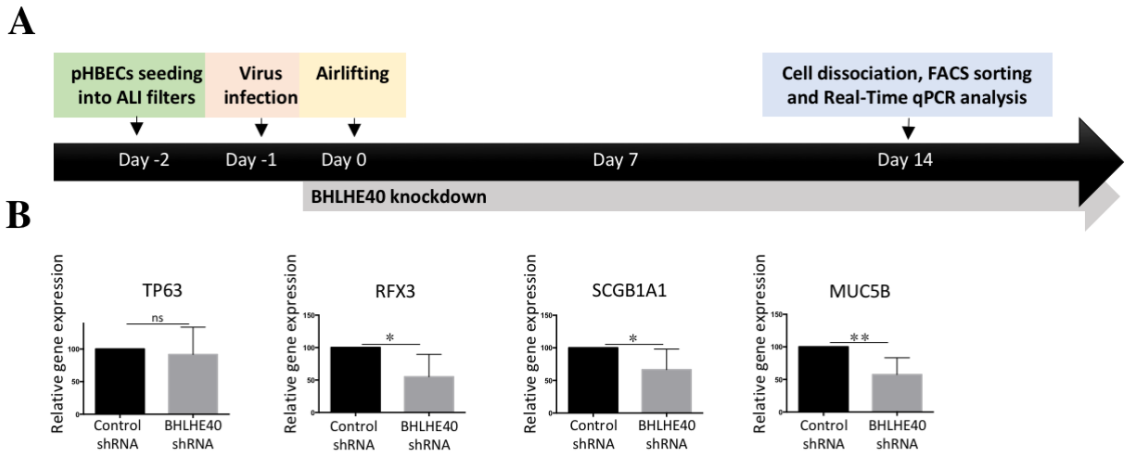

Figure 23. *BHLHE40* knockdown at day 0 reduced epithelial cell differentiation into ciliated and secretory cells without affecting basal cell gene expression at ALI day 14. **(A)** Schematic representation of *BHLHE40* knockdown strategy using the ALI culture: cells were infected with scramble or *BHLHE40* shRNA lentiviral particles. The next day, the cells were airlifted and allowed to differentiate. On day 14, the cells were dissociated with accutase for 1h at room temperature, then the transduced tGFP$^+$ cells were FACS sorted, and **(B)** gene expression of the airway epithelial markers was determined for each condition by Real-Time qPCR, (n=5) $^{**}P < 0.01$, $^{***}P < 0.001$. 5000 GFP$^+$ cells were sorted per patient per condition.

4.8 BHLHE40-GFP overexpression did not affect the total basal cell number or protein expression on days 14 and 21 of culture

Since BHLHE40 overexpressing basal cells were significantly reduced, we expected to see an overall decrease in the percentage of basal cell in the culture. To this end, we looked at the total basal cell number and protein expression on days 14 and 21. Surprisingly, BHLHE40 overexpression did neither affect the total basal cell number (Fig. 24A) nor the overall TP63 basal cell protein expression (Fig. 24B) on days 14 and 21. BHLHE40 overexpression induced the loss of basal cell fate and increased their differentiation, however, the total basal cell number remained unchanged. These data suggest the existence of a compensation mechanism for the loss of the transduced basal cells with BHLHE40 by the proliferation of non-transduced ones.

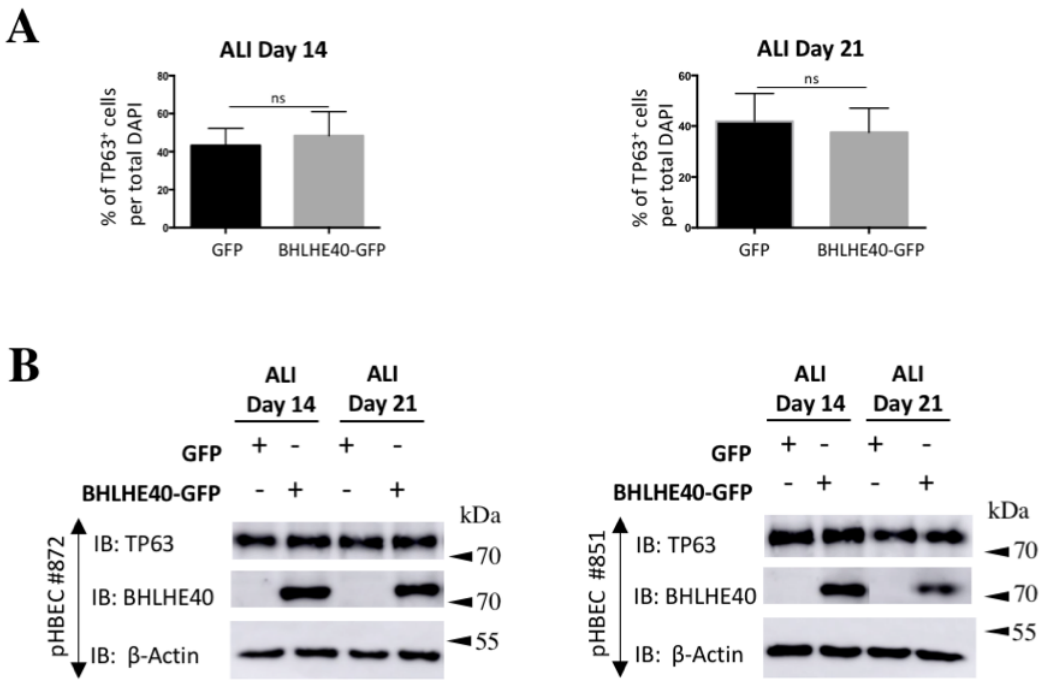

Figure 24. BHLHE40-GFP overexpression in the ALI did not affect the total basal cell number or protein expression on days 14 and 21. (A) Bar graph showing the percentage of TP63+ basal cells per total nuclei in the transduced ALI culture with GFP or BHLHE40-GFP on days 14 and 21, (n=4). (B) Lysates from transduced pHBECs with GFP or BHLHE40-GFP from ALI culture days 14 and 21 were immunoblotted and the protein expression of TP63 was determined on each timepoint (n=2). BHLHE40 antibody was used as the positive control for the overexpression and β-Actin was used as the loading control.

4.9 Compensatory proliferation of non-transduced cells likely replaced basal cell fate loss in BHLHE40-GFP overexpressing cells on day 3

BHLHE40 overexpression induced the loss of basal cell fate and increased their differentiation, however, the total basal cell number and TP63 protein expression remained unchanged compared to the control GFP transduced cells on days 14 and 21. To exclude the possibility that this is due to increased cell death of the transduced culture with control GFP, transduced cells with GFP or BHLHE40-GFP from days 1, 3, and 7 were stained with TUNEL (Terminal deoxynucleotidyl transferase dUTP Nick End Labeling) which enables the detection of DNA fragmentation during apoptosis (Fig. 25A, B). No significant difference in cell death was observed between the two conditions (Fig. 25C, D).

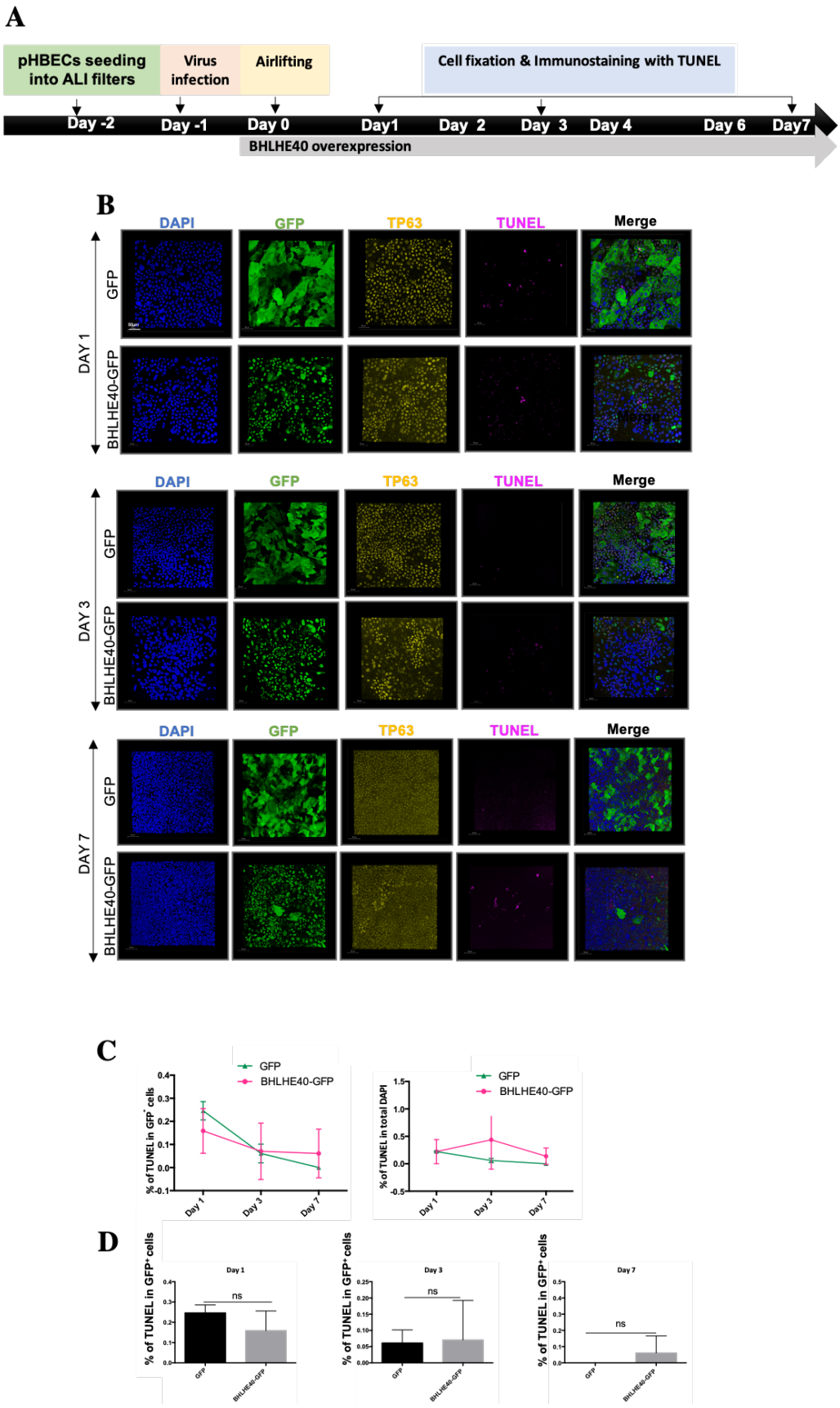
A
pHBECs seeding into ALI filters
Virus infection
Airlifting
Cell fixation & Immunostaining with TUNEL
Day -2
Day -1
Day 0
Day1
Day 2
Day 3
Day 4
Day 6
Day7
BHLHE40 overexpression
B
DAPI
GFP
TP63
TUNEL
Merge
DAY 1
DAY 3
DAY 7
BHLHE40-GFP
C
GFP
BHLHE40-GFP
% of TUNEL in GFP+ cells
% of TUNEL in total DAPI
Day 1
Day 3
Day 7
D
ns

Figure 25. BHLHE40-GFP overexpression did not affect airway epithelial cell apoptosis in the ALI culture on days 1, 3, or 7. (A) Schematic representation of the apoptosis assay strategy using the ALI system. Cells were infected with GFP or BHLHE40-GFP lentiviral particles. The next day, the cells were airlifted and allowed to grow for 7 days. Transduced cells were then fixed with 4% PFA on days 1, 3, and 7. **(B)** At each time point, the cells were stained with anti-GFP, anti-TP63 antibodies, and TUNEL. Nuclei were stained with DAPI. **(C)** Quantification data showing the percentage of TUNEL-positive cells in the transduced cells with GFP/BHLHE40-GFP or in total DAPI on days 1, 3, and 7. **(D)** Bar graph showing the percentage of TUNEL-positive cells in the transduced cells with GFP or BHLHE40-GFP on individual time points (n=3), *P < 0.05. A minimum of 1300 nuclei was counted for day 1-day 3 and 4000 nuclei for day 7.

To investigate the existence of a compensation mechanism for the loss of the transduced basal cells with BHLHE40 by the proliferation of non-transduced ones, the pHBECs in the ALI culture were treated with the DNA intercalating dye 5-ethynyl-2-deoxyuridine (EdU) for 16 hours on days 0, 2, 6, and 13, then fixed and stained the following days to check their proliferation (Fig. 26A). The proliferation of the non-transduced cells in the BHLHE40-GFP culture on days 1, 7, and 14 did not show any significant change, however, on day 3, the number of EdU^+ cells was significantly increased in the non-transduced cells in BHLHE40-GFP culture compared to the GFP transduced culture (Fig. 26B). Consistent with the previously observed BHLHE40-induced decrease in basal cell number, no significant increase in the proliferation of BHLHE40-GFP overexpressing basal cells was observed at any of the time points (Fig. 26C). Taken together, our results suggest the presence of a compensatory proliferation by the non-transduced cells in BHLHE40-GFP culture from day 3, which suggest a paracrine regulation between these two-cell populations.

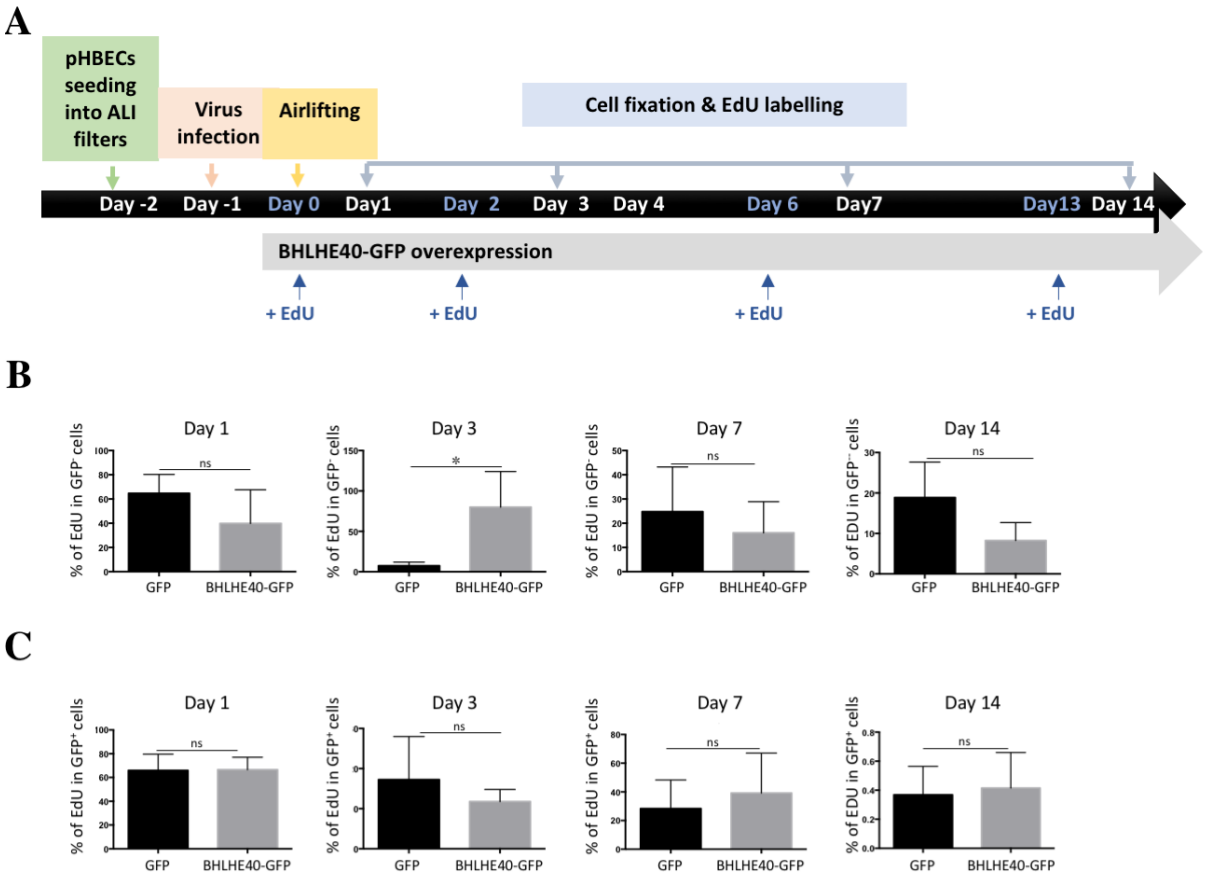

Figure 26. BHLHE40-GFP overexpression increased the proliferation of the non-transduced cells on day 3. (A) Schematic representation of the proliferation assay strategy using the ALI system. **(B)** Bar graph showing the percentage of EdU^- cells in the non-transduced cells in GFP or BHLHE40-GFP infected culture at days 1, 3, 7, and 14 (n=3), **(C)** Bar graph showing the percentage of EdU^+ cells in the transduced cells with GFP or BHLHE40-GFP infected cultures from (B).

4.10 BHLHE40 overexpression interfered with Notch signaling genes on day 14

BHLHE40-GFP overexpression increased human basal cell differentiation into ciliated, club, and goblet cells in the ALI culture on days 14 and 21. To investigate potential signaling pathway(s) involved in this phenotype, we looked at the bulk RNA sequencing data from the sorted BHLHE40-GFP cells from the ALI culture day 14. Since Notch signaling is known to be involved in airway epithelial cell differentiation (Rock et al., 2011; Stupnikov et al., 2019a; Tsao et al., 2009), the genes related to these pathways were analyzed. An overall decrease in Notch signaling genes was observed in BHLHE40-GFP overexpressing cells: Notch receptors (*NOTCH 1*, *NOTCH2*, *NOTCH3*, *NOTCH 4*), ligands (*JAG1*, *JAG2*, *DLL1*), and downstream effectors (*HEY1*, *HEY2*, *HES1*, *HES2*, *HES4*) had lower transcript levels. In contrast, Notch inhibitors *HES6*, *CIR1*, and *SAP30* known to be expressed in ciliated cells (Ruiz Garcia et al., 2019) had a higher expression in BHLHE40-GFP overexpressing cells

(Fig. 28A), consistent with the previously observed increase in ciliated cells in BHLHE40-GFP overexpression experiment.

A set of Notch signaling genes were analyzed by Real-Time qPCR for 3 biological replicates. Consistent with the bulk RNA sequencing data, BHLHE40-GFP overexpressing cells had a significantly lower level of the Notch receptors (*NOTCH1*), ligands (*JAG1*, *JAG2*, *DLL1*), and downstream effector (*HES1*). Also, BHLHE40-GFP overexpressing cells had a significantly higher expression of *HES6* (Fig. 28B). To better understand these changes in gene expression, we review literature about cell type-specific expression of Notch signaling genes in the human epithelium. Based on the single-cell RNA sequencing data of human nasal epithelial culture, *JAG1/2*, *DLL1*, and *NOTCH1* were mainly expressed in $TP63^{+}$ basal cells (Ruiz Garcia et al., 2019) (Fig. 28C). Accordingly, their lower expression in BHLE40-GFP overexpressing cells might be due to the lower proportion of basal cells in this sorted fraction compared to the control GFP sort. Similarly, the increased expression of *HES6* transcript in BHLE40-GFP overexpressing cells might be due to the higher proportion of ciliated cells in this sort compared to the control GFP sort. Taken together, this data indicates that the observed changes in Notch signaling gene expression might not be a direct effect of BHLHE40-GFP overexpression but rather due to differences in cell type proportion in the sorted cells between the two conditions.

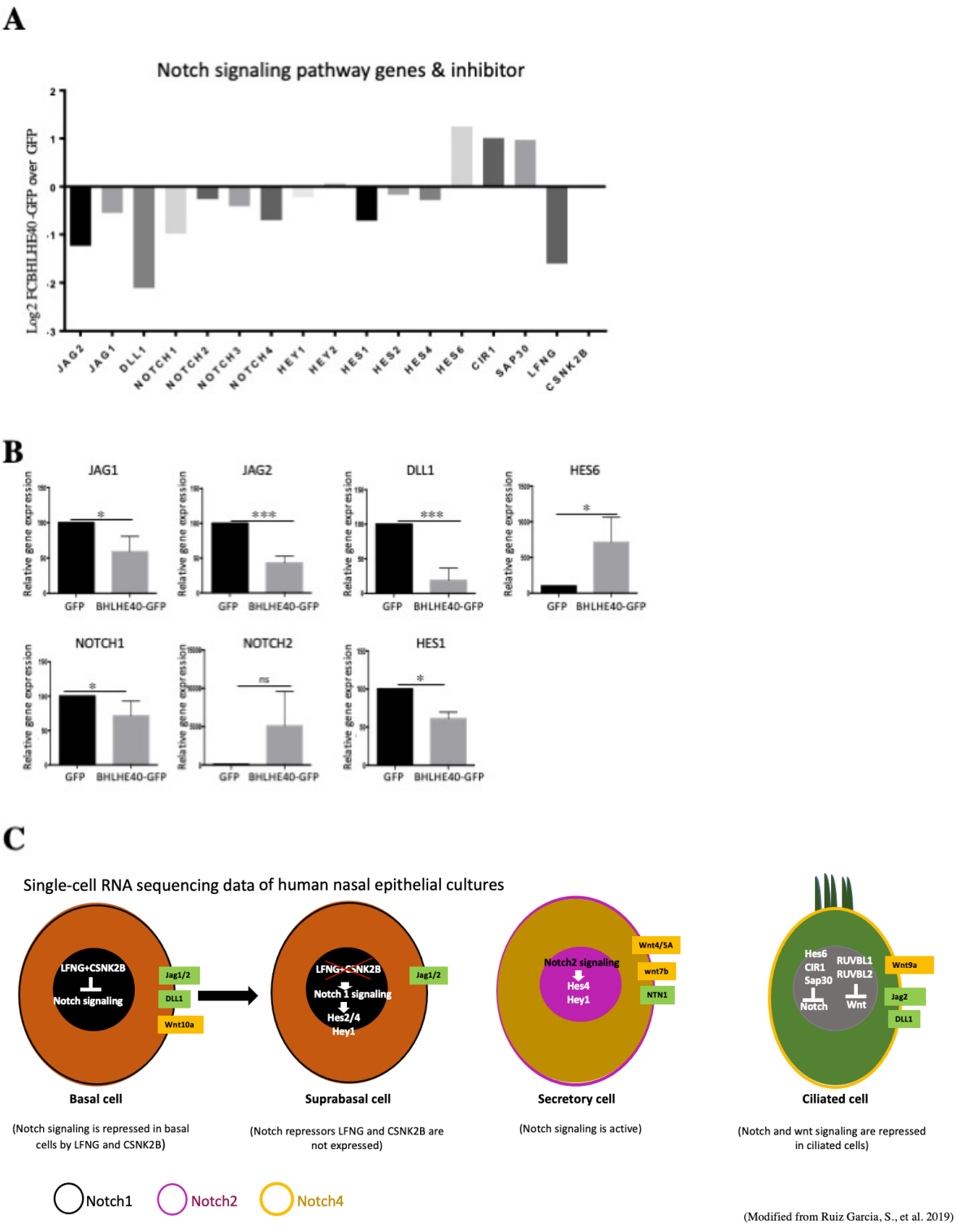

Figure 27. BHLHE40 overexpression correlates with a decreased Notch signaling gene expression in the ALI culture from day 14. (A) The log2FC of differentially expressed Notch-related genes and inhibitors in the FACS sorted BHLHE40-GFP⁺ cells compared to the GFP⁺ cells from ALI day 14 (n=1). **(B)** Real-time qPCR analysis of Notch signaling gene expression in the FACS sorted cells GFP⁺ or BHLHE40-GFP⁺ from the ALI culture day 14 (n=3), $*P < 0.05$, $***P < 0.001$. 5000 GFP⁺ cells were sorted per patient per condition, to validate the bulk sequencing data in Supl.Fig.4C. **(C)** Cell type-specific Notch signaling genes expression in human nasal epithelial cells based on single-cell RNA sequencing.

4.11 BHLHE40 overexpression did not increase ciliated cells at the expense of club cells on day 21 (day 10 induction)

Previous studies have shown that the inhibition of the NOTCH2 receptor in club cells leads to their trans-differentiation into ciliated cells in mice (Danahay et al., 2015). Since BHLHE40-induced increase in ciliated cells on day 14 correlated with a significant downregulation of Notch signaling genes, including *NOTCH2* and *HES1*, which are known to positively regulate the club cell fate (Morimoto et al., 2012), we hypothesized that BHLHE40 overexpression represses *NOTCH2* signaling in club cells, which in turn induces their trans-differentiation into ciliated cells (Fig. 28A). To this end, a lentiviral plasmid with a doxycycline-inducible promoter *(*Tet-On system) was used. The pHBECs in the ALI culture were transduced with BHLHE40-FLAG lentiviral particles and the overexpression was induced on day 10, when club cells $CC10^{+}$ begin to appear in the culture. The epithelial cell differentiation was then analyzed on day 21 (Fig. 28B). BHLHE40-FLAG overexpression decreased $TP63^{+}$ basal cell number. Consistent with the overexpression data from day 0, nearly all basal cells transduced with BHLHE40-FLAG shifted to the luminal layer as shown in the optical section of the ALI culture (Fig. 28C, G), suggesting that BHLHE40 later induction also negatively regulates the basal cell fate.

Furthermore, BHLHE40-FLAG-induced decrease in basal cells was confirmed with NGFR immunostaining (Fig. 28F, J). In addition, BHLHE40-FLAG overexpression increased differentiation toward ciliated cells $FOXJ1^{+}$ but also club cells $CC10^{+}$ (Fig. 28D, H, E, I). Taken together, BHLHE40-FLAG overexpressing cells did not show any reduction in club cell number at the detriment of ciliated cells, therefore it is unclear whether the BHLHE40-induced increase in ciliated cells arises from club cell trans-differentiation.

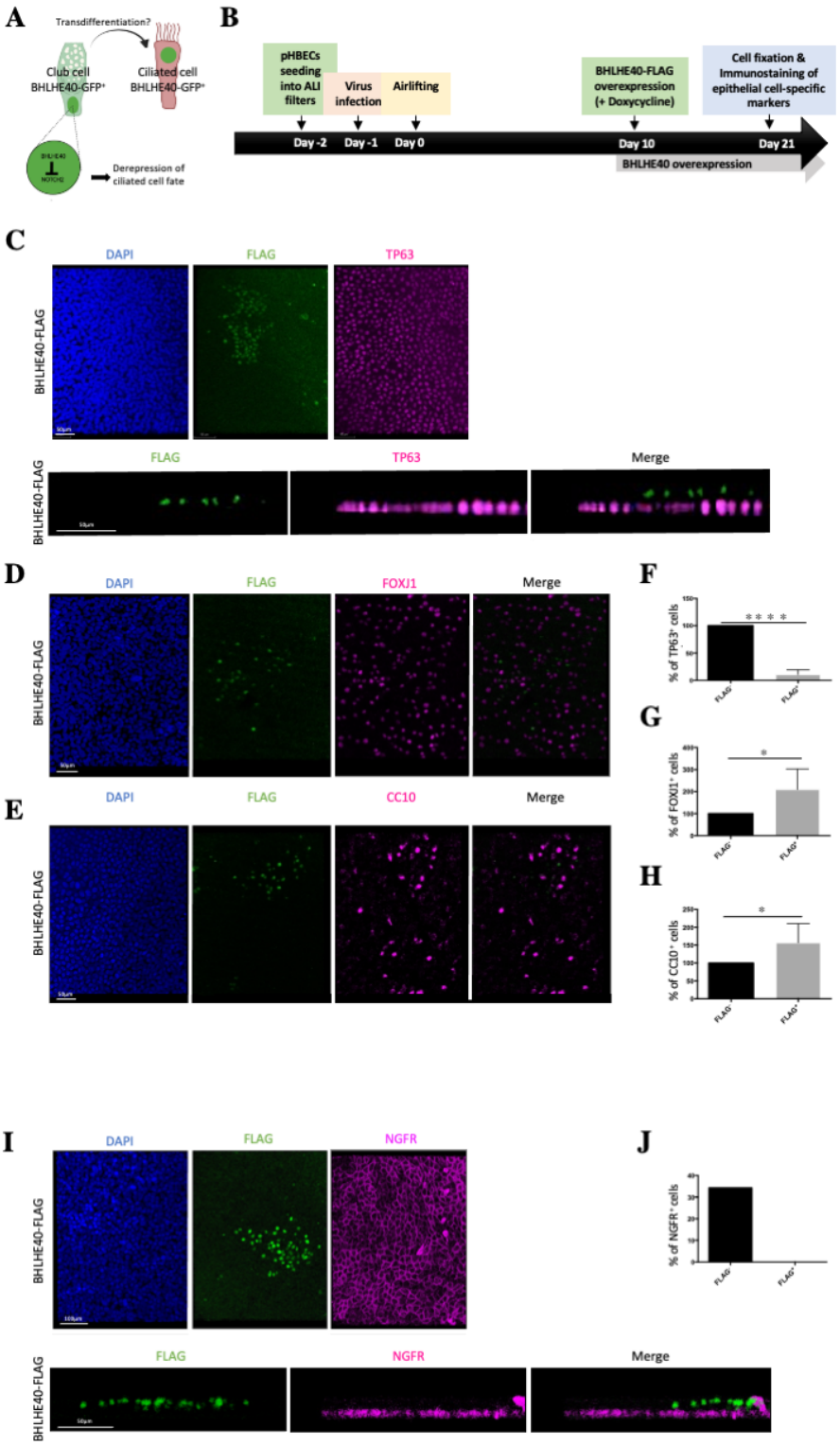

Figure 28. BHLHE40-FLAG overexpression on day 10 in the ALI increased in airway epithelial cell differentiation on day 21. (A) Proposed model: BHLHE40 represses Notch signaling in club cells, which in turn transdifferentiate into ciliated cells**. (B)** Schematic representation of BHLHE40-FLAG overexpression strategy using the ALI culture: primary cells were seeded in ALI filters and infected the next day with BHLHE40-FLAG lentiviral particles. The next day, the cells were airlifted and allowed to grow and differentiate over 21 days. BHLHE40-FLAG overexpression was induced on day 10 by adding doxycycline to the culture medium and cells were fixed with 4% PFA on day 21 prior to immunostaining

with epithelial cell-specific markers and confocal microscopy imaging. Airway epithelial cells transduced with BHLHE40-FLAG were stained on day 21 with the following specific antibodies for differentiation markers: **(C)** anti-TP63, **(D)** anti-FOXJ1, and **(E)** anti-CC10 antibodies. Anti-FLAG antibody was used to stain the transduced cells. In (C) and (I) are represented additional optical section images of the corresponding 3D reconstruction). **(F-G-H)** Bar graph showing the percentage of $TP63^+$ basal cells, $FOXJ1^+$ ciliated cells, and $CC10^+$ club cells, respectively, in the non-transduced ($FLAG^-$) or transduced cells with BHLHE40-FLAG ($FLAG^+$) on day 21 (n=4), $^{**}P < 0.01$, $^{***}P < 0.001$. 200 to 400 transduced cells were counted. **(I)** Airway epithelial cells transduced with BHLHE40-FLAG from day 21 were also stained for an additional basal cell marker using an anti-NGFR antibody. **(J)** Bar graph showing the percentage of $NGFR^+$ basal cells in $FLAG^-$ or $FLAG^+$ cells on day 21 (n=1).

4.12 BHLHE40 overexpression increased ciliated cells at the expense of club cells on day 28

As previously described, nearly all basal cells overexpressing BHLHE40-GFP had lost the basal cell fate and were found at the luminal surface by day 21. In this context, we thought that an extended culture would exclude any ‘’differentiation effect’’ from the basal cells overexpressing BHLHE40-GFP and would indicate if the increase in ciliated cells originates from the club cell trans-differentiation. For this purpose, we cultured the transduced pHBEC in ALI culture for 28 days, then FACS sorted the cells overexpressing GFP or BHLHE40-GFP, and analyzed epithelial marker gene expression. BHLHE40-GFP overexpressing cells show increased ciliated cell gene expression (*FOXJ1*, *TP73*, *MYB*) and decreased club cell gene expression (*SCGB1A1*), while the goblet cell marker *MUC5B* was still increased (Fig. 29). Even though the club cell marker *SCGB1A*1 was decreased, BHLHE40 overexpressing cells had increased *NOTCH2* gene expression, which can be attributed to the increased expression of the goblet cell marker *MUC5B*, as NOTCH2 has been shown to positively regulate also *MUC5B* gene expression (Danahay et al., 2015). Our data indicate that BHLHE40-induced increase in the ciliated cells may arise from club cell potential trans-differentiation, however further analysis with a larger number of biological replicates is needed to confirm this finding.

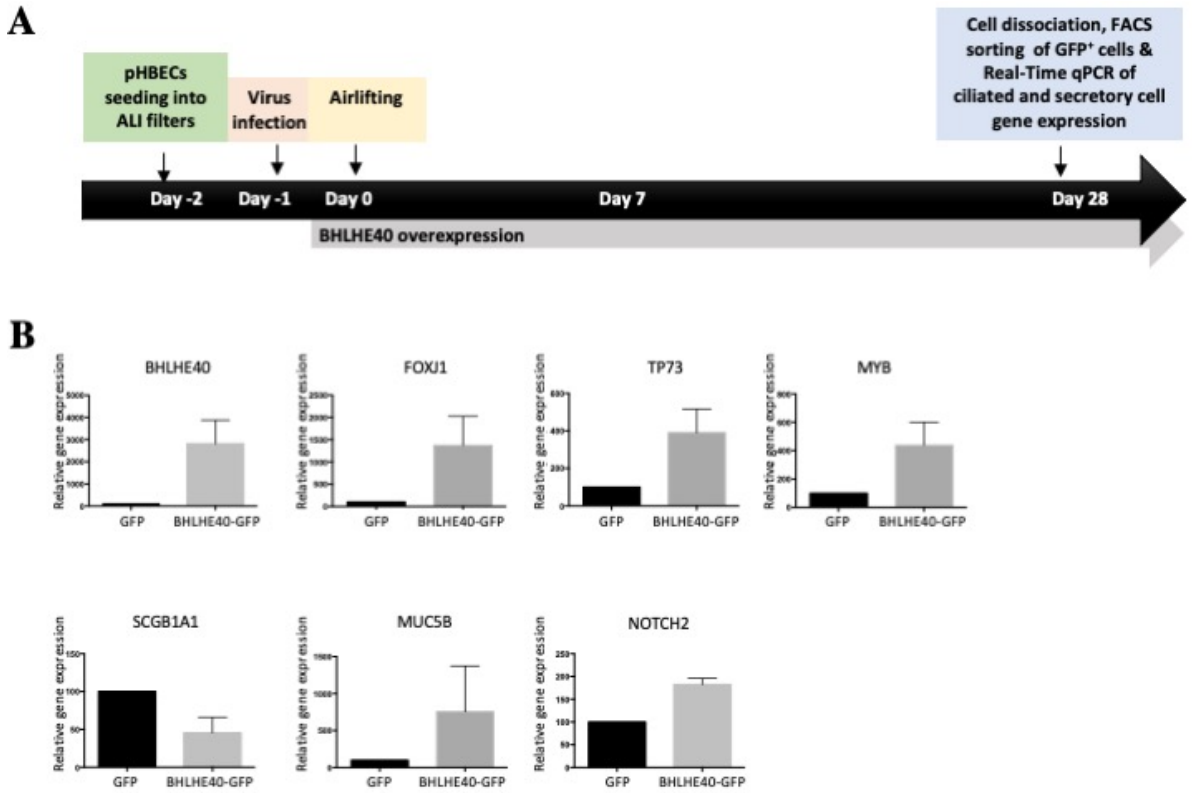

Figure 29. BHLHE40 overexpression increased ciliated and decreased club cell gene expression on day 28 of culture. (A) Schematic representation of BHLHE40-GFP overexpression experimental setup using the ALI system: cells were infected with GFP or BHLHE40-GFP lentiviral particles one day before airlifting. The next day, the cells were airlifted and allowed to differentiate. On day 28, the cells were dissociated with accutase for 1h at room temperature and the transduced GFP$^+$ cells were FACS sorted prior to gene expression analysis**. (B)** Real-time qPCR analysis of ciliated, club, goblet cell, and Notch-related gene expression in the FACS sorted cells GFP$^+$ or BHLHE40-GFP$^+$ from the ALI culture day 28. BHLHE40 gene expression was analyzed as the positive control. Statistical analysis was not performed due to the low number of biological replicates (n=2).

4.13 Identification of BHLHE40 transcriptional target involved in the basal-to-intermediate cell transition

4.13.1 Correlation of known BHLHE40 transcriptional targets with the human single-cell RNA sequencing data (pseudo-time analysis)

To understand how the transcription factor BHLHE40 negatively regulates basal cell fate, it is important to identify its potential direct transcriptional targets. To this end, we first compared the published BHLHE40 A549 ChIP-sequencing peaks to our differentially expressed transcription factors in the differentiation trajectory from the SMG-like basal cell-to-immature secretory-to-secretory cells. Since BHLHE40 is mainly described as a transcriptional repressor (Sun & Taneja, 2000), we reasoned that the genes that are downregulated upon *BHLHE40* upregulation are more likely to represent potential direct

transcriptional targets. For this purpose, we selected for this comparison only the 27 transcription factors that are upregulated in the SMG basal-like cluster and downregulated later in the immature secretory cell cluster upon *BHLHE40* upregulation (Fig. 30A). The correlation ended up in 8 potential transcriptional target genes (Fig. 30B). Second, to analyze whether BHLHE40 DNA binding to these targets is associated with their repression (Fig. 30C, D), we overexpressed BHLHE40-GFP in A549 cell lines and analyzed their gene expression 72 hours post-infection. Our result indicates that BHLE40 represses the expression of *FOS*, *HIF1α*, *MYC*, and *HMGA2*, but not *SOX9* (*BNC1*, *ZFP36L1*, and *FOSL1* could not be detected by Real-Time qPCR).

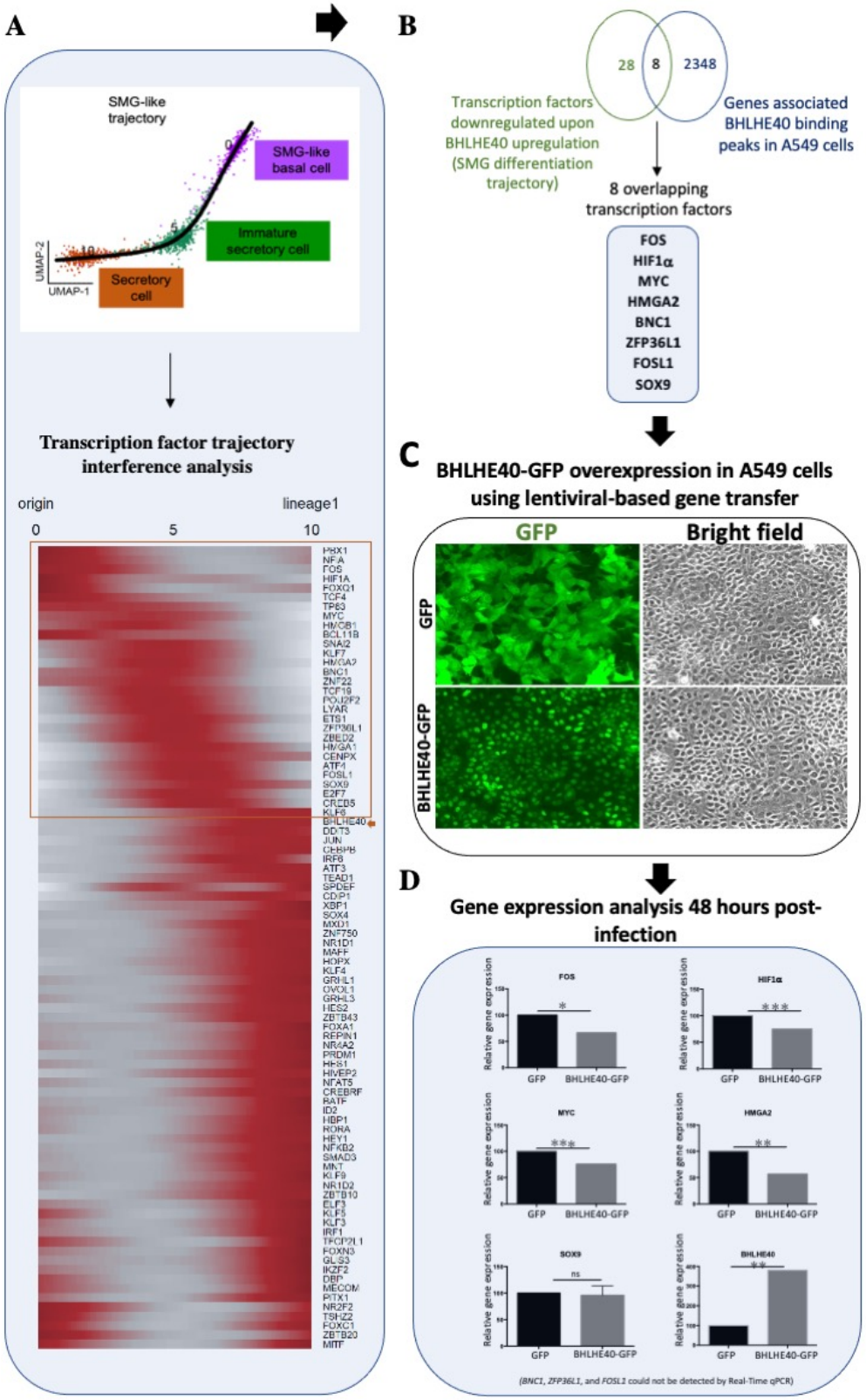

Figure 30. The strategy of selection of putative BHLHE40 transcriptional targets. **(A)** The differentially expressed transcription factors in the differentiation trajectory from the SMG-like basal cell-to-immature secretory-to-secretory cells were compared to the peaks from BHLHE40 ChIP-sequencing

data (A549 cell lines). The 27 genes selected for the comparison are shown in the box (these are the genes downregulated upon *BHLHE40* upregulation, which are more likely to be direct targets). **(B)** The comparison resulted in 9 transcription factors that are described to be direct transcriptional targets of BHLHE40 in A549 cell lines. **(C)** A549 cells were transduced with GFP or BHLHE40-GFP encoding lentiviral particles and **(D)** gene expression of the 8 identified transcription factors was analyzed 72 hours post-infection (n=3). *BHLHE40* gene expression was analyzed as a positive control for the overexpression.

4.13.2 Validation of BHLHE40 potential transcriptional targets using anti-BHLHE40 antibody in isolated nuclei (CUT&RUN)

To confirm BHLHE40 binding to the previously identified potential transcriptional targets in our ALI culture, we performed CUT&RUN experiments in differentiating epithelial cells from day 14. CUT&RUN is a technique used to specifically isolate the DNA regions bound by the protein of interest. BHLHE40-GFP was overexpressed from day 0 and transduced cultures were collected and dissociated using accutase on day 14 followed by nuclei isolation, then subjected to CUT and RUN experiment: the process begins with the target-specific primary antibody anti-BHLHE40 that binds to the protein of interest associated with chromatin. Then, a Protein A-Micrococcal Nuclease (MNase) fusion protein is introduced, where Protein A directly binds to the Fc region of the primary antibody anti-BHLHE40, bringing MNase in proximity to the target site. Upon activation by calcium ions (Ca^{2+}), MNase selectively cleaves DNA near the protein-DNA complex, generating precise DNA fragments. These fragments are then isolated and analyzed using Real-time qPCR with specific primers designed for the genomic regions of the selected targets. Interestingly, BHLHE40 bound to *HIF1α*, *BNC1*, *FOSL1*, *MYC*, *HMGA2*, and *ZFP36L1* at the described genomic regions, with varying levels of DNA enrichment (Fig. 31A). However, it did not bind to *FOS* enhancer region, nor to *HIF1α* coding sequence, which was used as a negative control. After that, to investigate whether BHLHE40 DNA binding to these targets is associated with their repression, we repeated BHLHE40-GFP overexpression experiment in the ALI culture and sorted the cells on day 14 to analyze gene expression. Among the 6 targets previously identified to be bound with BHLHE40, only *BNC1* was significantly reduced under BHLHE40 overexpression (Fig. 31B). Our result indicates that BHLHE40 transcriptionally represses the expression of the putative zinc finger transcription factor *BNC1*, but did not affect *HIF1α*, *FOSL1*, *MYC*, *HMGA2*, and *ZFP36L1* gene expression.

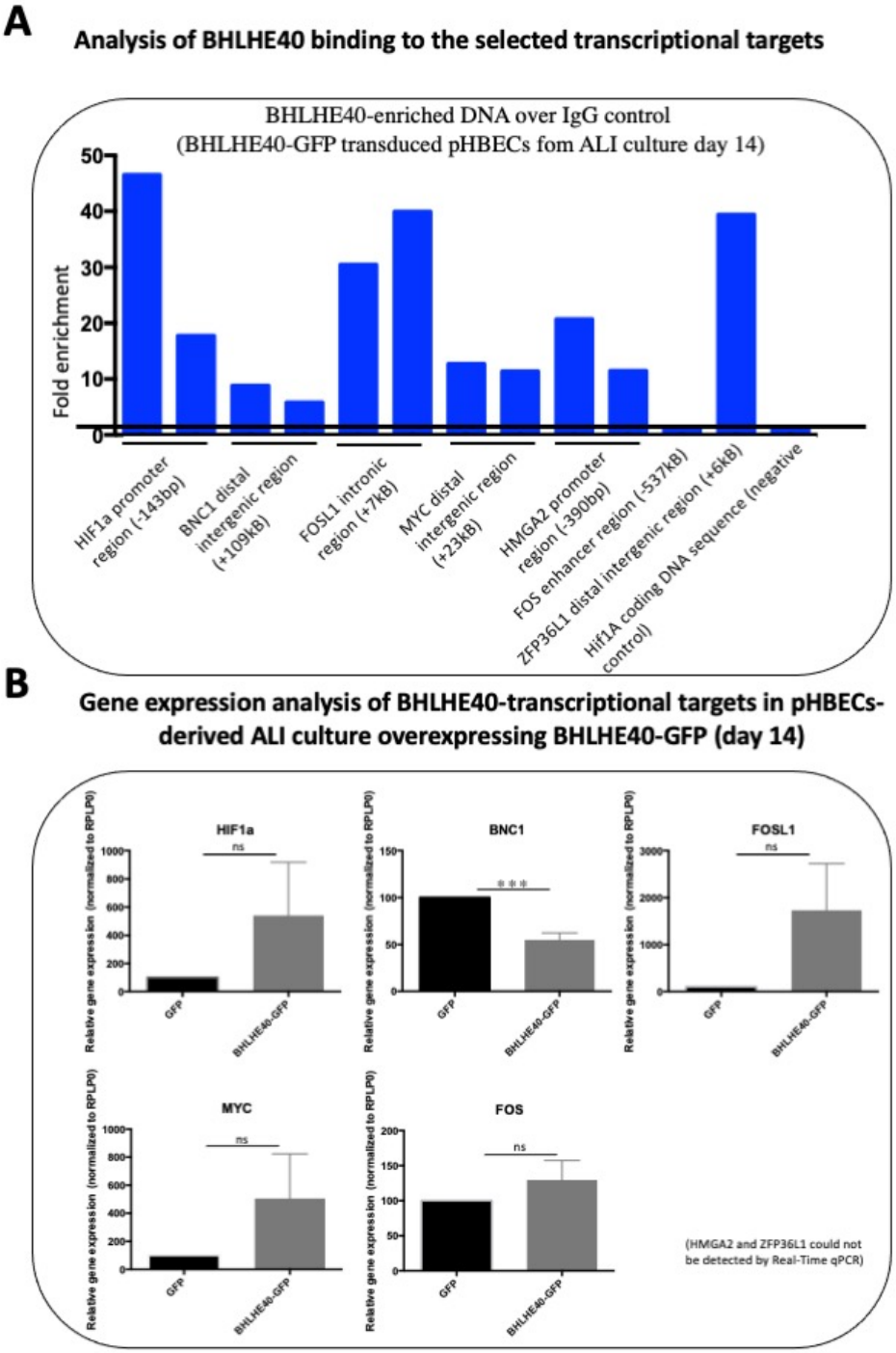

Figure 31. BHLHE40 transcriptionally represses BNC1 expression among the selected transcriptional targets. (**A**) Detection of BHLHE40 binding to the described genomic regions of the selected transcriptional targets, in ALI culture day14, using CUT&RUN Real-Time qPCR. IgG antibody was used as the negative control. **(B)** Gene expression of the 7 selected targets was analyzed by Real-time qPCR in FACS-sorted cells overexpressing GFP or BHLHE40-GFP from the ALI culture day 14 (n=3).

4.13.3 BHLHE40 overexpression decreased BNC1 expression exclusively in basal cells

To confirm that BNC1 protein expression is specific to basal cells, we analyzed its expression on day 14 by immunostaining (Fig. 32A, B). In addition to its specificity for SMG-like basal cells, as demonstrated in our previous pseudotime analysis of differentiating ALI cultures (Fig. 31A), BNC1 also shows specificity to the basal cells, where 99% of BNC1+ cells were $TP63^{+}$ on day 14 (Fig. 32A, B, C). Also, consistent with BHLHE40-mediated transcriptional repression of BNC1, BHLHE40 overexpression reduced the number of BNC1 expressing cells in the basal layer (Fig. 32D): 20% of BNC1+ cells in BHLHE40-GFP+ cells compared to 65% in control GFP+ cells; however, statistical significance could not be assessed due to the low number of biological replicates (n=2). Taken together, BHLHE40 overexpression is likely to reduce BNC1-positive cells specifically in the basal layer, a trend further supported by previous results showing BHLHE40-mediated transcriptional repression of *BNC1*. Nevertheless, further studies with a larger number of biological replicates are needed to confirm this observation.

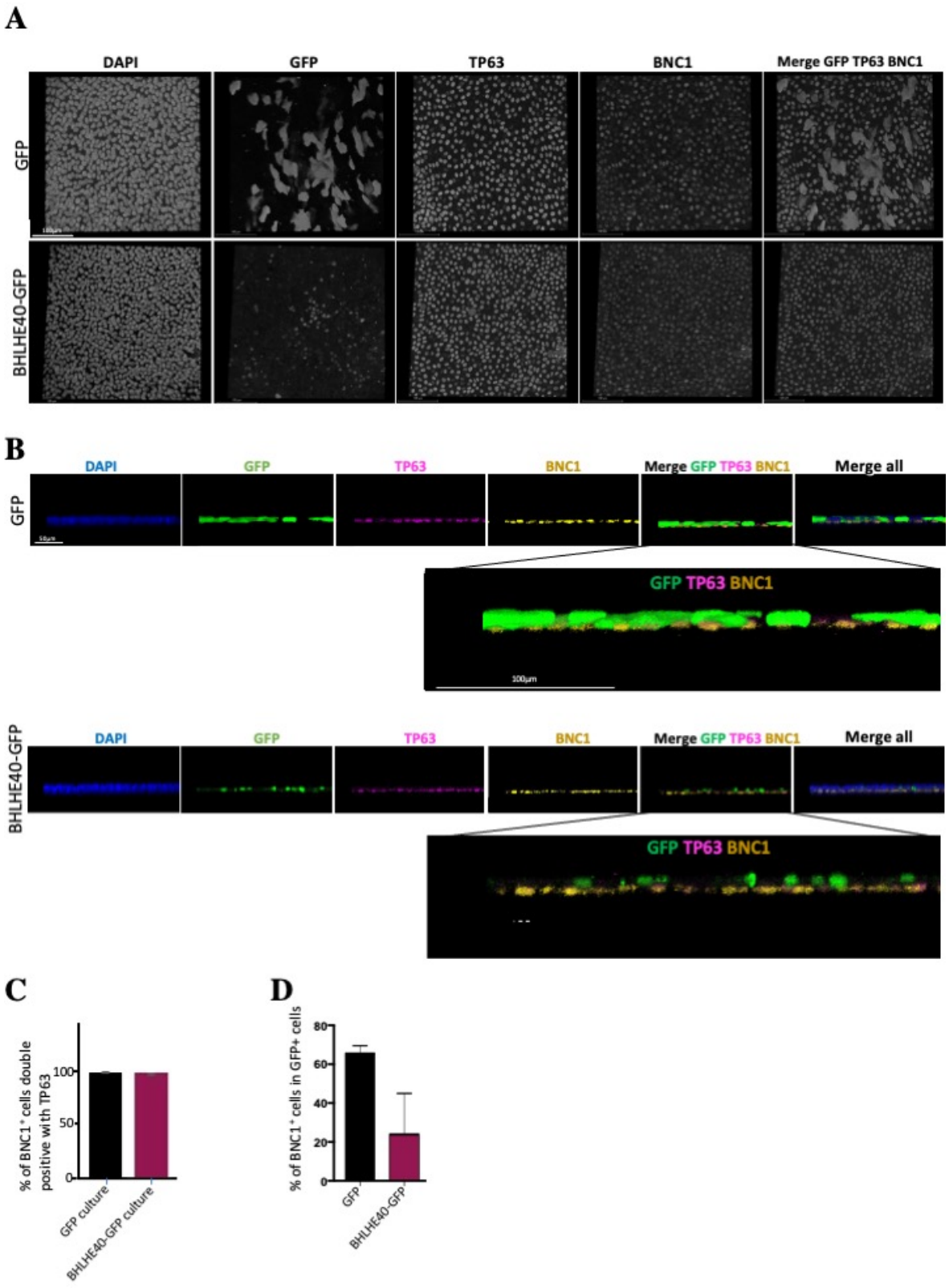

Figure 32. Overexpression of BHLHE40 decreases BNC1-positive cells, exclusively localized to the basal layer. ALI cultures from day 14 transduced with GFP or BHLHE40-GFP were stained with anti-GFP (transduced cells), anti-TP63, and anti-BNC1 antibodies. All nuclei were stained with DAPI. Confocal images from **(A)** the 3D reconstructions of the entire z-stack and **(B)** their corresponding optical section images showing BNC1 exclusive localization to the basal layer. **(C)** Quantification of BNC1$^+$ cells

that are double positive with TP63 or (**D**) double positive with GFP$^+$ transduced cells from ALI culture day 14. Statistical analysis was not performed due to the low number of biological replicates (n=2).

Our results indicate that the overexpression of BHLHE40 is likely to directly decrease *BNC1* expression in the basal layer via transcriptional repression, leading to a reduction in basal cell gene expression and facilitating the transition to an intermediate cell state (Fig. 33).

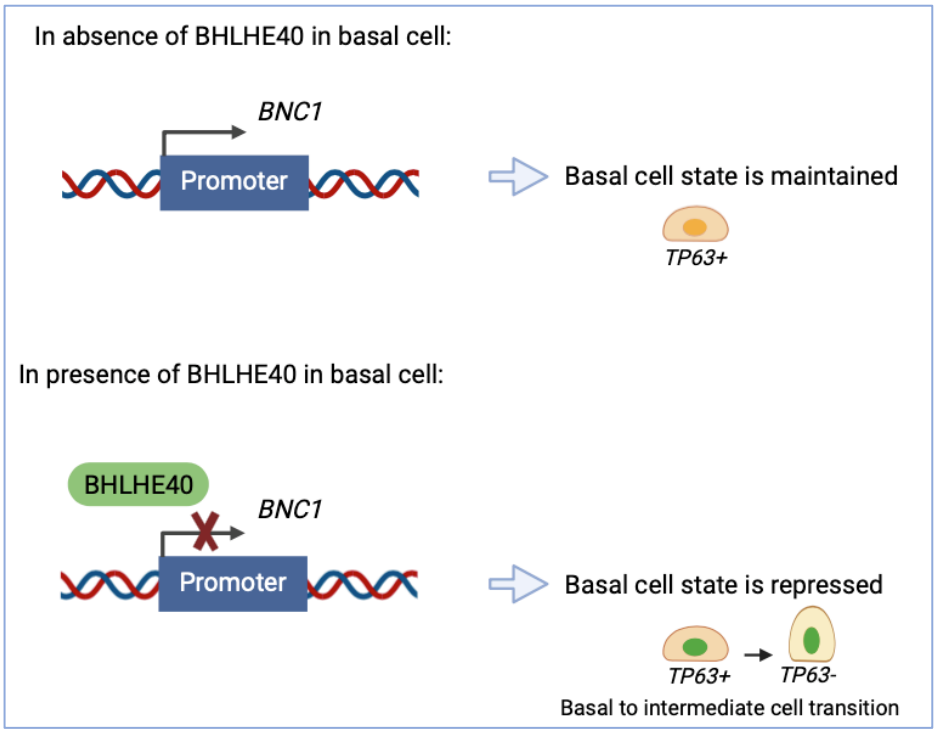

Figure 33. Proposed model depicting BHLHE40-induced transition from basal to intermediate cells through direct transcriptional repression of *BNC1*. In the absence of BHLHE40, *BNC1* is expressed in basal cells and maintains their undifferentiated state. However, when BHLHE40 is present in basal cells, it transcriptionally represses the expression of *BNC1*, consequently leading to basal cell transition to an intermediate cell and loss of basal cell marker gene expression.

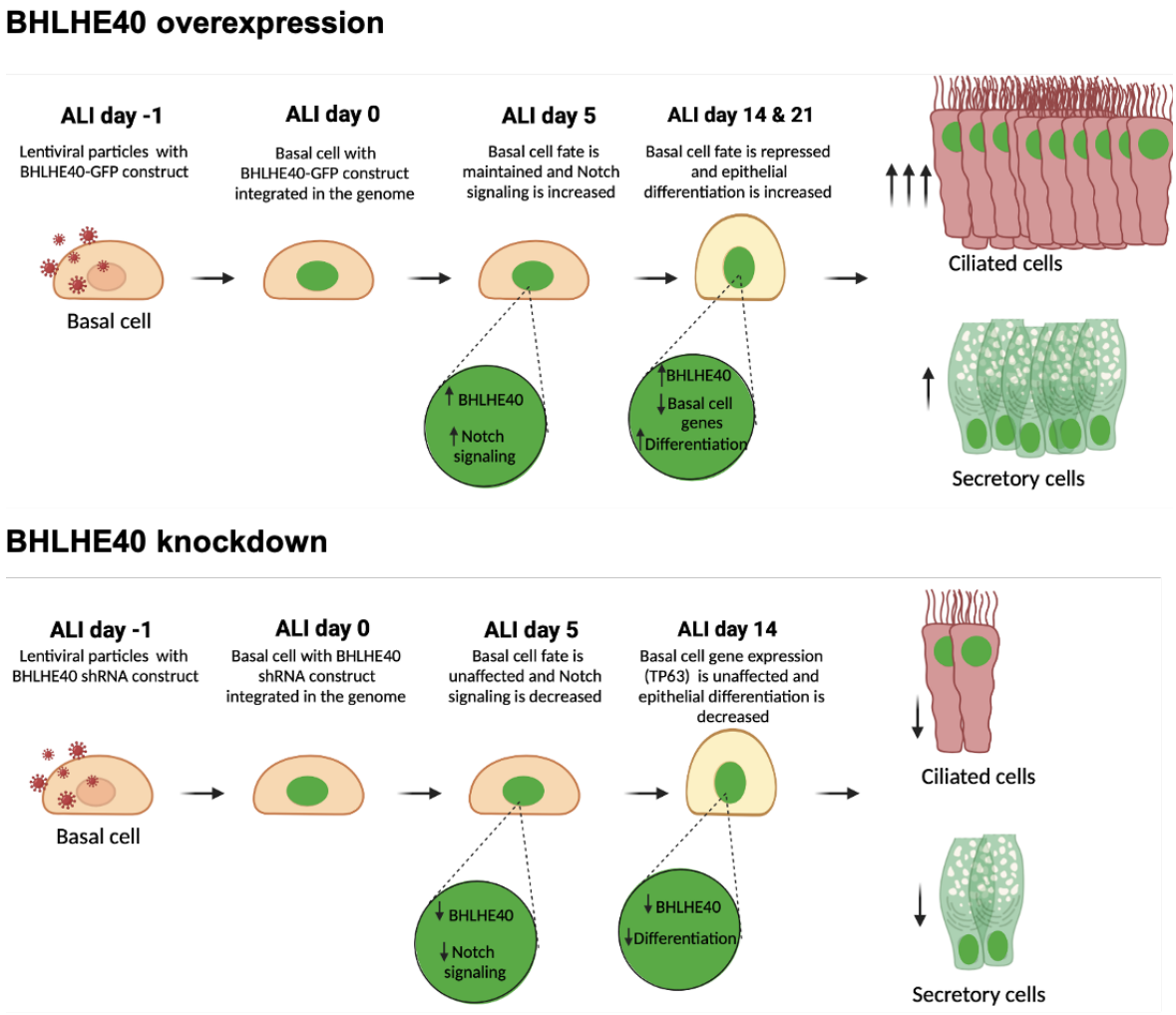

Figure 34. Schematic summary of BHLHE40 results in the ALI. Before differentiation, on day 5, BHLHE40 overexpression or knockdown in the ALI did not affect basal cell gene expression but increased or decreased Notch signaling, respectively. The increase in Notch signaling was followed by a gradual loss of basal fate during differentiation, which correlated with an increase in club, goblet, and predominantly ciliated cells. Consistently, *BHLHE40* knockdown reduced epithelial cell differentiation**.** Also, BHLHE40 overexpression did not affect basal cell proliferation or apoptosis.

5 Discussion

BHLHE40 overexpression induced the loss of basal cells and increased differentiation, however, the total basal cell number and TP63 protein expression remained unchanged. Therefore, we predicted the existence of a compensatory mechanism for the loss of the transduced basal cells overexpressing BHLHE40-GFP. This compensatory mechanism is expected to be mediated by the proliferation of non-transduced basal cells when their neighboring ones overexpressing BHLHE40-GFP are differentiating. Surprisingly, the proliferation of the non-transduced basal cells was not increased on day 14 (Fig. 26B), which is the time point when we observe a significant decrease in basal cells overexpressing BHLHE40-GFP due to their increased differentiation. This suggested that the replacement of basal cells through proliferation occurs at earlier time points. Our EdU incorporation experiment suggests that on day 3, the proliferation of non-transduced basal cells was significantly increased in the BHLHE40-GFP culture compared to the GFP-transduced culture (Fig. 26B). Notably, the BHLHE40-GFP transduced basal cells did not yet begin to differentiate, and as a result, their numbers were not reduced at this time point. To explain this observation, we propose that BHLHE40-GFP-expressing basal cells may have started to release signals that influenced their neighboring non-transduced basal cells, thereby stimulating an increase in their proliferation.

Taken together, our results suggest that on day 3, non-transduced basal cells in the BHLHE40-GFP transduced culture undergo compensatory proliferation. This observation implies a paracrine regulation, where the BHLHE40-GFP overexpressing basal cells signal to their non-transduced neighbors, thereby promoting an increase in their proliferation. However, further studies are needed to identify the specific signaling pathways involved in this paracrine regulation.

Based on our human single-cell RNA sequencing and pseudotime analysis of differentiating ALI cultures at different time points, we show a selective upregulation of the gene encoding the transcription factor BHLHE40 in differentiating immature secretory cells (Fig. 7D), where it distinctly correlated with the expression of Notch signaling genes *NOTCH2*, *NOTCH3*, *HES1*, and *HES2* on days 0 and 5 of the ALI culture, but also *NOTCH3* to a lesser extent (Fig. 8A, B, C, D). Consistently, we show that BHLHE40 overexpression or knockdown in our ALI culture increased or decreased *NOTCH1* and *2* receptors gene

expression, respectively (Fig. 17C, D). However, we could not detect a consistent change in *NOTCH3*, *HES1*, or *HEY2* gene expression (Fig. 17C, D, E, F). The absence of *HES1* upregulation on day 5 in BHLHE40 overexpressing cells even though *NOTCH1* and *2* receptors were upregulated, can be explained by the fact that *HES1* is not described as Notch downstream effector in basal or Suprabasal cells but rather in club cells (Kiyokawa & Morimoto, 2020; Morimoto et al., 2012). The presence of *BHLHE40* and *HES1* gene correlation in the single-cell sequencing data from day 5 can be attributed to the presence of *SCGB1A1* expressing club cells as early as day 5, which was not the case in BHLHE40 overexpression or knockdown experiments (Fig. 21). BHLHE40-induced Notch receptors upregulation may regulate *HES2* and *HEY1* at this stage of culture, known to be Suprabasal cell associated-Notch downstream effectors (Ruiz Garcia et al., 2019) (Fig.27 C). However, *HES2* and *HEY1* were undetectable in our Real-time qPCR analysis of FACS-sorted BHLHE40-GFP overexpressing cells from day 5. Nevertheless, *HES2 and HEY1* strongly correlated with *BHLHE40* high expression in our human single-cell RNA sequencing data from day 5 (Fig. 8 B).

Previous studies have shown that Notch1 signaling activation in basal cells of the murine airway epithelium is associated with the downregulation of basal cell genes and upregulation of luminal differentiation markers (Rock et al., 2011). Furthermore, N1ICD overexpression in primary epithelial cells from the human mammary epithelium reduced TP63 expression (Yalcin-Ozuysal et al., 2010). We hypothesized that BHLHE40-induced increase in Notch signaling genes on day 5 would correlate with the downregulation of basal cell genes prior to differentiation. To address this point, we analyzed basal cell gene expression in BHLHE40-GFP sorted cells from ALI day 5. Surprisingly, BHLHE40 overexpression or knockdown had no significant effect on *TP63*, *ITGA6*, *KRT5*, or *NGFR* basal cell gene expression (Fig. 17G, H), nor on the intermediate marker *KRT13* (Fig. 17I, J). Consistent with this result, we also found that BHLHE40 overexpression did not induce any precocious differentiation into ciliated or club cells (Fig. 21). Therefore, the absence of downregulation of basal cell genes on day 5 after BHLHE40 overexpression is likely due to the early time point of analysis (the differentiation did not start yet).

Furthermore, it has been shown that the downregulation of basal cell genes in primary human basal cells following *HES1* overexpression was shown after 4 days of culture, while in mice,

it has been shown after 2 weeks of N1ICD constitutive expression (Rock et al., 2011). Lacking a time course analysis of basal cell gene expression following Notch activation, we can't exclude that BHLHE40-induced increase in Notch signaling required additional time to reduce basal cell genes.

Expecting a decrease in basal cell genes at a later time point of culture, we re-analyzed their gene expression on day 14 and investigated further potential interesting targets. Using bulk RNA-sequencing of sorted BHLHE40-GFP overexpressing cells from day 14, we show that BHLHE40-GFP overexpressing cells had decreased basal cell gene expression (*TP63*, *ITGA6*, *KRT5*, *NGFR*), and increased differentiation marker gene expression (*FOXJ*, *MYB*, *TP73*, *SCGB1A1*, and *MUC5B*) (Fig. 18C, D). In line with our findings, we show that BHLHE40 overexpression decreased basal cell number and increased ciliated, club, and goblet cell numbers on days 14 and 21 (Fig. 19 and 34). Taken together, our results suggest that BHLHE40-induced decrease of basal cell marker genes and increased differentiation into secretory and ciliated lineages on day 14 is driven by the earlier BHLHE40-induced activation of Notch signaling on day 5.

Furthermore, based on our single-cell RNA sequencing of the pHBECs-derived ALI culture, we show that *BHLHE40* high expression correlates with the lowest *TP63* expression in all time points of culture (Fig. 8A, B, C, D), suggesting a negative correlation between *BHLHE40* high expression and *TP63*, and further supporting that BHLHE40 negatively regulate the undifferentiated basal cell state.

Supporting our hypothesis that BHLE40-induced loss of basal markers expression and progression toward the secretory lineage (club and goblet cells) on day 14 may be driven by the earlier BHLHE40-induced activation of Notch signaling on day 5, it was previously shown that sustained activation of N1ICD in murine basal cells promoted their differentiation into the secretory lineage, mainly into club and goblet cells, but not ciliated cells. Consistently, Notch pharmacological inhibition on day 1 prevented murine basal cell luminal differentiation in tracheosphere culture on day 7 (Rock et al., 2011), further supporting that Notch signaling activation is needed for the differentiation of basal epithelial cells into the secretory lineage. However, it does not explain our observed increase in ciliated cells. This led us to think that BHLHE40-induced increase in ciliated cells engages a different mechanism.

Interestingly, previous studies have shown the existence of two airway basal cell subpopulations following airway injury: Myb and N2ICD expressing basal cells, which regenerate the ciliated or the secretory lineage, respectively. Each of the pre-committed basal cells was shown co-express the intermediate marker KRT8, either with Myb or N2ICD before differentiation towards the ciliated or the secretory lineage (Pardo-Saganta, Law, et al., 2015). Considering our ALI culture as a re-generation model, we hypothesized that BHLHE40 acts separately in these intermediate cell populations to increase differentiation depending on their pre-commitment. In the pre-committed secretory lineage, BHLHE40 increases Notch2 signaling activation which in turn increases club and goblet cell numbers, while in the pre-committed ciliated cell, it increases Myb expression through transcriptional activation of *TP73* (Nemajerova et al., 2016). Supporting this, it has been shown that BHLHE40 in cooperation with HDAC8, transcriptionally increased the expression of *TP73*, a master regulator of ciliogenesis (Qian et al., 2014; Wallmeier et al., 2021). We speculate that the increase in ciliated cells arises from BHLHE40-increased transcriptional activation of *TP73* in intermediate cells Myb^{+}.

Furthermore, previous studies have shown that NOTCH2 inhibition using anti-NOTCH2 antagonist antibody or its genetic deletion in club cells increased ciliated cells at the expense of club cells (Lafkas et al., 2015; Pardo-Saganta, Law, et al., 2015). Also, inhibition of the NOTCH2 receptor in club cells induced their direct trans-differentiation into ciliated cells in mice (Danahay et al., 2015). Supporting these findings, Notch inhibition in ALI culture after cell differentiation, led to increased ciliated cells at the expense of secretory cells (Giuranno et al., 2020), further supporting that they arise from club cell trans-differentiation. Taken together, these data suggest that the effect of Notch inhibition on airway epithelial cell differentiation is timepoint-dependent (before and after differentiation) and involves different Notch receptors and cell types. Based on this, we reasoned that BHLHE40-induced increase in ciliated cells in our ALI culture results from club cell potential trans-differentiation driven by BHLHE40-induced repression of Notch2. This repression can take place on the protein level through BHLHE40 interacting with NICD thereby preventing its binding with RBPJk and the subsequent transcriptional activation of *HES1*, as described in muscle cells (Sun et al., 2007). Our bulk RNA sequencing of BHLHE40-GFP overexpressing cells from day 14 showed an overall decrease in Notch signaling genes including *NOTCH2* and *HES1*, however, we could only confirm the downregulation of *HES1* gene expression (Fig.27 A, B). The lack of *NOTCH2* downregulation can be explained by the increased number of goblet

cells MUC5B$^+$, as it is described to be also regulated by Notch2 signaling (Danahay et al., 2015; Pardo-Saganta, Law, et al., 2015), while *HES1* is club cell-specific (Kiyokawa & Morimoto, 2020; Morimoto et al., 2012). Another possibility is that BHLHE40 acts at the protein level and prevents N2ICD activation of downstream effectors as previously described, explaining therefore, the solitary downregulation of *HES1* gene expression.

To test if BHLHE40-induced increase in ciliated cells comes from club cell potential trans-differentiation, we induced BHLHE40-FLAG overexpression on day 10, when the club cells began to appear in the culture, and analyzed epithelial cell differentiation on day 21. Unexpectedly, BHLHE40-FLAG overexpressing cells did not show any reduction in club cell numbers, while the ciliated cells were increased (Fig. 28G, H). We reasoned that the absence of a decrease in club cell numbers could be attributed to their continuous and increased replacement by the basal/intermediate cells overexpressing BHLHE40-FLAG. To reduce the number of basal/intermediate cells overexpressing BHLHE40 and therefore diminish their replacement of club cells, we re-infected the cells with BHLHE40-GFP construct and extended the culture to 28 days (Fig. 29A). Since we have previously seen that BHLHE40 reduced basal cell numbers throughout the culture period from day 14 to 21, we expected a further decrease on day 28. Also, we chose BHLHE40-GFP construct for this experiment for its higher transduction efficiency. Interestingly, we show that BHLHE40-GFP overexpressing cells had increased ciliated cell gene expression at the expense of club cell genes (Fig. 29B). Also, the *MUC5B*$^+$ goblet cell marker gene expression was still increased, which explains the persistent upregulation of Notch2 expression and raises the possibility that the increase in ciliated cells is associated with the decrease in club cells. Unless club cells underwent apoptosis, we hypothesized that BHLHE40-induced increase in ciliated cells results from potential trans-differentiation of club cells, leading to their reduction. As previously discussed, BHLHE40-induced increase in ciliated can additionally arise from an intermediate pre-committed cell, which explains the predominant increase in ciliated cells.

Collectively, we propose that BHLHE40-induced increase in basal cell differentiation into club, goblet, and ciliated cells may involve three Notch signaling events (Fig. 35) and suggest a cell-type specific regulation of BHLHE40.

A first early event where BHLHE40 overexpression increases Notch1 signaling in basal cells, leading to their subsequent increased differentiation into intermediate progenitors (consistent

with the increase in *NOTCH1* expression on day 5 following BHLHE40 overexpression (Fig.17 C). We propose two intermediate subpopulations: one will lead to the increased secretory cells (club, goblet cells) due to a second BHLHE40-induced Notch2 event (consistent with the increase in *NOTCH2* expression on day 5 following BHLHE40 overexpression (Fig.17 C)), while a second intermediate subpopulation will lead to increased ciliated cells due to BHLHE40 selective transcriptional activation of *TP73* in a third event, known to bind and positively regulate *MYB* expression (Nemajerova et al., 2016). BHLHE40 selective positive regulation of the ciliated fate in the second intermediate subpopulation relies on unique molecular programs that distinguish it from the Notch2-intermediate subpopulation, however, the specific molecular programs defining each subpopulation remain to be elucidated (by further sub-clustering). However, we did not observe an increase in TP73 gene expression as early as day 5 following BHLHE40 overexpression (Fig. 21) but later on day 14 (Fig.18D), suggesting that the commitment of the intermediate cell population toward ciliated lineage mediated by BHLHE40 may require more time to occur. To confirm this hypothesis, further time course analysis should be done to analyze TP73 expression between days 5 and 14 following BHLHE40 overexpression.

Finally, a fourth Notch event, where BHLHE40 overexpression in club cells represses Notch2 signaling and induces their potential trans-differentiation into ciliated cells, while at the same time, the basal/intermediate cells overexpressing BHLHE40 are continuously replenishing the loss of club cells due to the first event (BHLHE40-induced increase in basal differentiation into intermediate secretory progenitors). Also, our hypothesis that the third and the fourth events give rise to ciliated cells may explain their predominant increase following BHLHE40 overexpression. This scenario cannot be addressed by temporally controlled overexpression or knockdown of BHLHE40 or Notch signaling components. It will require the more specific manipulation of their activity in target subpopulations of basal, Suprabasal, secretory, and ciliated cell types. The definition of specific enhancer elements targeting these cell types is a major future task.

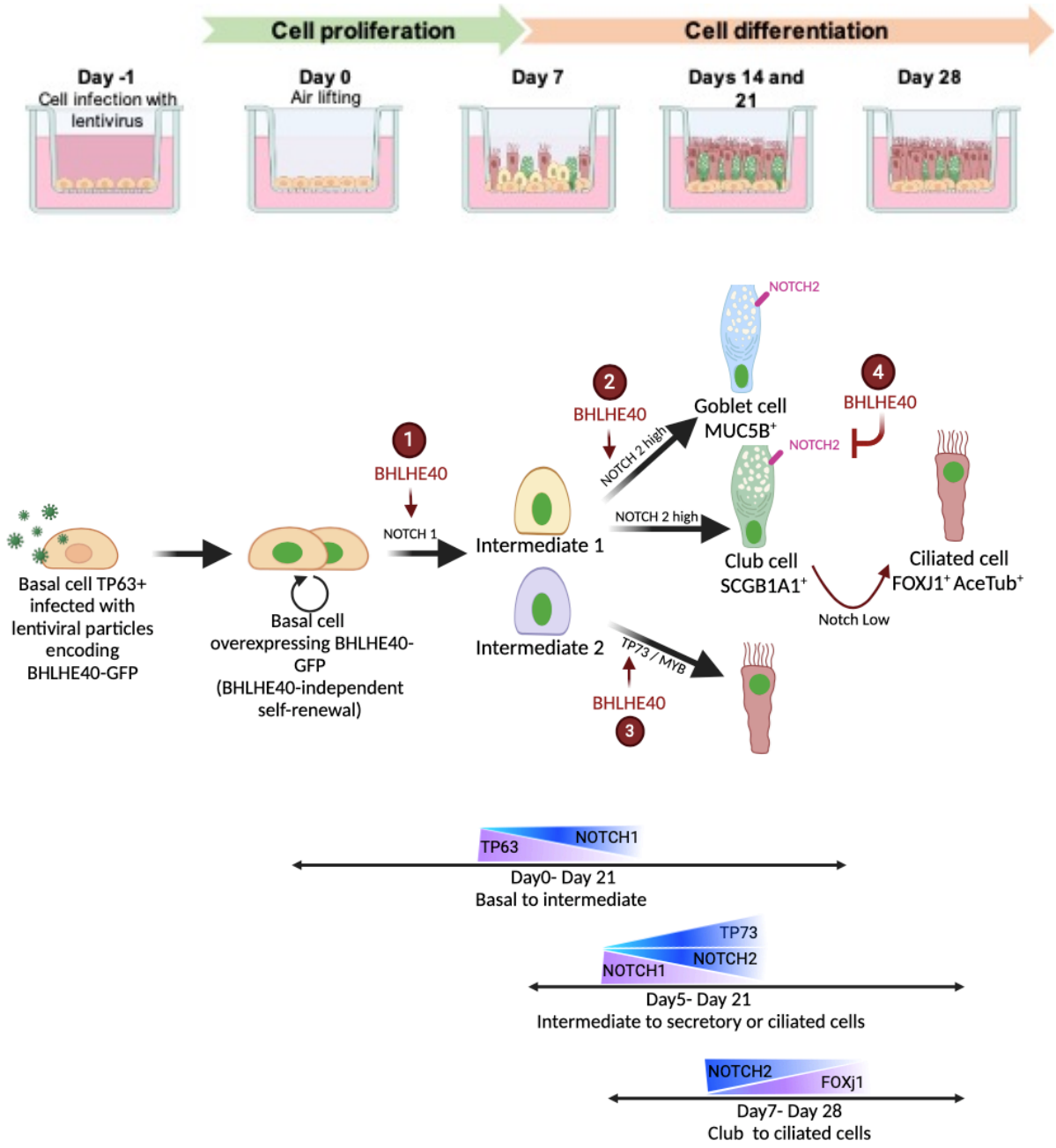

Figure 35. Proposed model explaining BHLHE40-induced increase in airway basal cell differentiation into club, goblet, and ciliated cells. Four events are at the origin of BHLHE40-induced increase in basal cell differentiation (3 Notch-dependent and 1 Notch-independent). **(1)** The first event is characterized by BHLHE40-induced increase in Notch1 signaling in basal cells, leading to their increased differentiation into two intermediate cell subpopulations. **(2)** The second event is characterized by BHLHE40-selective activation of Notch2 signaling in the first intermediate cell population, leading to increased secretory cell differentiation (club and goblet cells). **(3)** The third event is characterized by BHLHE40-selective transcriptional activation of *TP73* in the second intermediate cell population, which positively regulates *MYB* expression leading to increased ciliated cell differentiation. **(4)** The fourth event is characterized by BHLHE40-induced repression of Notch2 signaling in club cells leading to their trans-differentiation into ciliated cells. All events are continuous along the ALI culture and start in the time points indicated in the figure in the lower panel.

Taken together, our scenario suggests a cell-type distinct regulation of BHLHE40, which has been previously described in other epithelial cell types. For example, in contrast to our data, BHLHE40 has been shown to decrease the differentiation of keratinocytes, further supporting its context-dependent function (Qian et al., 2011).

To investigate the molecular mechanisms of BHLHE40-induced basal-to-intermediate cell transition (first event) and identify the direct transcriptional targets of BHLHE40 involved in Notch signaling activation driving this transition, we did a 3-step selection by performing a comparative analysis of three datasets (Fig. 30): the data from the published BHLHE40 A549 ChIP-sequencing, our differentially expressed transcription factors in the differentiation trajectory of the SMG-like basal cells toward secretory cells, and our Real-Time qPCR analysis of transduced A549 cells overexpressing GFP or BHLHE40-GFP.

Based on our human single-cell RNA seq data, we show that *FOS*, *HIF1α*, *MYC*, *HMGA2*, *BNC1*, *ZFP36L1*, *FOSL1,* and *SOX9* are downregulated upon BHLHE40 upregulation in the intermediate cell cluster along the SMG-like basal cell differentiation trajectory (Fig. 30A). Since BHLHE40 is mainly described as a transcriptional repressor (Sun & Taneja, 2000), we reasoned that these targets are more likely to be directly repressed by BHLHE40. In addition, we selected these 8 targets from others with similar patterns because they are described to be direct transcriptional targets of BHLHE40 in A549 cells (Fig. 30B). Aligning with this, our data shows that the overexpression of BHLHE40 in A549 cells reduced *FOS*, *HIF1α*, *MYC*, and *HMGA2* gene expression while BNC1, ZFP36L1, and FOSL1 expression were not detectable (Fig. 30C, D), providing further evidence that these genes are potentially direct transcriptional targets of BHLHE40 in our pHBECs-derived ALI culture.

Using our CUT&RUN DNA enrichment combined with gene expression analysis of transduced cells overexpressing BHLHE40-GFP from ALI day 14, we show that, although BHLHE40 bound to HIF1α, BNC1, FOSL1, MYC, HMGA2, and ZFP36L1 genomic regions, it only repressed BNC1 gene expression without affecting the other targets (Fig. 31A, B). The absence of BHLHE40-induced repression of these targets may be attributed to the mixed cell population overexpressing BHLHE40 that was used for this analysis, thereby diluting the repression effect occurring in basal cells. Unlike BNC1, which we have shown to be specific to basal cells at the protein level on day 14 (Fig. 32B, C), the other targets are not necessarily restricted to basal cells: while they were found to be specific to the SMG-like basal cells

within this particular differentiation trajectory, this does not rule out the possibility that they may also be specific to other cell type(s) in our ALI culture that were not included in this trajectory analysis. Since BHLHE40 has also been described as a transcriptional activator and not only a repressor (Qian et al., 2014; Jarjour et al., 2019; Nguyen et al., 2024), its function may vary depending on the cellular context. Consequently, in the absence of immunostaining to identify the cell-type specificity of these targets on day 14, we cannot rule out a cumulative effect from BHLHE40 transcriptional activity (repression and activation) across different cell types, which explains the absence of change in gene expression following BHLHE40 overexpression. To evaluate the repressive effect of BHLHE40 on these targets specifically in basal cells, isolating BHLHE40-GFP overexpressing basal cells from the rest of the culture on day 14 would be needed.

Furthermore, we show that BHLHE40 overexpression reduced the number of BNC1-expressing cells in the basal layer (Fig. 32D), further confirming BHLHE40-mediated transcriptional repression of BNC1 in basal cells.

Previous studies showed that BNC1 has a selectively high expression in basal cells of the skin epithelium, and is reduced in Suprabasal and differentiated layers. Consistently, its reduction is associated with the appearance of keratinocytes differentiation marker, suggesting its role in maintaining the undifferentiated basal cell state (Tseng & Green, 1994; Boudra et al., 2023). Consistently, our results show a correlation between the downregulation of BNC1 (Fig. 31B and 32D), the reduction of basal cell markers, and the increase in differentiation markers following BHLHE40 overexpression on day 14 (Fig. 18 and 19). Taken together, our data indicate that BHLHE40 transcriptionally represses BNC1 expression, which in turn induces the loss of basal cells and transition to an intermediate cell state. BHLHE40 direct transcriptional repression of BNC1 and the loss of basal cells occurred on day 14. We hypothesized that BHLHE40-mediated BNC1 repression triggered Notch activation, leading to basal cell loss. Since BHLHE40-induced increase in Notch signaling was observed on day 5, we suggest that this may reflect the early onset of BNC1 repression, continuing through day 14 when basal cells were lost. However, the lack of increased Notch1 signaling on day 14 in sorted cells overexpressing BHLHE40 is very likely due to the small proportion of basal cells and the larger proportion of ciliated cells where Notch signaling is repressed (Ruiz Garcia et al., 2019), as assessed by the expression of cell type-specific and corresponding Notch-related genes (Fig 18D and 28A, C). In contrast, we

show on day 5 that BHLHE40 overexpression increased the expression of NOTCH1, because the culture is more homogenous and mainly composed of basal cells at this time. However, how BNC1 induces the activation of Notch signaling driving basal to intermediate cell transition needs to be elucidated.

Since our scenario suggested that the basal-to-intermediate cell transition stems from BHLHE40-induced increase in Notch signaling, we expected that BHLHE40 transcriptionally repress Notch signaling inhibitor genes in basal cells, like *LFNG* and *CSNK2B* (Fig. 27C), leading therefore to Notch upregulation and subsequent basal-to-intermediate cell transition. Since neither BNC1 nor the other potential BHLHE40 transcriptional targets are described to be Notch inhibitor genes from the literature, the induced increase in Notch signaling is rather a secondary effect.

Lacking evidence that BHLHE40 transcriptionally represses *HIF1α*, *FOSL1*, *MYC*, *HMGA2*, and *ZFP36L1* gene expression, we hypothesized that BNC1 is the solely transcriptional target of BHLHE40 that is needed to maintain the undifferentiated basal cell state by negatively regulating Notch signaling in basal cells (e.g., through maintaining Notch inhibitor expression). In line with this, our bulk RNA sequencing data from the sorted BHLHE40-GFP cells from day 14 shows that gene expression of the basal cell-specific Notch inhibitor *LFNG* is reduced (Fig. 27A), suggesting that it could be the reason behind Notch activation in basal cells. Taken together, *LFNG* could be one of the downstream targets of BNC1 in basal cells which may be involved in the Notch-dependent basal-to-intermediate cell transition (Fig. 36).

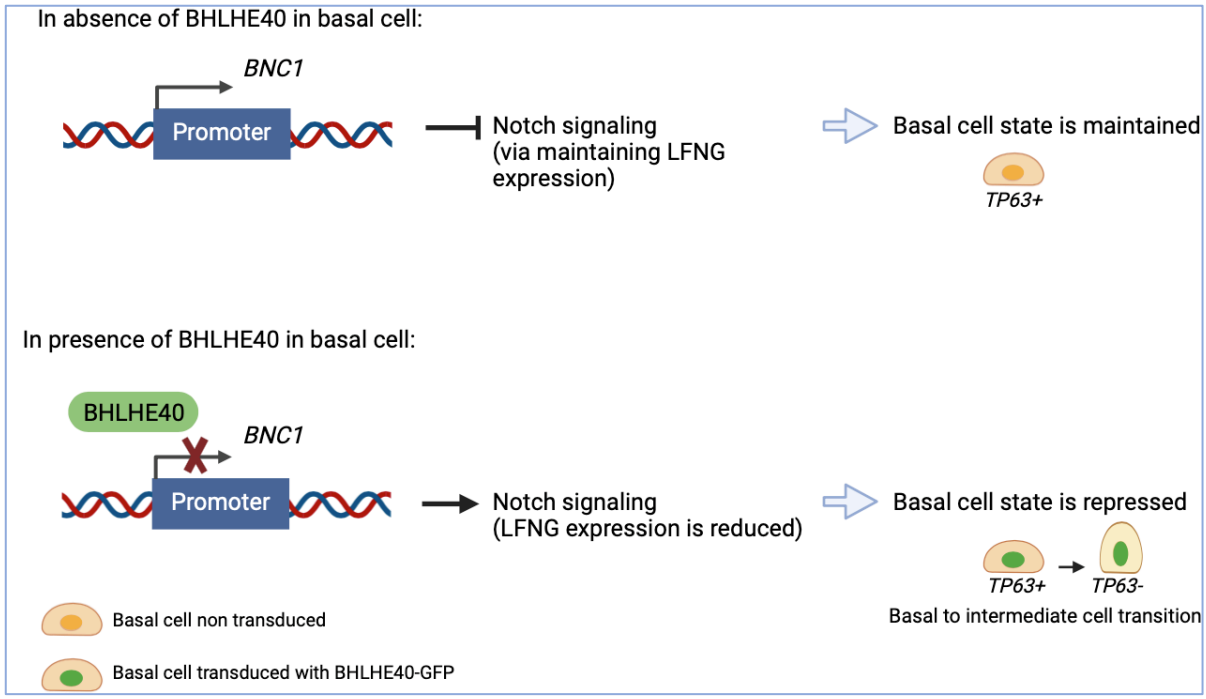

Figure 36. Proposed model explaining BHLHE40-induced basal to intermediate cell transition and the involved downstream target. In the absence of BHLHE40, the transcription factor *BNC1* is expressed in basal cells and negatively regulates Notch signaling possibly via maintaining the expression of the basal cell-specific Notch inhibitor LFNG. This Notch inhibition prevents basal cell differentiation and maintains their undifferentiated state. However, when BHLHE40 is present in basal cells, it transcriptionally represses the expression of *BNC1*, inducing the downregulation of *LFNG*, subsequent de-repression of Notch signaling, and basal to intermediate cell transition.

To confirm that *BNC1* repression mediates BHLHE40-induced loss of basal cell markers and transition to intermediate cells, *BNC1* knockdown should be performed to assess whether the phenotype of BHLHE40 overexpression in the ALI culture can be reproduced. Additionally, since TP63 expression is regulated by multiple signaling pathways in addition to Notch signaling (Yoh et al., 2015), further investigation is needed to deepen our understanding of the molecular mechanisms underlying BHLHE40-BNC1-induced loss of basal cells TP63^{+}, focusing on identifying BNC1 downstream targets, which our results suggest as a potential starting point for future studies. This will determine how BNC1 maintains TP63 expression in the human airway epithelium and whether Notch signaling is solely involved in this BHLHE40-mediated regulation of basal cell differentiation.

In addition, previous studies have shown that the expression of MYC and HIF1α maintain the basal cell genes in different epithelial cell contexts. Their loss of function is associated with the loss of basal cell-specific genes (Schwab LP et al, 2012; Xi Y et al, 2017; Hishida T et al, 2022; Wang F et al, 2022). Also, HMGA2 repression was shown to positively regulate osteogenic differentiation (Wei J et al, 2014) while its expression seemed to be required in

adult stem cells to allow self-renewal and block differentiation (Parisi S et al, 2020). Therefore, it would be valuable to investigate the role of these additional potential BHLHE40 transcriptional targets in maintaining the basal cell state by first validating their BHLHE40-transcriptional repression. As previously discussed, sorting basal cells overexpressing BHLHE40-GFP from the rest of the culture on day 14 would be needed to evaluate BHLHE40 repressive effect specifically in basal cells, without being influenced by other cell types in the culture.

Future experiments to identify the unique molecular programs that distinguish the pre-committed basal/intermediate cells toward a secretory or a ciliated cell program, to predict which co-factors interact with BHLHE40 to regulate the expression of which target(s) in each specific cell type/subtype, and to further validate the proposed BHLHE40 spatio-temporal regulation along the pHBECs-derived ALI culture (Fig. 35), we will need a combination of single-cell RNA and ATAC-sequencing of BHLHE40 overexpressing basal cells at different time point of ALI culture. This will enable the identification of the differentially expressed transcription factors, Notch activators, and inhibitors genes, in parallel to the differentially accessible chromatin regions in the genome along the differentiation trajectory from basal cells towards intermediate/presecretory cells, in a cell-type specific manner (in BHLHE40 overexpressing versus non-overexpressing basal cells). In this way, we will better predict which Notch genes are being regulated with which transcription factor(s) downstream of BHLHE40, then we could confirm this specific regulation using a specific antibody-targeted DNA binding approach.

Considering our pHBEC-derived ALI culture as a regeneration model, our data suggest that BHLHE40 has the potential to enhance human airway epithelial regeneration upon injury by promoting basal cell differentiation. This highlights the need to further investigate the molecular mechanisms through which BHLHE40 contributes to this process. Additionally, our pseudotime analysis of differentiating ALI culture suggested the involvement of BHLHE40 in the SMG-like basal cell differentiation trajectory towards secretory cells (Fig. 7D). Since basal cells of the SMGs have been shown to contribute to the surface airway epithelium (SAE) regeneration upon injury (Hegab et al., 2011; Levlev et al., 2022; Lynch et al., 2018), we propose that BHLHE40 may enhance regeneration by promoting differentiation of basal progenitor cells not only of the SAE but also of the SMGs. To investigate the contribution of BHLHE40 in airway epithelial cell regeneration *in vivo*, an inducible

BHLHE40 basal cell-specific knockout or knock-in mouse model (with a reporter) combined with naphthalene injury or diphtheria toxin-induced luminal epithelial cell ablation, is needed. Furthermore, to distinguish BHLHE40 contribution to epithelial regeneration via basal cells of the SAE versus SMG, additional studies are needed to identify unique SMG basal cell markers for lineage tracing upon injury, in the presence or absence of BHLHE40. In addition, it would be interesting to assess whether BHLHE40 also contributes to distal lung regeneration by influencing LNEPs, a stem cell population that activates the TP63/KRT5 basal cell program in a Notch-dependent manner, to regenerate alveolar epithelium upon injury (Kathiriya et al., 2020; Vaughan et al., 2015).

Last but not least, our analysis of *Bhlhe40*-global knockout adult mice (Dr. Alexandra Firsova) did not show any difference in airway epithelial cell numbers compared to the control lungs in the tracheal and airway epithelium (data not shown), excluding a role of BHLHE40 in murine airway epithelium differentiation during homeostasis.

To exclude a redundant function of BHLHE40, we show that its knockdown resulted in the reduction, but not the absence of epithelial cell differentiation into club, goblet, and ciliated cells (Fig. 22 and 23). To account for this, we propose that not all cells expressing *BHLHE40* shRNA had efficiently prevented the expression of *BHLHE40*. This is supported by the previously observed partial decrease in *BHLHE40* gene expression in the sorted cells overexpressing *BHLHE40* shRNA (Fig. 16D), and also aligns with the expected low level of *BHLHE40* expression in a knockdown experiment, as opposed to a knockout. Therefore, we propose that the cells overexpressing *BHLHE40* shRNA that had still differentiated did not efficiently reduce BHLHE40 gene expression, which can be attributed to epigenetic factors-silencing of the lentiviral construct (Knight et al., 2012; Sun et al., 2022). A second scenario to explain the reduction, but not the absence of epithelial cell differentiation following the knockdown, is that BHLHE40 is not a master regulator of differentiation but rather increases or decreases the rate of differentiation in cooperation with other transcription factors, suggesting its supportive rather than driving role in cell differentiation. Its knockdown reduces differentiation but does not completely block it, as other factor(s) provide partial functionality in its absence, though they cannot fully compensate for its loss. Taken together, these findings suggest that BHLHE40 is important but not essential to driving airway epithelial cell differentiation.

6 Summary

Airway basal cells are multipotent stem cell progenitors, which are crucial to maintaining the pseudostratified epithelium. Understanding the molecular mechanisms that regulate their differentiation is essential to unravel how normal and pathological airway epithelial regeneration occurs. With this aim, we performed single-cell RNA sequencing and pseudotime analysis of primary human bronchial epithelial cells (pHBECs) differentiated on air-liquid-interface (ALI) culture, revealing a selective upregulation of the transcription factor BHLHE40 in differentiating intermediate epithelial cells. Using our ALI cultures in combination with lentiviral-based gene transfer, we show that the overexpression of BHLHE40 in human basal cells increased their differentiation into club, goblet, and ciliated cells. Consistent with the overexpression results, the knockdown of *BHLHE40* in the ALI cultures reduced basal epithelial cell differentiation. Interestingly, we demonstrate that BHLHE40-mediated loss of basal cell fate through increased differentiation was preceded earlier in the culture by an increase in Notch signaling on day 5. Previous studies have shown that Notch1 signaling activation in basal cells of the murine airway epithelium is associated with the downregulation of basal cell genes and upregulation of luminal differentiation markers. Furthermore, N1ICD overexpression in primary epithelial cells from the human mammary epithelium reduced TP63 expression. Taken together, we propose that BHLHE40-induced loss of basal cells and transition to an intermediate state involves Notch signaling.

To investigate the molecular mechanisms of BHLHE40-induced basal-to-intermediate cell transition and identify its direct transcriptional targets involved in Notch signaling activation driving this transition, we did a 3-step selection by performing a comparative analysis of three datasets: the data from the published BHLHE40 A549 ChIP-sequencing, our differentially expressed transcription factors in the differentiation trajectory of the Submucosal glands (SMGs)-like basal cells toward secretory cells, and our Real-Time qPCR analysis of transduced A549 cells overexpressing GFP or BHLHE40-GFP. We ended up with 8 potential BHLHE40 targets: *FOS*, *HIF1α*, *MYC*, *HMGA2*, *BNC1*, *ZFP36L1*, *FOSL1,* and *SOX9*. To confirm that they are transcriptional targets of BHLHE40 in our pHBECs-derived ALI culture, we used CUT&RUN DNA enrichment combined with gene expression analysis of transduced cells overexpressing BHLHE40-GFP from ALI day 14. We show that, although BHLHE40 has bound to *HIF1α*, *BNC1*, *FOSL1*, *MYC*, *HMGA2*, and *ZFP36L1* genomic

regions, it only repressed *BNC1* gene expression without affecting the other targets. Consistently, we show that BHLHE40 overexpression reduced the number of BNC1-expressing cells in the basal layer and that BNC1 expression was exclusive to basal cells, further confirming BHLHE40-mediated transcriptional repression of BNC1 in basal cells.

Previous studies showed that BNC1 has a selectively high expression in basal cells of the skin epithelium, which goes down in the Suprabasal and differentiated layers. Consistently, its reduction was associated with the appearance of keratinocytes differentiation marker, suggesting its role in maintaining the undifferentiated basal cell state. In line with our results, we show a correlation between the downregulation of *BNC1*, the reduction of basal cell markers, and the increase in epithelial cell differentiation following BHLHE40 overexpression on day 14. Taken together, our data indicate that BHLHE40 transcriptionally represses *BNC1* expression, which in turn induces the loss of basal cells and their differentiation. We hypothesized that BNC1 is the solely transcriptional target of BHLHE40 that is needed to maintain the undifferentiated basal cell state by negatively regulating Notch signaling in basal cells (e.g., by activating Notch inhibitor). Bulk RNA sequencing of sorted BHLHE40-GFP cells from ALI day 14 identified LFNG, a basal cell-specific Notch inhibitor, as a potential downstream target of BNC1, as its expression decreased following BHLHE40 overexpression. However, it remains unclear whether LFNG or other mediators contribute to the BHLHE40-BNC1-induced transition from basal to intermediate cells.

Additionally, since TP63 expression is regulated by multiple signaling pathways in addition to Notch signaling, further investigation is needed to deepen our understanding of the molecular mechanisms driving BHLHE40-BNC1-mediated loss of $TP63^{+}$ basal cells, focusing on identifying BNC1 downstream targets, which our findings suggest as a promising starting point for future studies. This will determine how BNC1 maintains TP63 expression in the human airway epithelium and whether Notch signaling is solely involved in BHLHE40-mediated regulation of basal cell differentiation.

Considering our pHBECs-derived ALI culture as a re-generation model, our data suggest a potential of BHLHE40 to enhance the regeneration of the human airway epithelium upon airway injury through increasing differentiation. Also, our single-cell RNA sequencing and pseudotime analysis of differentiating ALI culture suggested the involvement of BHLHE40 in the SMGs-like basal cell differentiation trajectory towards secretory cells. Since basal cells

of the SMGs have been shown to contribute to the surface airway epithelium (SAE) regeneration upon injury, we propose a potential role of BHLHE40 in enhancing regeneration via increasing differentiation of basal progenitor cells, both in the SAE and the SMGs. Collectively, we propose that BHLHE40 could serve as a target for therapeutic strategies aimed at enhancing tissue repair and regeneration in the airway epithelium.

7 Zusammenfassung

Die Basalzellen der Atemwege sind multipotente Stammzellvorläufer, die für die Aufrechterhaltung des pseudostratifizierten Epithels von entscheidender Bedeutung sind. Das Verständnis der molekularen Mechanismen, die ihre Differenzierung regulieren, ist essenziell, um zu verstehen, wie die normale und pathologische Regeneration des Atemwegepithels abläuft. Zu diesem Zweck führten wir eine Einzelzell-RNA-Sequenzierung und Pseudotime-Analyse von primären menschlichen bronchialen Epithelzellen (*primary human bronchial epithelial cells*, pHBECs), die in einer *Air-Liquid-Interface* (ALI)-Kultur differenziert wurden, durch. Dabei zeigte sich eine selektive Hochregulation des Transkriptionsfaktors BHLHE40 in differenzierenden intermediären Epithelzellen. Mit unseren ALI-Kulturen in Kombination mit lentivirusbasiertem Gentransfer zeigten wir, dass die Überexpression von BHLHE40 in menschlichen Basalzellen deren Differenzierung in Club-, Becher- und Zilienzellen erhöhte. Im Einklang mit den Überexpressionsergebnissen verringerte der Knockdown von *BHLHE40* in den ALI-Kulturen die Differenzierung der Basalzellen. Interessanterweise demonstrierten wir, dass der BHLHE40-vermittelte Verlust der Basalzellen durch eine verstärkte Differenzierung in den frühen Kulturtagen mit einer Zunahme der Notch-Signalgebung am Tag 5 einherging. Frühere Studien haben gezeigt, dass die Aktivierung des Notch1-Signals in Basalzellen des murinen Atemwegepithels mit einer Herabregulierung der Basalzellgene und einer Hochregulierung von Markern der luminalen Differenzierung verbunden ist. Darüber hinaus führte die Überexpression von N1ICD in primären Epithelzellen des menschlichen Mamma Epithels zu einer Reduktion der TP63-Expression. Zusammenfassend konnten wir zeigen, dass der BHLHE40-induzierte Verlust von Basalzellen und der Übergang zu einem intermediären Zustand durch Notch-Signaling vermittelt wird.

Um die molekularen Mechanismen der BHLHE40-induzierten Basalzellen-zu-intermediären Zellen-Transition zu untersuchen und seine direkten Transkriptionsziele zu identifizieren, die an der Aktivierung der Notch-Signalgebung beteiligt sind, führten wir eine dreistufige Selektion durch, indem wir eine vergleichende Analyse von drei Datensätzen vornahmen: die Daten der veröffentlichten BHLHE40 A549 ChIP-Sequenzierung, unsere differentiell exprimierten Transkriptionsfaktoren in dem Differenzierungverlauf der submukosalen Drüsen (SMGs)-ähnlichen Basalzellen, hin zu sekretorischen Zellen und unsere RT (*real time*) qPCR-Analyse von transduzierten A549-Zellen, die entweder GFP oder BHLHE40-

GFP überexprimierten. Wir identifizierten 8 potenzielle BHLHE40-Ziele: *FOS*, *HIF1α*, *MYC*, *HMGA2*, *BNC1*, *ZFP36L1*, *FOSL1* und *SOX9*. Um zu bestätigen, dass es sich bei diesen um Transkriptionsziele von BHLHE40 in unserer pHBECs-abgeleiteten ALI-Kultur handelt, verwendeten wir CUT&RUN DNA-Anreicherung in Kombination mit einer Genexpressionsanalyse von transduzierten Zellen, die BHLHE40-GFP an Tag 14 der ALI-Kultur überexprimierten. Wir zeigten, dass BHLHE40 an den Genomregionen von *HIF1α*, *BNC1*, *FOSL1*, *MYC*, *HMGA2* und *ZFP36L1* gebunden war, jedoch nur die *BNC1*-Genexpression unterdrückte, ohne die anderen Ziele zu beeinflussen. Konsistent damit zeigte sich, dass die Überexpression von BHLHE40 die Anzahl der BNC1-exprimierenden Zellen in der Basalschicht reduzierte und dass die BNC1-Expression exklusiv in Basalzellen auftrat, was die BHLHE40-vermittelte Transkriptionsrepression von BNC1 in Basalzellen weiter bestätigte.

Frühere Studien haben gezeigt, dass *BNC1* eine selektiv hohe Expression in Basalzellen des Hautepithels aufweist, die in den suprabasalen und differenzierten Schichten abnimmt. In Übereinstimmung damit, wurde seine Reduktion mit dem Auftreten von Differenzierungsmarkern der Keratinozyten in Verbindung gebracht, was auf seine Rolle bei der Aufrechterhaltung des undifferenzierten Basalzell-Zustands hinweist. Im Einklang mit unseren Ergebnissen zeigen wir eine Korrelation zwischen der Herabregulierung von BNC1, der Reduktion von Basalzellmarkern und der Zunahme der epithelialen Differenzierung nach Überexpression von BHLHE40 an Tag 14. Zusammengefasst deuten unsere Daten darauf hin, dass BHLHE40 die BNC1-Expression transkriptionell repressiert, was wiederum den Verlust von Basalzellen und deren Differenzierung induziert. Wir nahmen an, dass BNC1 das einzig transkriptionelle Ziel von BHLHE40 ist, das notwendig ist, um den undifferenzierten Basalzell-Zustand durch negative Regulation der Notch-Signalgebung in Basalzellen aufrechtzuerhalten (z. B. durch Aktivierung des Notch-Inhibitors). Die Gesamt-RNA-Sequenzierung von sortierten BHLHE40-GFP-Zellen aus der ALI-Kultur am Tag 14 identifizierte LFNG, einen Basalzell-spezifischen Notch-Inhibitor, als potenzielles downstream Ziel von BNC1, da dessen Expression nach Überexpression von BHLHE40 abnahm. Es bleibt jedoch unklar, ob LFNG oder andere Mediatoren zur BHLHE40-BNC1-induzierten Transition von Basalzellen zu intermediären Zellen beitragen.

Da die TP63-Expression durch mehrere Signalwege, einschließlich der Notch-Signalgebung, reguliert wird, sind zusätzlich weitere Untersuchungen erforderlich, um unser Verständnis der

molekularen Mechanismen zu vertiefen, die den BHLHE40-BNC1-vermittelten Verlust von TP63+ Basalzellen antreiben. Dabei sollte der Fokus auf der Identifikation von BNC1-regulierten Zielgenen liegen, die unsere Ergebnisse als vielversprechenden Ausgangspunkt identifizieren konnte. Dies könnte erklären, wie BNC1 die TP63-Expression im menschlichen Atemwegepithelium aufrechterhält und ob die Notch-Signalgebung ausschließlich in die BHLHE40-vermittelte Regulation der Basalzell-Differenzierung involviert ist.

Im Hinblick auf unsere pHBECs-abgeleitete ALI-Kultur als Modell für Regeneration legen unsere Daten nahe, dass BHLHE40 das Potenzial besitzt, die Regeneration des menschlichen Atemwegepithels nach Atemwegsverletzungen durch verstärkte Differenzierung zu fördern. Unsere Einzelzell-RNA-Sequenzierung und Pseudotime-Analyse der differenzierenden ALI-Kultur deuteten ebenfalls darauf hin, dass BHLHE40 in dem Differenzierungsverlauf der SMGs-ähnlichen Basalzellen hin zu sekretorischen Zellen eine Rolle spielt. Da gezeigt wurde, dass Basalzellen der SMGs zur Regeneration des Oberflächen-Atemwegepithels (SAE) nach Verletzungen beitragen, besitzt BHLHE40 eine potenzielle Rolle bei der Förderung der Regeneration durch verstärkte Differenzierung der basalen Vorläuferzellen, sowohl im SAE als auch in den SMGs, vor. Dementsprechend könnte BHLHE40 als Ziel für therapeutische Strategien dienen, die auf die Förderung der Gewebeheilung und Regeneration im Atemwegepithelium abzielen.

References

Augustyn, A., Borromeo, M., Wang, T., Fujimoto, J., Shao, C., Dospoy, P. D., Lee, V., Tan, C., Sullivan, J. P., Larsen, J. E., Girard, L., Behrens, C., Wistuba, II, Xie, Y., Cobb, M. H., Gazdar, A. F., Johnson, J. E., & Minna, J. D. (2014). ASCL1 is a lineage oncogene providing therapeutic targets for high-grade neuroendocrine lung cancers. *Proc Natl Acad Sci U S A*, *111*(41), 14788-14793. https://doi.org/10.1073/pnas.1410419111

Bi, H., Li, S., Qu, X., Wang, M., Bai, X., Xu, Z., Ao, X., Jia, Z., Jiang, X., Yang, Y., & Wu, H. (2015). DEC1 regulates breast cancer cell proliferation by stabilizing cyclin E protein and delays the progression of cell cycle S phase. *Cell Death Dis*, *6*, e1891. https://doi.org/10.1038/cddis.2015.247

Boudjelal, M., Taneja, R., Matsubara, S., Bouillet, P., Dolle, P., & Chambon, P. (1997). Overexpression of Stra13, a novel retinoic acid-inducible gene of the basic helix-loop-helix family, inhibits mesodermal and promotes neuronal differentiation of P19 cells. *Genes Dev*, *11*(16), 2052-2065. https://www.ncbi.nlm.nih.gov/pubmed/9284045

Boudra, R., Patenall, B. L., King, S., Wang, D., Best, S. A., Ko, J. Y., Xu, S., Padilla, M. G., Schmults, C. D., Barthel, S. R., Lian, C. G., & Ramsey, M. R. (2023). PRMT1 Inhibition Selectively Targets BNC1-Dependent Proliferation, but not Migration in Squamous Cell Carcinoma. *bioRxiv*. https://doi.org/10.1101/2023.03.27.533164

Byers, D. E., Alexander-Brett, J., Patel, A. C., Agapov, E., Dang-Vu, G., Jin, X., Wu, K., You, Y., Alevy, Y., Girard, J. P., Stappenbeck, T. S., Patterson, G. A., Pierce, R. A., Brody, S. L., & Holtzman, M. J. (2013). Long-term IL-33-producing epithelial progenitor cells in chronic obstructive lung disease. *J Clin Invest*, *123*(9), 3967-3982. https://doi.org/10.1172/JCI65570

Chang, H. C., Kao, C. H., Chung, S. Y., Chen, W. C., Aninda, L. P., Chen, Y. H., Juan, Y. A., & Chen, S. L. (2019). Bhlhe40 differentially regulates the function and number of peroxisomes and mitochondria in myogenic cells. *Redox Biol*, *20*, 321-333. https://doi.org/10.1016/j.redox.2018.10.009

Chen, G., Korfhagen, T. R., Xu, Y., Kitzmiller, J., Wert, S. E., Maeda, Y., Gregorieff, A., Clevers, H., & Whitsett, J. A. (2009). SPDEF is required for mouse pulmonary goblet cell differentiation and regulates a network of genes associated with mucus production. *J Clin Invest*, *119*(10), 2914-2924. https://doi.org/10.1172/JCI39731

Cho, Y., Noshiro, M., Choi, M., Morita, K., Kawamoto, T., Fujimoto, K., Kato, Y., & Makishima, M. (2009). The basic helix-loop-helix proteins differentiated embryo chondrocyte (DEC) 1 and DEC2 function as corepressors of retinoid X receptors. *Mol Pharmacol*, *76*(6), 1360-1369. https://doi.org/10.1124/mol.109.057000

Danahay, H., Pessotti, A. D., Coote, J., Montgomery, B. E., Xia, D., Wilson, A., Yang, H., Wang, Z., Bevan, L., Thomas, C., Petit, S., London, A., LeMotte, P., Doelemeyer, A., Velez-Reyes, G. L., Bernasconi, P., Fryer, C. J., Edwards, M., Capodieci, P., . . . Jaffe, A. B. (2015). Notch2 is required for inflammatory cytokine-driven goblet cell metaplasia in the lung. *Cell Rep*, *10*(2), 239-252. https://doi.org/10.1016/j.celrep.2014.12.017

Giuranno, L., Roig, E. M., Wansleeben, C., van den Berg, A., Groot, A. J., Dubois, L., & Vooijs, M. (2020). NOTCH inhibition promotes bronchial stem cell renewal and epithelial barrier integrity after irradiation. *Stem Cells Transl Med*, *9*(7), 799-812. https://doi.org/10.1002/sctm.19-0278

Guha, A., Deshpande, A., Jain, A., Sebastiani, P., & Cardoso, W. V. (2017). Uroplakin 3a(+) Cells Are a Distinctive Population of Epithelial Progenitors that Contribute to Airway

Maintenance and Post-injury Repair. *Cell Rep*, *19*(2), 246-254. https://doi.org/10.1016/j.celrep.2017.03.051

Guha, A., Vasconcelos, M., Cai, Y., Yoneda, M., Hinds, A., Qian, J., Li, G., Dickel, L., Johnson, J. E., Kimura, S., Guo, J., McMahon, J., McMahon, A. P., & Cardoso, W. V. (2012). Neuroepithelial body microenvironment is a niche for a distinct subset of Clara-like precursors in the developing airways. *Proc Natl Acad Sci U S A*, *109*(31), 12592-12597. https://doi.org/10.1073/pnas.1204710109

Hegab, A. E., Ha, V. L., Gilbert, J. L., Zhang, K. X., Malkoski, S. P., Chon, A. T., Darmawan, D. O., Bisht, B., Ooi, A. T., Pellegrini, M., Nickerson, D. W., & Gomperts, B. N. (2011). Novel stem/progenitor cell population from murine tracheal submucosal gland ducts with multipotent regenerative potential. *Stem Cells*, *29*(8), 1283-1293. https://doi.org/10.1002/stem.680

Hishida, T., Vazquez-Ferrer, E., Hishida-Nozaki, Y., Takemoto, Y., Hatanaka, F., Yoshida, K., Prieto, J., Sahu, S. K., Takahashi, Y., Reddy, P., O'Keefe, D. D., Rodriguez Esteban, C., Knoepfler, P. S., Nunez Delicado, E., Castells, A., Campistol, J. M., Kato, R., Nakagawa, H., & Izpisua Belmonte, J. C. (2022). Myc Supports Self-Renewal of Basal Cells in the Esophageal Epithelium. *Front Cell Dev Biol*, *10*, 786031. https://doi.org/10.3389/fcell.2022.786031

Hogan, B. L., Barkauskas, C. E., Chapman, H. A., Epstein, J. A., Jain, R., Hsia, C. C., Niklason, L., Calle, E., Le, A., Randell, S. H., Rock, J., Snitow, M., Krummel, M., Stripp, B. R., Vu, T., White, E. S., Whitsett, J. A., & Morrisey, E. E. (2014). Repair and regeneration of the respiratory system: complexity, plasticity, and mechanisms of lung stem cell function. *Cell Stem Cell*, *15*(2), 123-138. https://doi.org/10.1016/j.stem.2014.07.012

Honma, S., Kawamoto, T., Takagi, Y., Fujimoto, K., Sato, F., Noshiro, M., Kato, Y., & Honma, K. (2002). Dec1 and Dec2 are regulators of the mammalian molecular clock. *Nature*, *419*(6909), 841-844. https://doi.org/10.1038/nature01123

Hughes, M., Dobric, N., Scott, I. C., Su, L., Starovic, M., St-Pierre, B., Egan, S. E., Kingdom, J. C., & Cross, J. C. (2004). The Hand1, Stra13 and Gcm1 transcription factors override FGF signaling to promote terminal differentiation of trophoblast stem cells. *Dev Biol*, *271*(1), 26-37. https://doi.org/10.1016/j.ydbio.2004.03.029

Ivanova, A. V., Ivanov, S. V., & Lerman, M. L. (2005). Association, mutual stabilization, and transcriptional activity of the STRA13 and MSP58 proteins. *Cell Mol Life Sci*, *62*(4), 471-484. https://doi.org/10.1007/s00018-004-4423-2

Iwata, T., Kawamoto, T., Sasabe, E., Miyazaki, K., Fujimoto, K., Noshiro, M., Kurihara, H., & Kato, Y. (2006). Effects of overexpression of basic helix-loop-helix transcription factor Dec1 on osteogenic and adipogenic differentiation of mesenchymal stem cells. *Eur J Cell Biol*, *85*(5), 423-431. https://doi.org/10.1016/j.ejcb.2005.12.007

Jackson, P. K., & Attardi, L. D. (2016). p73 and FoxJ1: Programming Multiciliated Epithelia. *Trends Cell Biol*, *26*(4), 239-240. https://doi.org/10.1016/j.tcb.2016.03.001

Jarjour, N. N., Schwarzkopf, E. A., Bradstreet, T. R., Shchukina, I., Lin, C. C., Huang, S. C., Lai, C. W., Cook, M. E., Taneja, R., Stappenbeck, T. S., Randolph, G. J., Artyomov, M. N., Urban, J. F., Jr., & Edelson, B. T. (2019). Bhlhe40 mediates tissue-specific control of macrophage proliferation in homeostasis and type 2 immunity. *Nat Immunol*, *20*(6), 687-700. https://doi.org/10.1038/s41590-019-0382-5

Kathiriya, J. J., Brumwell, A. N., Jackson, J. R., Tang, X., & Chapman, H. A. (2020). Distinct Airway Epithelial Stem Cells Hide among Club Cells but Mobilize to Promote Alveolar Regeneration. *Cell Stem Cell*, *26*(3), 346-358 e344. https://doi.org/10.1016/j.stem.2019.12.014

Kim, C. F., Jackson, E. L., Woolfenden, A. E., Lawrence, S., Babar, I., Vogel, S., Crowley, D., Bronson, R. T., & Jacks, T. (2005). Identification of bronchioalveolar stem cells in normal lung and lung cancer. *Cell*, *121*(6), 823-835. https://doi.org/10.1016/j.cell.2005.03.032

Kiyokawa, H., & Morimoto, M. (2020). Notch signaling in the mammalian respiratory system, specifically the trachea and lungs, in development, homeostasis, regeneration, and disease. *Dev Growth Differ*, *62*(1), 67-79. https://doi.org/10.1111/dgd.12628

Knight, S., Zhang, F., Mueller-Kuller, U., Bokhoven, M., Gupta, A., Broughton, T., Sha, S., Antoniou, M. N., Brendel, C., Grez, M., Thrasher, A. J., Collins, M., & Takeuchi, Y. (2012). Safer, silencing-resistant lentiviral vectors: optimization of the ubiquitous chromatin-opening element through elimination of aberrant splicing. *J Virol*, *86*(17), 9088-9095. https://doi.org/10.1128/JVI.00485-12

Knowles, M. R., & Boucher, R. C. (2002). Mucus clearance as a primary innate defense mechanism for mammalian airways. *J Clin Invest*, *109*(5), 571-577. https://doi.org/10.1172/JCI15217

Lafkas, D., Shelton, A., Chiu, C., de Leon Boenig, G., Chen, Y., Stawicki, S. S., Siltanen, C., Reichelt, M., Zhou, M., Wu, X., Eastham-Anderson, J., Moore, H., Roose-Girma, M., Chinn, Y., Hang, J. Q., Warming, S., Egen, J., Lee, W. P., Austin, C., . . . Siebel, C. W. (2015). Therapeutic antibodies reveal Notch control of transdifferentiation in the adult lung. *Nature*, *528*(7580), 127-131. https://doi.org/10.1038/nature15715

Lembrechts, R., Brouns, I., Schnorbusch, K., Pintelon, I., Timmermans, J. P., & Adriaensen, D. (2012). Neuroepithelial bodies as mechanotransducers in the intrapulmonary airway epithelium: involvement of TRPC5. *Am J Respir Cell Mol Biol*, *47*(3), 315-323. https://doi.org/10.1165/rcmb.2012-0068OC

Levlev, V., Jensen-Cody, C. C., Lynch, T. J., Pai, A. C., Park, S., Shahin, W., Engelhardt, J. F. (2022). Sox9 and Lef1 Regulate the Fate and Behavior of Airway Glandular Progenitors in Response to Injury. *Stem Cells, 40*(8), 778-790. doi:10.1093/stmcls/sxac038

Linnoila, R. I. (2006). Functional facets of the pulmonary neuroendocrine system. *Lab Invest*, *86*(5), 425-444. https://doi.org/10.1038/labinvest.3700412

Liu, H., Kennard, S., & Lilly, B. (2009). NOTCH3 expression is induced in mural cells through an autoregulatory loop that requires endothelial-expressed JAGGED1. *Circ Res*, *104*(4), 466-475. https://doi.org/10.1161/CIRCRESAHA.108.184846

Liu, N., Hargreaves, V. V., Zhu, Q., Kurland, J. V., Hong, J., Kim, W., Sher, F., Macias-Trevino, C., Rogers, J. M., Kurita, R., Nakamura, Y., Yuan, G. C., Bauer, D. E., Xu, J., Bulyk, M. L., & Orkin, S. H. (2018). Direct Promoter Repression by BCL11A Controls the Fetal to Adult Hemoglobin Switch. *Cell*, *173*(2), 430-442 e417. https://doi.org/10.1016/j.cell.2018.03.016

Liu, Q., Liu, K., Cui, G., Huang, X., Yao, S., Guo, W., Qin, Z., Li, Y., Yang, R., Pu, W., Zhang, L., He, L., Zhao, H., Yu, W., Tang, M., Tian, X., Cai, D., Nie, Y., Hu, S., . . . Zhou, B. (2019). Lung regeneration by multipotent stem cells residing at the bronchioalveolar-duct junction. *Nat Genet*, *51*(4), 728-738. https://doi.org/10.1038/s41588-019-0346-6

Lynch, T. J., Anderson, P. J., Rotti, P. G., Tyler, S. R., Crooke, A. K., Choi, S. H., Montoro, D. T., Silverman, C. L., Shahin, W., Zhao, R., Jensen-Cody, C. W., Adamcakova-Dodd, A., Evans, T. I. A., Xie, W., Zhang, Y., Mou, H., Herring, B. P., Thorne, P. S., Rajagopal, J., . . . Engelhardt, J. F. (2018). Submucosal Gland Myoepithelial Cells Are Reserve Stem Cells That Can Regenerate Mouse Tracheal Epithelium. *Cell Stem Cell*, *22*(5), 779. https://doi.org/10.1016/j.stem.2018.04.007

Marshall, C. B., Mays, D. J., Beeler, J. S., Rosenbluth, J. M., Boyd, K. L., Santos Guasch, G. L., Shaver, T. M., Tang, L. J., Liu, Q., Shyr, Y., Venters, B. J., Magnuson, M. A., &

Pietenpol, J. A. (2016). p73 Is Required for Multiciliogenesis and Regulates the Foxj1-Associated Gene Network. *Cell Rep*, *14*(10), 2289-2300. https://doi.org/10.1016/j.celrep.2016.02.035

Montoro, D. T., Haber, A. L., Biton, M., Vinarsky, V., Lin, B., Birket, S. E., Yuan, F., Chen, S., Leung, H. M., Villoria, J., Rogel, N., Burgin, G., Tsankov, A. M., Waghray, A., Slyper, M., Waldman, J., Nguyen, L., Dionne, D., Rozenblatt-Rosen, O., . . . Rajagopal, J. (2018). A revised airway epithelial hierarchy includes CFTR-expressing ionocytes. *Nature*, *560*(7718), 319-324. https://doi.org/10.1038/s41586-018-0393-7

Mori, M., Mahoney, J. E., Stupnikov, M. R., Paez-Cortez, J. R., Szymaniak, A. D., Varelas, X., Herrick, D. B., Schwob, J., Zhang, H., & Cardoso, W. V. (2015). Notch3-Jagged signaling controls the pool of undifferentiated airway progenitors. *Development*, *142*(2), 258-267. https://doi.org/10.1242/dev.116855

Morimoto, M., Nishinakamura, R., Saga, Y., & Kopan, R. (2012). Different assemblies of Notch receptors coordinate the distribution of the major bronchial Clara, ciliated and neuroendocrine cells. *Development*, *139*(23), 4365-4373. https://doi.org/10.1242/dev.083840

Nakashima, A., Kawamoto, T., Honda, K. K., Ueshima, T., Noshiro, M., Iwata, T., Fujimoto, K., Kubo, H., Honma, S., Yorioka, N., Kohno, N., & Kato, Y. (2008). DEC1 modulates the circadian phase of clock gene expression. *Mol Cell Biol*, *28*(12), 4080-4092. https://doi.org/10.1128/MCB.02168-07

Nemajerova, A., Kramer, D., Siller, S. S., Herr, C., Shomroni, O., Pena, T., Gallinas Suazo, C., Glaser, K., Wildung, M., Steffen, H., Sriraman, A., Oberle, F., Wienken, M., Hennion, M., Vidal, R., Royen, B., Alevra, M., Schild, D., Bals, R., . . . Lize, M. (2016). TAp73 is a central transcriptional regulator of airway multiciliogenesis. *Genes Dev*, *30*(11), 1300-1312. https://doi.org/10.1101/gad.279836.116

Nguyen, C., Kudek, M., Zander, R., Niu, H., Shen, J., Bauer, A., Alson, D., Khatun, A., Chen, Y., Sun, J., Drobyski, W., Edelson, B. T., & Cui, W. (2024). Bhlhe40 Promotes CD4+ T Helper 1 Cell and Suppresses T Follicular Helper Cell Differentiation during Viral Infection. *Journal of immunology (Baltimore, Md. : 1950)*, *212*(11), 1829–1842. https://doi.org/10.4049/jimmunol.2300355

Pardo-Saganta, A., Law, B. M., Tata, P. R., Villoria, J., Saez, B., Mou, H., Zhao, R., & Rajagopal, J. (2015). Injury induces direct lineage segregation of functionally distinct airway basal stem/progenitor cell subpopulations. *Cell Stem Cell*, *16*(2), 184-197. https://doi.org/10.1016/j.stem.2015.01.002

Pardo-Saganta, A., Tata, P. R., Law, B. M., Saez, B., Chow, R. D., Prabhu, M., Gridley, T., & Rajagopal, J. (2015). Parent stem cells can serve as niches for their daughter cells. *Nature*, *523*(7562), 597-601. https://doi.org/10.1038/nature14553

Parisi, S., Piscitelli, S., Passaro, F., & Russo, T. (2020). HMGA Proteins in Stemness and Differentiation of Embryonic and Adult Stem Cells. *Int J Mol Sci*, *21*(1). https://doi.org/10.3390/ijms21010362

Qian, Y., Jung, Y. S., & Chen, X. (2011). DeltaNp63, a target of DEC1 and histone deacetylase 2, modulates the efficacy of histone deacetylase inhibitors in growth suppression and keratinocyte differentiation. *J Biol Chem*, *286*(14), 12033-12041. https://doi.org/10.1074/jbc.M110.207241

Qian Y, Zhang J, Jung YS, Chen X. (2014) DEC1 coordinates with HDAC8 to differentially regulate TAp73 and ΔNp73 expression. PLoS One. 2014 Jan 3;9(1):e84015. doi: 10.1371/journal.pone.0084015.

Rauschmeier, R., Gustafsson, C., Reinhardt, A., N, A. G., Tortola, L., Cansever, D., Subramanian, S., Taneja, R., Rossner, M. J., Sieweke, M. H., Greter, M., Mansson, R., Busslinger, M., & Kreslavsky, T. (2019). Bhlhe40 and Bhlhe41 transcription

factors regulate alveolar macrophage self-renewal and identity. *EMBO J*, *38*(19), e101233. https://doi.org/10.15252/embj.2018101233

Rawlins, E. L., & Hogan, B. L. (2008). Ciliated epithelial cell lifespan in the mouse trachea and lung. *Am J Physiol Lung Cell Mol Physiol*, *295*(1), L231-234. https://doi.org/10.1152/ajplung.90209.2008

Rawlins, E. L., Okubo, T., Xue, Y., Brass, D. M., Auten, R. L., Hasegawa, H., Wang, F., & Hogan, B. L. (2009). The role of Scgb1a1+ Clara cells in the long-term maintenance and repair of lung airway, but not alveolar, epithelium. *Cell Stem Cell*, *4*(6), 525-534. https://doi.org/10.1016/j.stem.2009.04.002

Rawlins, E. L., Ostrowski, L. E., Randell, S. H., & Hogan, B. L. (2007). Lung development and repair: contribution of the ciliated lineage. *Proc Natl Acad Sci U S A*, *104*(2), 410-417. https://doi.org/10.1073/pnas.0610770104

Reynolds, S. D., Reynolds, P. R., Pryhuber, G. S., Finder, J. D., & Stripp, B. R. (2002). Secretoglobins SCGB3A1 and SCGB3A2 define secretory cell subsets in mouse and human airways. *Am J Respir Crit Care Med*, *166*(11), 1498-1509. https://doi.org/10.1164/rccm.200204-285OC

Rock, J. R., Gao, X., Xue, Y., Randell, S. H., Kong, Y. Y., & Hogan, B. L. (2011). Notch-dependent differentiation of adult airway basal stem cells. *Cell Stem Cell*, *8*(6), 639-648. https://doi.org/10.1016/j.stem.2011.04.003

Rock, J. R., & Hogan, B. L. (2011). Epithelial progenitor cells in lung development, maintenance, repair, and disease. *Annu Rev Cell Dev Biol*, *27*, 493-512. https://doi.org/10.1146/annurev-cellbio-100109-104040

Rock, J. R., Onaitis, M. W., Rawlins, E. L., Lu, Y., Clark, C. P., Xue, Y., Randell, S. H., & Hogan, B. L. (2009). Basal cells as stem cells of the mouse trachea and human airway epithelium. *Proc Natl Acad Sci U S A*, *106*(31), 12771-12775. https://doi.org/10.1073/pnas.0906850106

Rogers, D. F. (1994). Airway goblet cells: responsive and adaptable front-line defenders. *Eur Respir J*, *7*(9), 1690-1706. https://www.ncbi.nlm.nih.gov/pubmed/7995400

Rogers, D. F. (2003). The airway goblet cell. *Int J Biochem Cell Biol*, *35*(1), 1-6. https://doi.org/10.1016/s1357-2725(02)00083-3

Rokicki, W., Rokicki, M., Wojtacha, J., & Dzeljijli, A. (2016). The role and importance of club cells (Clara cells) in the pathogenesis of some respiratory diseases. *Kardiochir Torakochirurgia Pol*, *13*(1), 26-30. https://doi.org/10.5114/kitp.2016.58961

Ruiz Garcia, S., Deprez, M., Lebrigand, K., Cavard, A., Paquet, A., Arguel, M. J., Magnone, V., Truchi, M., Caballero, I., Leroy, S., Marquette, C. H., Marcet, B., Barbry, P., & Zaragosi, L. E. (2019). Novel dynamics of human mucociliary differentiation revealed by single-cell RNA sequencing of nasal epithelial cultures. *Development*, *146*(20). https://doi.org/10.1242/dev.177428

Salwig, I., Spitznagel, B., Vazquez-Armendariz, A. I., Khalooghi, K., Guenther, S., Herold, S., Szibor, M., & Braun, T. (2019). Bronchioalveolar stem cells are a main source for regeneration of distal lung epithelia in vivo. *EMBO J*, *38*(12). https://doi.org/10.15252/embj.2019102099

Sato, F., Muragaki, Y., & Zhang, Y. (2015). DEC1 negatively regulates AMPK activity via LKB1. *Biochem Biophys Res Commun*, *467*(4), 711-716. https://doi.org/10.1016/j.bbrc.2015.10.077

Schwab, L. P., Peacock, D. L., Majumdar, D., Ingels, J. F., Jensen, L. C., Smith, K. D., Cushing, R. C., & Seagroves, T. N. (2012). Hypoxia-inducible factor 1alpha promotes primary tumor growth and tumor-initiating cell activity in breast cancer. *Breast Cancer Res*, *14*(1), R6. https://doi.org/10.1186/bcr3087

Shen, M., Yoshida, E., Yan, W., Kawamoto, T., Suardita, K., Koyano, Y., Fujimoto, K., Noshiro, M., & Kato, Y. (2002). Basic helix-loop-helix protein DEC1 promotes chondrocyte differentiation at the early and terminal stages. *J Biol Chem*, *277*(51), 50112-50120. https://doi.org/10.1074/jbc.M206771200

Silva, S., Bicker, J., Falcão, A., & Fortuna, A. (2023). Air-liquid interface (ALI) impact on different respiratory cell cultures. *European journal of pharmaceutics and biopharmaceutics: official journal of Arbeitsgemeinschaft fur Pharmazeutische Verfahrenstechnik e.V*, *184*, 62–82. https://doi.org/10.1016/j.ejpb.2023.01.013

Song, H., Yao, E., Lin, C., Gacayan, R., Chen, M. H., & Chuang, P. T. (2012). Functional characterization of pulmonary neuroendocrine cells in lung development, injury, and tumorigenesis. *Proc Natl Acad Sci U S A*, *109*(43), 17531-17536. https://doi.org/10.1073/pnas.1207238109

Stupnikov, M. R., Yang, Y., Mori, M., Lu, J., & Cardoso, W. V. (2019a). Jagged and Delta-like ligands control distinct events during airway progenitor cell differentiation. *Elife*, *8*. https://doi.org/10.7554/eLife.50487

Stupnikov, M. R., Yang, Y., Mori, M., Lu, J., & Cardoso, W. V. (2019b). Jagged and Delta ligands control distinct events during airway progenitor cell differentiation. *Elife*, *8*. https://doi.org/10.7554/eLife.50487

Sun, D., Llora Batlle, O., van den Ameele, J., Thomas, J. C., He, P., Lim, K., Tang, W., Xu, C., Meyer, K. B., Teichmann, S. A., Marioni, J. C., Jackson, S. P., Brand, A. H., & Rawlins, E. L. (2022). SOX9 maintains human foetal lung tip progenitor state by enhancing WNT and RTK signalling. *EMBO J*, *41*(21), e111338. https://doi.org/10.15252/embj.2022111338

Sun, H., Li, L., Vercherat, C., Gulbagci, N. T., Acharjee, S., Li, J., Chung, T. K., Thin, T. H., & Taneja, R. (2007). Stra13 regulates satellite cell activation by antagonizing Notch signaling. *J Cell Biol*, *177*(4), 647-657. https://doi.org/10.1083/jcb.200609007

Sun, H., & Taneja, R. (2000). Stra13 expression is associated with growth arrest and represses transcription through histone deacetylase (HDAC)-dependent and HDAC-independent mechanisms. *Proc Natl Acad Sci U S A*, *97*(8), 4058-4063. https://doi.org/10.1073/pnas.070526297

Swift, J., & Coruzzi, G. M. (2017). A matter of time - How transient transcription factor interactions create dynamic gene regulatory networks. *Biochim Biophys Acta Gene Regul Mech*, *1860*(1), 75-83. https://doi.org/10.1016/j.bbagrm.2016.08.007

Tata, P. R., Mou, H., Pardo-Saganta, A., Zhao, R., Prabhu, M., Law, B. M., Vinarsky, V., Cho, J. L., Breton, S., Sahay, A., Medoff, B. D., & Rajagopal, J. (2013). Dedifferentiation of committed epithelial cells into stem cells in vivo. *Nature*, *503*(7475), 218-223. https://doi.org/10.1038/nature12777

Travaglini, K. J., Nabhan, A. N., Penland, L., Sinha, R., Gillich, A., Sit, R. V., Chang, S., Conley, S. D., Mori, Y., Seita, J., Berry, G. J., Shrager, J. B., Metzger, R. J., Kuo, C. S., Neff, N., Weissman, I. L., Quake, S. R., & Krasnow, M. A. (2020). A molecular cell atlas of the human lung from single-cell RNA sequencing. *Nature*, *587*(7835), 619-625. https://doi.org/10.1038/s41586-020-2922-4

Tsao, P. N., Vasconcelos, M., Izvolsky, K. I., Qian, J., Lu, J., & Cardoso, W. V. (2009). Notch signaling controls the balance of ciliated and secretory cell fates in developing airways. *Development*, *136*(13), 2297-2307. https://doi.org/10.1242/dev.034884

Tseng, H., & Green, H. (1994). Association of basonuclin with ability of keratinocytes to multiply and with absence of terminal differentiation. *J Cell Biol*, *126*(2), 495-506. https://doi.org/10.1083/jcb.126.2.495

Vaughan, A. E., Brumwell, A. N., Xi, Y., Gotts, J. E., Brownfield, D. G., Treutlein, B., Tan, K., Tan, V., Liu, F. C., Looney, M. R., Matthay, M. A., Rock, J. R., & Chapman, H.

A. (2015). Lineage-negative progenitors mobilize to regenerate lung epithelium after major injury. *Nature*, *517*(7536), 621-625. https://doi.org/10.1038/nature14112

Wallmeier, J., Bracht, D., Alsaif, H. S., Dougherty, G. W., Olbrich, H., Cindric, S., Dzietko, M., Heyer, C., Teig, N., Thiels, C., Faqeih, E., Al-Hashim, A., Khan, S., Mogarri, I., Almannai, M., Al Otaibi, W., Alkuraya, F. S., Koerner-Rettberg, C., & Omran, H. (2021). Mutations in TP73 cause impaired mucociliary clearance and lissencephaly. *Am J Hum Genet*, *108*(7), 1318-1329. https://doi.org/10.1016/j.ajhg.2021.05.002

Wang, C., Liu, W., Liu, Z., Chen, L., Liu, X., & Kuang, S. (2015). Hypoxia Inhibits Myogenic Differentiation through p53 Protein-dependent Induction of Bhlhe40 Protein. *J Biol Chem*, *290*(50), 29707-29716. https://doi.org/10.1074/jbc.M115.688671

Watson, J. K., Rulands, S., Wilkinson, A. C., Wuidart, A., Ousset, M., Van Keymeulen, A., Gottgens, B., Blanpain, C., Simons, B. D., & Rawlins, E. L. (2015). Clonal Dynamics Reveal Two Distinct Populations of Basal Cells in Slow-Turnover Airway Epithelium. *Cell Rep*, *12*(1), 90-101. https://doi.org/10.1016/j.celrep.2015.06.011

Wei, J., Li, H., Wang, S., Li, T., Fan, J., Liang, X., Li, J., Han, Q., Zhu, L., Fan, L., & Zhao, R. C. (2014). let-7 enhances osteogenesis and bone formation while repressing adipogenesis of human stromal/mesenchymal stem cells by regulating HMGA2. *Stem Cells Dev*, *23*(13), 1452-1463. https://doi.org/10.1089/scd.2013.0600

Xi, Y., Kim, T., Brumwell, A. N., Driver, I. H., Wei, Y., Tan, V., Jackson, J. R., Xu, J., Lee, D. K., Gotts, J. E., Matthay, M. A., Shannon, J. M., Chapman, H. A., & Vaughan, A. E. (2017). Local lung hypoxia determines epithelial fate decisions during alveolar regeneration. *Nat Cell Biol*, *19*(8), 904-914. https://doi.org/10.1038/ncb3580

Yalcin-Ozuysal, Ö., Fiche, M., Guitierrez, M. *et al*. Antagonistic roles of Notch and p63 in controlling mammary epithelial cell fates. *Cell Death Differ* **17**, 1600–1612 (2010). https://doi.org/10.1038/cdd.2010.37

Yoh, K., & Prywes, R. (2015). Pathway Regulation of p63, a Director of Epithelial Cell Fate. *Frontiers in endocrinology*, *6*, 51. https://doi.org/10.3389/fendo.2015.00051

Zhao, M., Xiaofei, L., Gang, C., Wei, L., Jing, X., Gang, H., Ruini, C., Rui, N., Wei, S., Jian, Y., & Bingfang, Y. (2012). DEC1 binding to the proximal promoter of CYP3A4 ascribes to the downregulation of CYP3A4 expression by IL-6 in primary human hepatocytes. *Biochem Pharmacol*, *84*(5), 701-711. https://doi.org/10.1016/j.bcp.2012.06.010

Acknowledgments

I would like to express my sincere gratitude to Prof. Dr. Christos Samakovlis for granting me the opportunity to undertake this doctoral research, as well as for his invaluable guidance and the profound insights I have gained from him throughout this journey. His expertise has been instrumental in developing my scientific thinking and approach. I would like to extend my heartfelt thanks to Dr. Ramesh for his invaluable supervision, both technically and scientifically, which has been essential to the success of this project. I am also very grateful to Dr. Janine Koepke for her valuable advice and support throughout this journey as well as for taking the time to read my thesis and providing me with constructive feedback. I would like to thank Dr. Christina Ortiz for her valuable supervision and for the technical skills I have gained under her guidance, particularly in molecular cloning.

A special thanks to Dr. Athanasios Fysikopoulos for guiding me through all aspects of mouse work and handling, as well as for sharing his valuable knowledge. I would like to Thank Dr. Anoop Vadakan Cherian for his immense support with confocal microscopy and imaging software. I am grateful to Dr. Martin Hardt for granting me access to use IMARIS software and for his kindness. I would like to thank Dr. Pamela Millar Büchner for taking the time to read my thesis and sharing insightful feedback. I also would like to thank Eleni Bouloukou, Dr. Andres Alberro Brage, and Antonella D'Ambrosio for their support and for creating a nice work environment. I would like to thank Dr. Alexandros Sountoulidis for his valuable contribution of the human single-cell RNA sequencing data, which has greatly contributed to the success of this project. A special thanks also to Dr. Alexandra Firsova for her valuable work with the BHLHE40 knockout mice. I would also like to thank Prof. Dr. Marek Bartkuhn for his valuable assistance with the CUT&RUN data analysis and his insightful advice. Also, to David Glaser for his effort in analyzing the data. I am grateful to the MBML program for providing me with this great opportunity and for the invaluable knowledge I have gained throughout the lectures and retreats. A special thanks to Dr. Elie El Agha for his valuable tutoring throughout the program.

Finally, a heartfelt thanks to my dearest friends Dr. Hiba Hasan and Reem Jamous for embellishing this journey with their sincere and warm hearts. My deepest gratitude goes to my parents for their unconditional love and unwavering support. Dedicated to the dearest memory of my beloved aunt Saida Hichri.